University of Nairobi

PETROLOGY AND GEOCHEMISTRY OF ROCKS HOSTING NIOBIUM-TANTALUM, TIN AND TUNGSTEN BEARING MINERALS IN RUNYANKEZI AREA, NORTHERN BURUNDI

BY

DIDACE NTIRAMPEBA

I56/8347/2017

A Dissertation submitted for examination in partial fulfillment of the requirements for award of the degree of Master of Science in Geology of the University of Nairobi.

2020

DECLARATION

I hereby declare, that this is my original work and it has not been submitted for a degree in any other university.

Signed ……..date……..

Didace NTIRAMPEBA
I56/8347/2017
Department of **Geology**
School of **Physical Sciences**
University of Nairobi

This dissertation is submitted for examination with our approval as supervisors:

Signed ……..date……..

Dr. D. W. Ichang'i
Department of Geology
University of Nairobi
P.O.Box 30197-00100, Nairobi, Kenya
dichangi@uonbi.ac.ke

Signed ……..date……..

Dr. A.K. Waswa
Department of Geology
University of Nairobi
aaronwaswa@gmail.com

UNIVERSITY OF NAIROBI

DECLARATION OF ORIGINALITY FORM

This form must be completed and signed for all works submitted to the University for Examination.

Name of student: DIDACE NTIRAMPEBA
Registration number: I56/8347/2017
College: BIOLOGICAL AND PHYSICAL SCIENCES
Faculty/School/Institute: SCHOOL OF PHYSICAL SCIENCES
Department: GEOLOGY
Course name: Master of Science in Geology
Title of the work: PETROLOGY AND GEOCHEMISTRY OF ROCKS HOSTING NIOBIUM-TANTALUM, TIN AND TUNGSTEN BEARING MINERALS IN RUNYANKEZI AREA, NORTHERN BURUNDI

DECLARATION

1. I understand what is plagiarism is and I am aware of the university's policy in this regard.
2. I declare that this **dissertation** is my original work and has not been submitted elsewhere for examination, award of a degree or publication. Where others people's work, or my own work has been used, this has properly been acknowledged and referenced in accordance with the University of Nairobi's requirements.
3. I have not sought or used the services of any professional agencies to produce this work
4. I have not allowed, and shall not allow anyone to copy my work with the intention of passing it off as his/her own work
5. I understand that any false claim in respect of this work shall result in disciplinary action, in accordance with University Plagiarism policy.

Signature:

Date:

DEDICATION

This dissertation is dedicated to my Mother **BARAGASIKA Cécile** and my beloved Spouse **IRATUNGA Suavis**, to my two Sons **NTIRAMPEBA Guy Dorian** and **NTIRAMPEBA Davis Rey**, and in memory of my late Father **NYANDWI Evariste.**

ACKNOWLEDGEMENT

I would like to thank my Supervisors sincerely, **Dr. D. W. Ichang'I and Dr. A.K. Waswa,** for their advice, their constructive comments, their patience and their availability. I would also like to thank the lecturers of the University of Nairobi, particularly those of the Department of Geology, who supported me during this academic journey.

I also thank the Burundian Minister of Hydraulics, Energy and Mines, **Hon. Côme MANIRAKIZA** and his Permanent Secretary Mr. **Siméon HABONIMANA** for their moral support and their understandings. I would also like to thank the NTEGA Holding Burundi Company for the funding which it granted me during this academic course as well as its facilitation during the fieldwork in the Runyankezi area.

I wish to pass my gratitude to the team of Society Ntega Holding Burundi for their professional support and exchanges. I wish to thank all my colleagues and friends who participated directly or indirectly in the realization of this project. My gratitude goes to **Miss BANGURAMBONA Fidès** for her courtesy and zeal that she has shown me.

In conclusion, I would like to warmly and sincerely thank my **Dear Wife IRATUNGA Suavis** for her patience, understanding, respect, loyalty, competence and above all, for her encouragement and support, that she finds happiness and respect at the end of this work.

ABSTRACT

Runyankezi area occur in the northern part of Burundi in Kirundo and Ngozi Provinces. It occurs in the Meso- to- Neoproterozoic Karagwe-Ankole belt that has a huge mineral potential. Runyankezi is historically known to have mineralization of cassiterite, columbo-tantalite, and more rarely Tungsten. This belt is composed of metasedimentary rocks subjected to different episodes of deformations and metamorphism. The lack of knowledge regarding characteristics of tantalum, tin, and tungsten (3Ts) bearing rocks in Runyankezi and the genesis of their associated mineralizations was the base of the choice of this research. The main objective of this research was to investigate the geological context of the 3Ts-bearing host lithologies and their related mineralization and the petrogenesis of the 3Ts' minerals in Runyankezi area in northern part of Burundi. The tools used in this research included geological field observations for stratigraphy and micro-structure, rock sampling, and geochemical analysis. Geological field observations revealed that all mineralization of 3Ts in the study area is from pegmatites. Petrography showed that principal minerals in rocks hosting 3Ts in the Runyankezi are Li-rich tourmaline (Elbaite), muscovite, biotite with zircon inclusion, hornblende, feldspars (orthoclase), sericite, and quartz. It is noted that muscovite, biotite, sericite, and tourmaline occur as a result of hydrothermal alteration. Geochemistry showed that 3Ts bearing rocks are Subalkaline and peraluminous. Trace elements (High Field Strength Elements and Large Ion Lithophile Elements) and rare-earth elements (REE) analyses revealed that pegmatites with high mineralization are of Lithium-Caesium-Tantalum type (LCT-Type) and are far from the granitic intrusion. They are associated with S-type granites. Their formation took place at low temperature and are evolved with Ta>Nb. These pegmatites occur in Buvyukana. In contrast, pegmatites with low concentration are of Niobium-Yettrium-Fluorine type (NYF-Type) and are close to granitic intrusion. They are associated with I-type granites. Those granites are not mantellic but crustal with high Rb concentration, the formation of derived pegmatites took place at high temperature, they are not more evolved, with Nb>Ta and occur in Nyanza-Burenge site;

- Those pegmatites have undergone post-magmatic alteration evidenced by Rb/Sr and Ba/Rb ratios;
- The genetic setting of Tin, Tungsten, and Columbo-Tantalite is associated with hydrothermal alterations. These alterations are sericitization, albitization, tourmalinization, muscovitization, kaolinization, and greissenization.

In both sites, mineralization occur at the muscovite-rich portion and decreases as the core of the pegmatite approaches. It also increases as the distance from the granitic batholiths increases.

It has been confirmed that the Buvyukana location within the study area has potential tantalite mineral that can be exploited. For further research, an investigation of the source of the fluid which gave independent pegmatites of Buvyukana site in Ntega is with high interest.

TABLE OF CONTENTS

DECLARATION.....i

DECLARATION OF ORIGINALITY FORM.....ii

DEDICATION.....iii

ACKNOWLEDGEMENT.....iv

ABSTRACT.....v

TABLE OF CONTETS.....vii

LIST OF TABLES.....xi

LIST OF FIGURES.....xii

LIST OF ABBREVIATIONS AND ACRONYMS.....xv

CHAPTER ONE: INTRODUCTION AND LITERATURE REVIEW.....1

1.1 BACKGROUND INFORMATION.....1

1.2 GENERAL FRAMEWORK.....2

1.3 PROBLEMS STATEMENTS.....3

1.4 OBJECTIVES.....3

1.4.1 Main Objective.....3

1.4.2 Specific Objectives.....3

1.5 JUSTIFICATION AND SIGNIFICANCE OF THE RESEARCH.....4

1.6 THESIS LAYOUT.....4

1.7 GEOGRAPHY OF THE STUDY AREA.....5

1.7.1 Location.....5

1.7.2 Climate.....7

1.7.3 Relief, land use, drainage and vegetation.....7

1.7.4 GENERAL GEOLOGY OF RUNYANKEZI.....9

CHAPTER TWO: LITERATURE REVIEW.....11

2.1 HISTORICAL EMPLACEMENT OF MESO-TO NEOPROTEROZOIC (1,000 TO 542Ma) KIBARAN BELT AND IT'S MINERALIZATION.....11

2.2 GEOLOGY AND STRUCTURES OF BURUNDI 12
2.3 GEOLOGY OF NORTHERN BURUNDI 14
2.3.1 The Lower Burundian with a thickness of about 7000m 14
2.3.2 The Average Burundian with a thickness of about 2500m 14
2.3.3 Upper Burundian about 1350m thick: 14
2.4 METAMORPHISM OF BURUNDIAN SEDIMENTS 15
2.5 DEFORMATION AND FOLDING OF BURUNDIAN FORMATIONS 15
2.6 THE AGE OF OROGENY AND MAGMATISM OF BURUNDIAN 16
2.7 GLOBAL OVERVIEW ON 3Ts 17
2.7.1 Geology and Occurrence of Tin 17
2.7.2 Geology and Occurrence of Tungsten 18
2.7.3 Geology and Occurrence of Nb and Ta 20
2.7.4 Igneous rocks hosting Nb and Ta 21
2.7.5 Concentration of Nb and Ta in Sedimentary rocks 21
2.7.6 Geochemistry of Nb and Ta 23
2.7.7 The behavior and formation of Nb-Ta during Magma crystallization 25
2.7.8 Primary and secondary Resources of Nb-Ta for Industries 26
2.7.9 Use of Niobium and Tantalum 26
2.7.10 Processing and Mining of Nb-Ta 27
2.7.11 Reserve of Niobium-Tantalum in the World 29
2.8 MINING ACTIVITY AND ITS EVOLUTION IN BURUNDI 30
2.8.1 Mining potential in Burundi 30
2.8.2 History and evolution of the mining activity of rare metals in Burundi 32
2.9 LEGAL FRAMEWORK AND TRANSPARENCY OF THE MINING SECTOR IN BURUNDI 35
2.9.1 Legal framework of the mining sector in Burundi 35
2.9.2 Transparency of the mining sector 35

CHAPTER THREE: MATERIAL AND METHODS.....36

3.1 GEOLOGICAL ASSESSMENT 36

3.1.1 Geological field work 36

3.1.2 Petrology investigation 38

3.2 GEOCHEMICAL ASSESSMENT 39

3.2.1 Digging, Sampling and Standards Operating Procedures (sops).....39

3.2.1.2 Standard Operating Procedures (SOPs) 41

3.2.2 Analytical Methods.....42

3.2.2.1 Sample preparation and dispatch 42

3.6 USE OF GIS DURING THIS WORK 46

CHAPTER FOUR: RESULTS AND DISCUSSION 47

4.1 MINERALIZATION AND OCCURRENCE OF (Nb-Ta, Sn, W) BEARING ROCKS IN RUNYANKEZI 47

4.1.1 Occurrence of specific 3Ts bearing lithologies and their classification 47

4.1.2 Rock description and location of mineralization in the rock.....48

4.2 INVESTIGATION OF MINERALOGY, PETROLOGY, AND GEOCHEMISTY OF NIOBIUM-TANTALUM, TIN AND TUNGSTEN BEARING ROCKS IN RUNYANKEZI 52

4.2.1 Mineralogy investigation.....53

4.2.1.1 Mineralogy of Mpindo-kigaga Granite and its associated Pegmatite 53

4.2.1.2 Mineralogy of Granite from Ndurumu River and its associated Pegmatite.....55

4.2.1.3 Mineralogy of Granite from Rurambo-Nyanza (South part of the study area)....57

4.2.2 Composition and classification of sampled rocks in burenge-nyanza using major elements 59

4.2.2.1 Rock classification: Total alkalis- silica diagram (TAS) and SiO_2 vs K_2O diagram 64

4.2.2.2 Tectonic Setting 67

4.2.2.3 Harker variation diagrams.....68

4.2.3 Whole rock geochemical of sampled rocks in runyankezi 69

4.2.3.1 Use of Nb/Ta and/or Ta/Nb ratios in Genetic setting of 3Ts minerals 69

4.2.3.2 Analysis and Discussion of plotted Diagrams 70

4.3 CHARACTERIZATION OF 3T'S MINERALIZATION IN THE RUNYANKEZI AREA, NORTHERN BURUNDI 84

4.3.1 Overview on pegmatites rocks and nb-ta deposits 84

4.3.2 Classification of pegmatites.....85

4.3.3 Origin of pegmatites 86

4.3.4 Style of mineralization in runyankezi area 87

4.3.5 Association and type of deposits in runyankezi 88

4.4 DISCUSSION 89

CHAPTER FIVE: CONCLUSION AND RECOMMENDATIONS 91

REFERENCES.....93

LIST OF APPENDICES 105

Appendix A: Chemical analyses of Whole Rock from Buvyukana (in ppm).....105

Appendices B: Chemical analyses of Whole Rock from NYANZA-BURENGE (in ppm) 115

LIST OF TABLES

CHAPTER 1

Table 1. 1 Runyankezi Coordinate and area 5

Table 1. 2 Different Formations and their associated rocks 10

CHAPTER 2

Table 2. 1 Major types of Tungsten deposits, with their Geological environment (Sinclair, 1986). 19

Table 2. 2 Major types of niobium and tantalum deposits, with key characteristics and examples.Modified from British Geological Survey (2011). 22

Table 2. 3 Major minerals of Nb-Ta (British Geologic survey, 2011) 24

Table 2. 4 World Tantalum producers (Schulz et al., 2017).....30

Table 2. 5 Mining potential of Burundi (OBM, 2019) 31

Table 2. 6 The production of artisanal mining from 1933 to 1979 (OBM, 2019).....33

Table 2. 7 Mining production from 1989 to 2018 (OBM, 2019).....34

CHAPTER 4

Table 4. 1 Chemical analysis of twenty samples from Nyanza-Burenge and their normalized values. 60

LIST OF FIGURES

CHAPTER 1

Figure 1. 1 Location of Runyankezi in Ngozi and Kirundo Provinces, north Burundi 6

Figure 1. 2 Profile reflecting the relief of Runyankezi. 8

Figure 1. 3 Geological Map of Runyankezi (Modified from Burundian Quarry and Mine Office, 2019) 9

CHAPTER 2

Figure 2. 1 Regional tectonic setting of the Karagwe-Ankole Belt (KAB) and the Kibaran belt (KIB) (Dewaele et al., 2011).....11

Figure 2. 2 Geological Map of Burundi (Nahimana, 2008 modified from the Ministry of Energy and Mines and RMCA, 1990). 13

Figure 2. 3 Process scheme for Nb and Ta production (Arrachart et al., 2015) 29

CHAPTER 3

Figure 3. 1 Contact between host rocks and pegmatites (field investigation) 36

Figure 3. 2 Sampling map.....37

Figure 3. 3 Gallery (Adit) with Wooden Support.....40

Figure 3. 4 Sampling and description within the gallery at 26 m of the depth.....41

Figure 3. 5 Control chart for AMIS0338 for Tantalum 45

Figure 3. 6 chart for AMIS0339 for Tin 45

CHAPTER4

Figure 4. 1 Outcrop Granite together with pegmatite in north part of Runyankezi.....48

Figure 4. 2 Sequence of Stratigraphy in well define unit in the study area 49

Figure 4. 3 High weathered pegmatites at Buvyukana site.....50

Figure 4. 4 Stockworks veins in weathered pegmatite (a) and diaclases (b) 50

Figure 4. 5 Contact between Granite and Pegmatite.....51

Figure 4. 6 Photomicrographs of foliated granite from Mpindo-Kigaga. Fs=Feldspar, Hbl=Hornblende, Musc=Muscovite, Ser= Sericite, Waypoint: X: 29.94712; Y:-2.6163. 53

Figure 4. 7 Photomicrographs of Pegmatite from Mpindo-Kigaga. Fs=Feldspar, Musc=Muscovite, Tourm= Tourmaline, Bio= Biotite. Waypoint: X: 29.94712; Y:-2.6163. .54

Figure 4. 8 Photomicrographs of granite from Ndurumu River. Fs=Feldspar, Musc=Muscovite, Hbl=Hornblende, Bio= Biotite, Waypoint: X: 29,98636; Y:-2,72552. 55

Figure 4. 9 Photomicrographs of pegmatite from Ndurumu River. Fs=Feldspar, Musc=Muscovite, Hbl=Hornblende, Tourm=Tourmaline. Waypoint: X: 29,98636; Y:-2,72552.....56

Figure 4. 10 Photomicrographs of granite from Rurambo-Nyanza. Fs=Feldspar, Musc=Muscovite, Qtz=Quartz, Bio= Biotite. Waypoint: X: 29,99773; Y : -2,73845. 58

Figure 4. 11 a-b.Composition and classification diagram of Nyanza-Burenge rocks (MackDonald, 1968 and Le Maitre et al., 1989), c-d.Subdivision of subalkaline rocks of Nyanza-Burenge using the K_2O vs SiO_2 (Le Maitre et al., 1989). 65

Figure 4. 12 Classification diagram of Nyanza-Burenge rocks based on Alumina saturation (Shand, 1943).....66

Figure 4. 13 a.Bivariate plot of Al_2O_3 versus TiO_2 showing environment related to different Geological fields (After Muller et al., 1992), b.Bivariate plot of Fe_2O_3+MgO versus TiO_2 showing geological fields (After Bhatia, 1983).....67

Figure 4. 14 Harker variation diagram for major elements in Nyanza-Burenge site.....68

Figure 4. 15 Rare Earth element abundances in Buvyukana pegmatites and granites, normalized to Condritic values after Thompson (1982). 72

Figure 4. 16 Plot of K/Rb vs Nb/Ta highlighting pegmatite-hydrothermal evolution (Shaw, 1968 and Ballouard et al., 2016).....73

Figure 4. 17 Correlation of Sr with: Rb, Nb, Ta, Zr, Ba, and Sn in Pegmatite.....74

Figure 4. 18 Correlation of Sn with: Nb, and Ta in Pegmatite. 75

Figure 4. 19 Correlation of Rb with: Nb, Sn, and Ta in Pegmatite. 75

Figure 4. 20 Plot of Zr/Hf vs Nb/Ta as geochemical indicator of the fertility of granitic rocks (Linnen and Keppler, 2002; Claiborne et al., 2006 and Ballouard et al., 2016).....76

Figure 4. 21 Plot of Rb/Sr Vs Ba/Rb to test post-magmatic alteration (Imeokparia, 1981). ...76

Figure 4. 22 Rare Earth element abundances in Nyanza- Burenge pegmatites and granites, normalized to Condritic values after Thompson (1982). 78

Figure 4. 23 Plot of Zr/Hf vs Nb/Ta as geochemical indicator of the fertility of granitic rocks (Linnen and Keppler, 2002; Claiborne et al., 2006 and Ballouard et al., 2016).....79

Figure 4. 24 Plot of Rb/Sr Vs Ba/Rb to test post-magmatic alteration (Imeokparia, 1981)....80

Figure 4. 25 Correlation of Cs with: Nb, Sn, Ta, Rb, Zr, Ba, U, Sr, W, and Hf in Pegmatite.81

Figure 4. 26 Correlation of Sn with: Nb, Ta, and W in Pegmatite; Correlation of Nb with: Ta, and W in Pegmatite; and Correlation of Ta with: W in Pegmatite 82

Figure 4. 27 Correlation of Sr with: Nb, Sn, Ta, and W in Pegmatite.....83

Figure 4. 28 Schematic representation of regional zoning and evolution from a simple biotite granite to a complex pegmatite, applied to the studied pegmatites (Modified from Trueman and Cerny, 1982 and London, 2008) 86

Figure 4. 29 Location of the mineralization.....87

Figure 4. 30 Plot of Ta vs Ta/Nb highlighting the type of deposit (Stepanov et al., 2014).....88

Figure 4. 31 Plot of Ta vs Ta/Nb highlighting the type of deposit is (Stepanov et al., 2014) .89

LIST OF ABBREVIATIONS AND ACRONYMS

3Ts: Tin, Tungsten, Niobium-Tantalum

HFSE: High Field Strength Elements

LILE: Large Ion Lithophile Element

REE: Rare Earth Elements

LCT: Lithium, Caesium, Tantalum

LOI: Loss on Ignition

NYF: Niobium, Yettrium, Fluorine

RM: Rare Metals

DRC: Democratic Republic of Congo

KAB: Karagwe-Ankole Belt

KIB: Kibaran Belt

CGM: Colombite Group Minerals

DTM: Digital Terrain Model

MT: Million Tons

OBM : Office Burundais des Mines et Carrières

VMA: Vision Minière Africaine

PPP: Public-Private Partnership

EITI: Extractive Industries Transparency Initiative

ICGLR: International Conferenc of Great Lakes Region

BC: Before Christ

ASI: Aluminium Saturation Index

HSLA: High Strength Low-Alloy

NMRI: Nuclear Magnet Resonance Instrulents

RoW: Remain of the World

LIMS: Laboratory Information Management System

QA: Quality Assurance

QC: Quality Control

PPL: Plane polarized light

XPL: Cross polarized light

CHAPTER ONE: INTRODUCTION AND LITERATURE REVIEW

1.1 BACKGROUND INFORMATION

Burundi is a country located in Central Africa and is a member of the East-African Community with an area of approximately 27,834 km^2.

Since the colonial era, Burundi is known to have different mineralizations such as rare metals in northern Burundi, but also rare earth elements (Gakara) in the west of the country in addition to nickel in the south-east and central of the country in Musongati and Nyabikere respectively, and others including, for example, vanadium in Mukanda.

The rare metals (RM) of the north of the country have been exploited since the 1930s. These mineralizations were long considered together with those of Rwanda, and the DRC, and were ignored during research regarding their characterization.

Various initiatives for the development of the Mining sector in Burundi have been set up by the Government, research assays have been conducted for several years, but it is to be noted that these mineralizations are not well known at the world level from the point of view of specific characteristics of their genesis as well as their hosting rocks, whereas they have been exploited for several years until today.

The Mesoproterozoic Kibaran Orogeny in Central Africa host various granites related rare elements mineralizations such as Columbite-Tantalite "Coltan", Cassiterite, Wolframite, beryl, Spodumene as typical minerals. Rocks hosting 3Ts-bearing minerals in north Burundi region are known to be related to Mesoproterozoic Kibaran belt orogeny (Brinckmann et al., 2001; Tack et al., 1994; Lavreau and Liégeois, 1982; Tack et al., 2010; Fernandez-Alonso et al., 2012; Melcher, 2017) which is characterized by enrichment in rare metals such as Niobium-Tantalum, Tin "Sn", Tungsten.

Those metals are the main mineralizations in quartz veins, greisen and pegmatites, but secondary mineralization in alluvial and eluvial deposits (Brinckmann et al., 1987).
The young granites "Tin-granite" or "Sn-granite" are formed at 986±10 (Tack et al., 2006 and Mutima, 2010) and appeared in Kibaran belt as intrusion where they represent the most important magmatic event in terms of metallogenic evolution.
These Kibara granites of fourth-generation (G4) have recently been dated with U-Pb SHRIMP zircon at 986±10 Ma (Tack et al. 2006 and 2008).

Tack *et al.* (2006 and 2008) in their studies show that pegmatites were emplaced at 968±8 Ma whereas the intrusion of the young granites is at 986±10 Ma.

Dewaele *et al*. (2007a and 2008) by their investigation indicate that the Columbite-Tantalite mineralizations are contemporaneous with the crystallization of the pegmatites, whereas the cassiterite present in the pegmatites formed during a later phase of intense K-alteration (sericitisation and muscovitisation).

In Rutongo area, Dewael *et al.* (2010) obtained in their investigation new apparent age (869±7 Ma) much younger than the accepted ages of the G4-granites, younger than the Kibaran pegmatites and associated Columbite-tantalum mineralization and younger than the age reported for the Sn-mineralised quartz vein.

But former researches showed almost the same age as it is shown below:

- ✓ Monteyne-Poulaert *et al*. (1962a, b) obtained Rb-Sr ages of muscovites and Sn-mineralised quartz veins from D.R Congo (Kivu), Rwanda and Burundi that range between Ca 1100 and 870 Ma.
- ✓ Cahen and Snelling (1966) place the formation of post-tectonic pegmatites and veins with cassiterite and sulphides between 1000±30 Ma and 870±26 Ma for the Rwandese-Burundese part of the Kibara orogeny, based on published K/Ar, Rb/Sr, U/Pb and Pb-Pb ages.
- ✓ Brinckmann (1988) dated muscovite crystals from Sn-mineralised quartz vein and altered host-rocks at Mulehe, Burundi which gave an Rb-Sr age of 936±82 Ma.

Considering these previous works, it is evident that the geological context of rocks hosting 3Ts-bearing minerals is not well known in the investigated area. The findings of this research will help in the orientation of miners regarding the genesis of enriched or depleted rocks to know where they can focus their exploitation activities. It will also provide the idea of the enrichment of the rocks for possible exploration campaigns to minimize the exploration expenditures.

1.2 GENERAL FRAMEWORK

During this research project, the interest was the Petrology and the whole rock Geochemistry of rocks hosting Niobium-Tantalum, Tin and Tungsten (3Ts) bearing minerals. The remain of the rocks, which were not associated with those mineralizations, were not included in this investigation.

1.3 PROBLEMS STATEMENT

Different projects and researches have been conducted in Northern part of Burundi. Still, no particular attention has been focused to the Petrology and whole-rock Geochemistry of rocks hosting 3Ts-bearing minerals in the north region, particular in Runyankezi area. They are known to be in Karagwe-Ankole segment, the way they are said in general, combining three countries (Burundi, Rwanda and Uganda) which make the north part of the entire Kibaran Belt; those rocks in Burundi are not yet investigated as it has been done in Rwanda, and DRC.

The kibaran belt in which the study area is contained is known to have major provinces of rare metals in the world, much documentations and investigations have been done by different authors and were based on the geology and the age of various generations of granites which intruded that belt, among those authors figured (Brinckmann et al., 2001; Tack et al., 1994; Lavreau and Liégeois, 1982 Tack et al., 2010; Fernandez-Alonso et al., 2012; Melcher, 2017).

A partial investigation on mineralization of Pegmatites of Northwestern Burundi and an assay of characterization of mineral indicators of coltan mineralization in northern Burundi has been done in neighbouring localities of the study area (Ntirandekura, 2015 and Nikobahoze, 2015).

Understandably, these rocks hosting 3Ts-bearing minerals in the study area are not well known. Their petrology and Geochemistry are not well understood to highlight the petrogenesis of those rocks and genetic setting of those 3Ts minerals. Besides that, the characterization of those rocks and their mineralizations was of high interest.

1.4 OBJECTIVES

1.4.1 Main Objective

The main objective of this research was to characterize the geological context of the 3Ts-bearing lithologies and their related mineralizations in Runyankezi area in the Northern part of Burundi using data on petrology and geochemistry of the whole rock.

1.4.2 Specific Objectives

1. To investigate field occurrences of 3T's bearing rocks to establish mineralizations location and occurrences;

2. To investigate the mineralogy, petrology, and geochemistry of the Nb-Ta, Sn, and W bearing rocks in Runyankezi Area, Northern Burundi;
3. To characterize the 3T's mineralizations in the Runyankezin Area, Northern BURUNDI in order to highlight the type of deposits, the association between mineralizations, and the style of the appearance of mineralization in the rock.

1.5 JUSTIFICATION AND SIGNIFICANCE OF THE RESEARCH

Today, rare metals such as Niobium-Tantalum, Tin, and Tungsten are highly needed because of their demand related to the modern utilization and manufacturing of electronic devices especially the use of Tantalum and niobium in alloy steel production. These metals are available within various geological contexts and have different geneses. Their exploitation in Burundi is artisanal (craft activities), and that activity represents a valuable contribution to Burundi's economy. Even that exploitation is conducted, those rocks hosting 3Ts-bearing minerals and their associated mineralizations are still not well understood, and their geneses need to be investigated by the use of petrology and the whole rock geochemistry of these rocks hosting 3Ts- bearing minerals.

Today, Runyankezi area is known to have mineralization of 3Ts, but, as it has been done for some areas surrounding, these rocks hosting 3Ts-bearing minerals are still not well understood in that locality. Then, it is better to assess the petrology and the geochemistry of these rocks hosting 3Ts- bearing minerals. This research will lead to a good and interpretative of the genesis of those rocks and their associated mineralizations in order to distinguish them if they are pure magmatic or magmatic-hydrothermal. Besides, this research will help exploiters to differentiate the location of enriched rocks related to depleted rocks.

1.6 THESIS LAYOUT

This thesis is based on several Chapters as follows:

Chapter one: Introduction, it gives the main objective, specific objectives, the geology of Runyankezi and background of the Study Area.

Chapter two: Literature review, highlights different pieces of information regarding the Niobium-Tantalum, Tin, and Tungsten geology and geochemistry, the geology of Burundi in general, the geology of Kibaran belt and its mineralization as well as the Mining activity in Burundi.

Chapter three: Materials and methods, which include the methods and materials used to achieve the objectives of this research. That includes field observation, geological survey, geochemical survey, and analytical procedures.

Chapter four: Results and discussion, it includes three main points:

- Mineralization and occurrence of (Nb-Ta, Sn, W) bearing rocks in Runyankezi. The existence of specific 3T's bearing lithologies and their classification, rock description and location of mineralization in the rock are evaluated in this subchapter;
- Investigation of mineralogy, petrology, and geochemistry of niobium-tantalum, tin and tungsten bearing rocks in Runyankezi;
- Characterization of 3Ts mineralization in the runyankezi area, Northern Burundi. This sub-chapter talks about: the style of the mineralization in the rock, association of the mineralization, and the type of the ore deposit

Chapter five: Conclusion and Recommendations.

1.7 GEOGRAPHY OF THE STUDY AREA

1.7.1 Location

The study area is located in Northern Burundi shared between Kirundo and Ngozi provinces, it contains a part of Ngozi in south and southwest, part of Kirundo in north and northeast whereas in the northwest is bordered by the Republic of Rwanda. The area is bordered by following coordinates:

Table 1. 1 Runyankezi Coordinate and area

Peak	X_coord	Y_cood	Area
A	29°55'50"	2°37'11"	313.9 km^2
B	30°04'50"	2°37'11"	
C	30°04'50"	2°49'11"	
D	29°54'50"	2°44'22"	
E	29°54'50''	2°42'26''	

The accessibility of the area from Kirundo and Ngozi is facilitated by dirt road which has other local and narrow roads throughout the region.

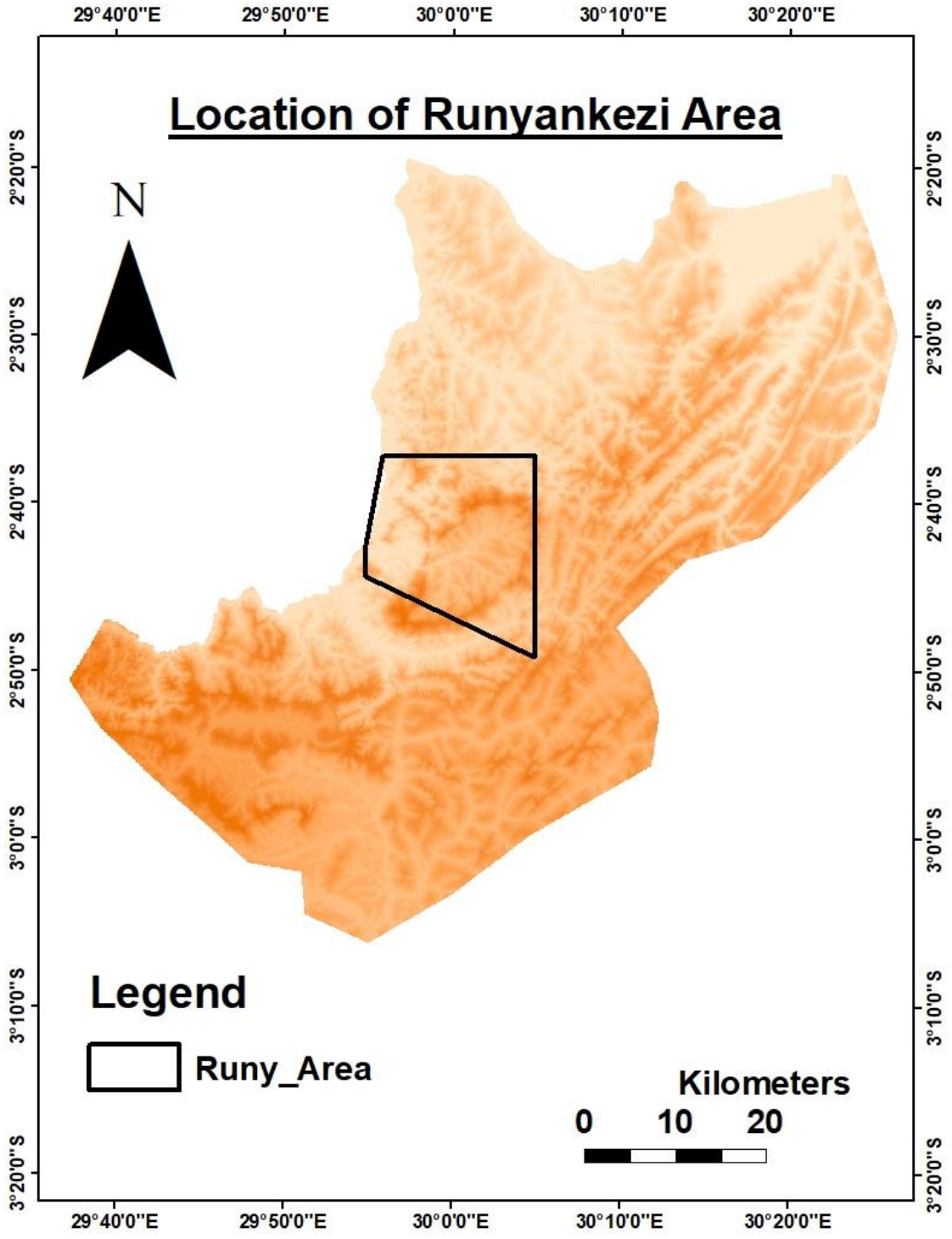

Figure 1. 1 Location of Runyankezi in Ngozi and Kirundo Provinces, north Burundi

1.7.2 Climate

The study area is generally rainy and wet; it belongs to the tropical climate. According to Burundi's environment, it is conditioned by the relief, and is characterized by four seasons: two rainy seasons September to November (Agatasi) and February to may (Impeshi), and two dry seasons (Ici) (Jun to august and December to January).

Annual temperatures usually vary from 15.4 to 24.1° C, while the annual rainfall varies between 794mm and 1678mm (ISABU, 2002).

1.7.3 Relief, land use, drainage and vegetation

The global relief of Burundi accounts five units which are from west to east the low Imbo land corresponding to the western graben of the rift where Tanganyika is located, the steep Mirwa region, the mountainous area corresponding to western Horst of the rift, the central highland, and the Kumoso depression (Bidou, 1991). The altitude is 774m at the rim of the Lake Tanganyika and 2670 on the Congo-Nile Ridge and 1200 m in the east of the country.

The study area has an intricate and various reliefs with highlands and depression alternatively (Fig.1.2). All the area under investigation is used for agriculture (crop farming) except the small part of the area in the north with eucalyptus plantations. The primary seed crops grown include maize, beans, sorghum, cassava, suit potatoes and banana. That crop farming is coupled with livestock farming of goat, sheep, fowl and cattle (fieldwork observations). Otherwise, this relief is conditioned by the lithology. The last is composed usually by silt, schist and outcrops of quartzite, granitic rocks, and basic rocks. These quartzite rocks sometimes are exploited for construction materials while the areas dominated by silt are used for agriculture. The essential sources of water are located in the depression, whereas the highlands are humid because of the rainfall and are covered by green vegetation mainly composed of crop farming. Rivers are not too many, but marsh areas are everywhere and surrounded by crop farming.

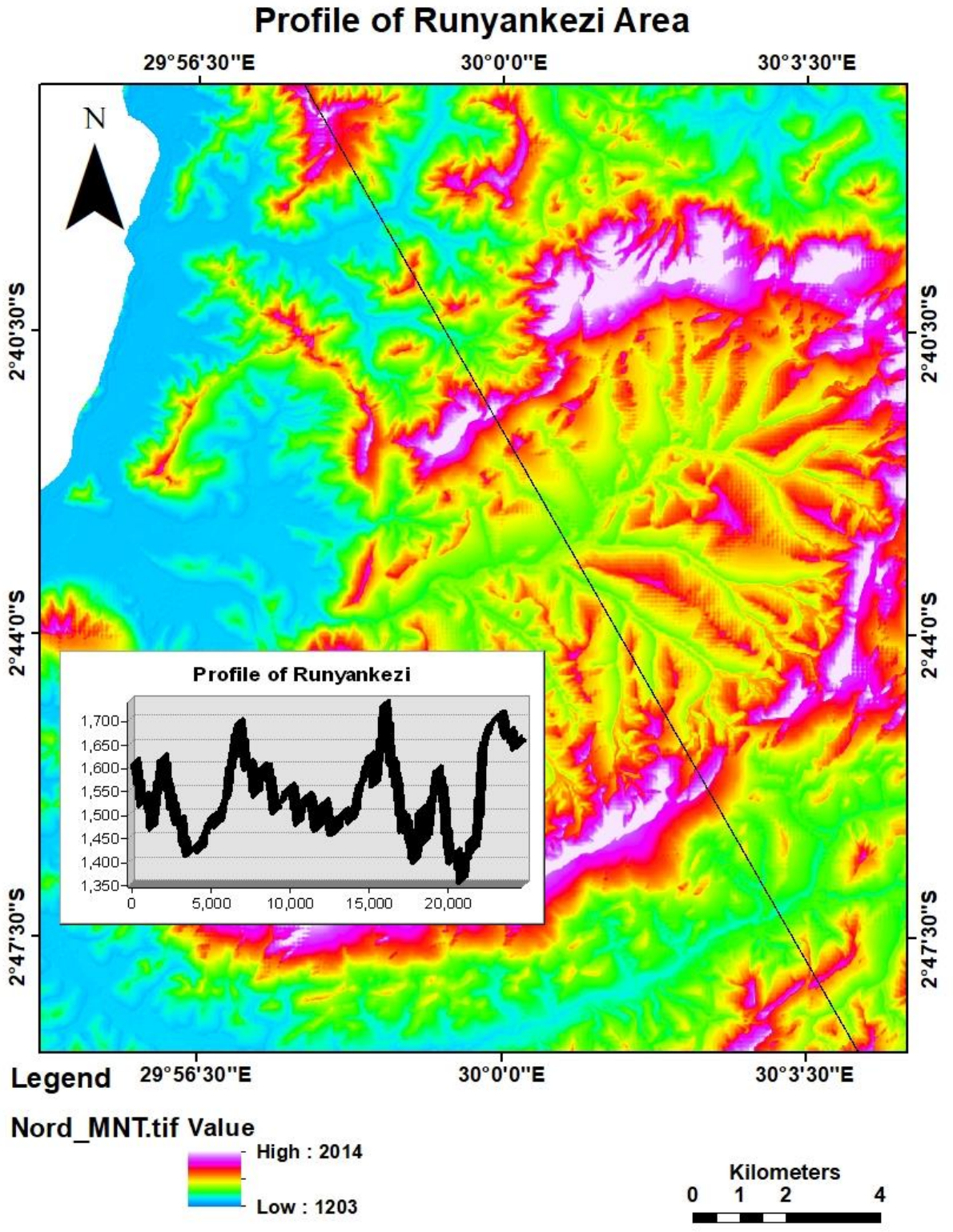

Figure 1. 2 Profile reflecting the relief of Runyankezi.

1.7.4 GENERAL GEOLOGY OF RUNYANKEZI

The geology of Runyankezi area corresponds to the formation belonging to Mesoproterozoic and Cenozoic deposits. Otherwise, it contains Cenozoic rocks and Precambrian rocks which belong to Kanyaru Super Mesoproterozoic.

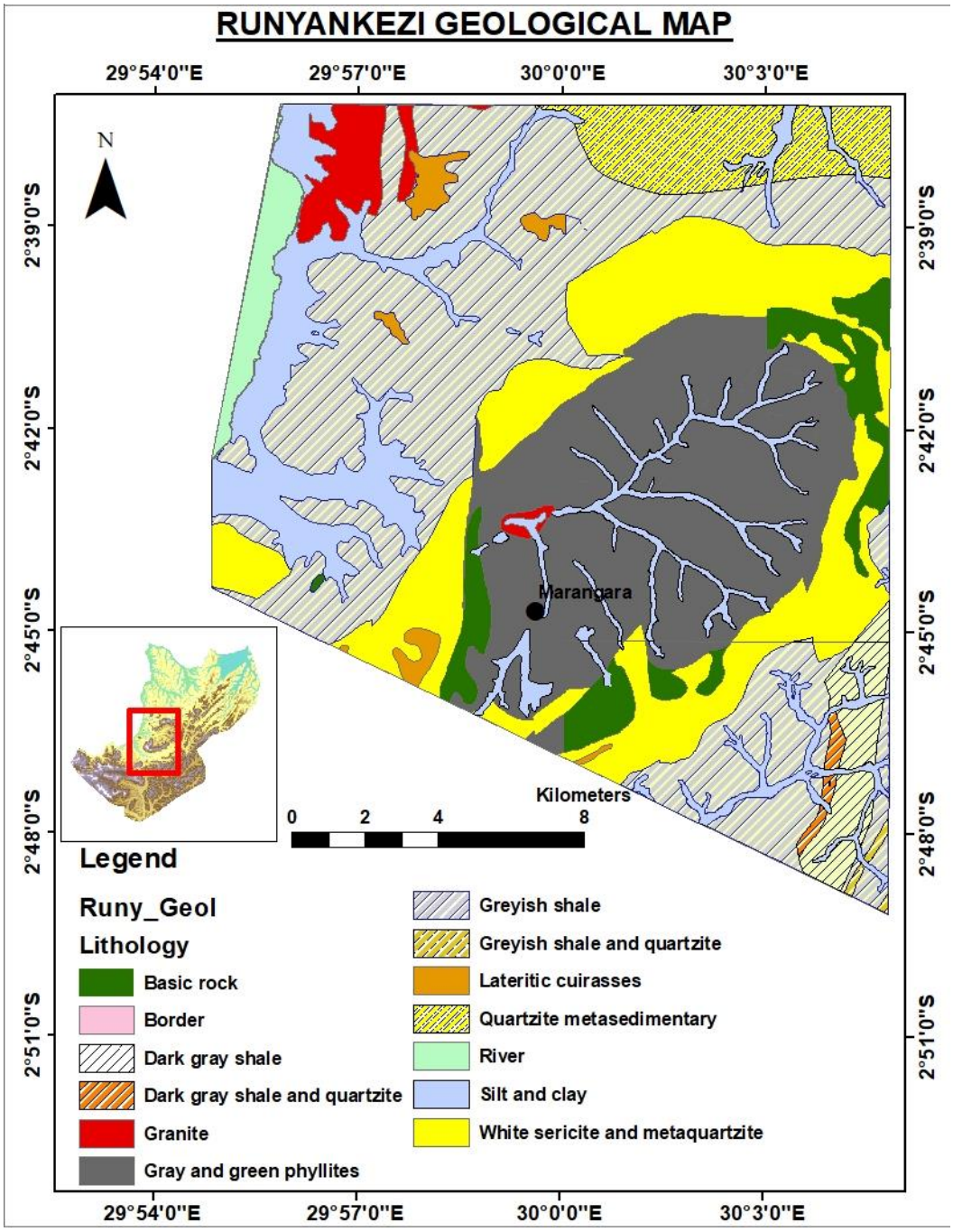

Figure 1. 3 Geological Map of Runyankezi (Modified from Burundian Quarry and Mine Office, 2019)

By fieldwork investigations and existing geological map, following lithologies have been confirmed.

Table 1. 2 Different Formations and their associated rocks

Geological time		**Type of formation/ Lithologies Symboles**	**Rocks/lithology**
Cenozoic		Ho: valley bottom and low terrace alluvium	Recent Sediments (Silt and Clays)
Mesoproterozoic Supergroup of Kanyaru	The Upper Group	Gisha (Gi)	dark gray shales, banded and altered in red hues
		Nyabihanga and Ngozi (Ny / Ng)	greyish Gresoschists with interlocations of misclassified quartzites and microconglomerate with sedimentary structure
		Ruganza (Ru)	white Sericite metaquartzites often being cut into platelets parallel to the stratification and alternating with more homogeneous, massive and greyish metaquartzites locally oblique stratification.
		Migendo (Md)	Metasediment mainly quartzite in nature and generally loaded with tourmaline appearing in isolated outcrops in a granitic and pegmatitic arena
	The Lower Group	Rukago (Rk),	gray and green phyllites sometimes sandstone with intercalation of quartzite beds. It presents in places near granite, a micaschistous appearance and are locally feldspathized.
		Rukago (Rkb), Ngozi (NgG), Ruganza (RuGb), Rug	Basic rock points in the Rukago, Lateritic cuirasses and soils Misclassified , Quartzites and microconglomerate interbedded with sedimentary structure are observed in the Nyabihanga and Gisha formations.
		RuLat / RuLt/ Ng Lat	Lateritic cuirasses and soils in Ruganza and Ngozi formation
		Migendo formation with Granite (MdGr)	Granite points in finely grained, muscovite-oriented metamorphic granite.

CHAPTER TWO: LITERATURE REVIEW

2.1 HISTORICAL EMPLACEMENT OF MESO-TO NEOPROTEROZOIC (1,000 TO 542Ma) KIBARAN BELT AND IT'S MINERALIZATION

The Mesoproterozoic Kibaran Belt goes through five countries, namely Democratic Republic of Congo (DRC), Burundi, Rwanda, Uganda, and a small part in Tanzania. It is made of two different segments which are separated by a northwest-trending "Rusizi Ubende belt" basement (Fig.2.1). The Kibaran Belt is from the southeast of DRC to southwest of Uganda. The southern part occupies part of Katanga Province in DRC whereas the northern portion extends into the Kivu-Maniema region of the DRC, to the east of the western Rift. The portion in the east of western Rift has for a long time been referred to as the "Northeastern Kibaran Belt" (Tack et al., 1994; Tack et al., 2002). It covers southwestern Uganda (Ankole Province), northwestern Tanzania (Karagwe province), Kivu-Maniema, Burundi and Rwanda. The Kibaran Belt occurs between the Archaean/Palaeoproterozoic Congo craton to the west and the north, and the Archaean Tanzania Craton and Palaeoproterozoic Bangweulu Block to the east and the south (Tack et al., 2002; Dewaele et al., 2013) **(**Fig .2. 1).

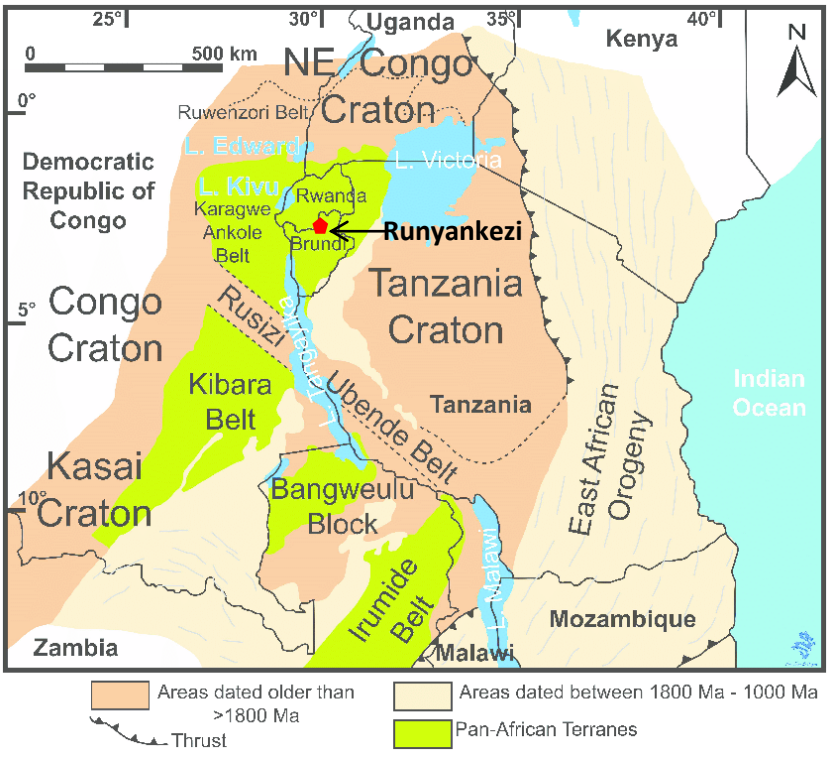

Figure 2. 1 Regional tectonic setting of the Karagwe-Ankole Belt (KAB) and the Kibaran belt (KIB) (Dewaele et al., 2011).

Ankole and Karagwe segments together make one unit known on the name of Karagwe-Ankole Belt (KAB) and cover countries such as Kivu-Maniema, Burundi, Rwanda, southwesthern part of Uganda, and the northwestern part of Tanzania whereas the southern part is called Kibaran Belt which covers Katanga Province and Kivu-Maniema Belt (KIB) (Fig .2.1) (Tack et al., 2010). The entire Karagwe-Ankole and Kibara Belt stretch over a strike distance of 1,300 km from south-western Uganda via Rwanda and Burundi into the Katanga region of the DRC and onward towards the Angola-Zambia DRC border (Tack et al., 2010; Fernandez-Alonso et al., 2012; Melcher, 2017).

They are composed of metasedimentary rocks which consist of monotonous siliciclastic pelite and arenite sequences, interpreted as shallow-water turbidity deposits. Carbonate rocks are present (Tack et al., 2010).

The two parts have been intruded by various generations of granitoid massifs and subordinate mafic bodies (Tacket al., 2010 and Fernandez-Alonso et al., 2012) where the first main granite generation is related to thermodynamic "tectono-magmatic" event at almost 1375 Ma during the time of prominent bimodal magmatism and extension tectonics, while the orogeny occurred during Rodinia amalgamation at around 1000 Ma (Fernandez-alonso et al., 2012). The generations related to the amalgamation Rodinia are considered as fertile granites also called "Tin-Granites" that have been emplaced around 986 Ma and are associated with rare metal pegmatites and Sn-W mineralized quartz veins. Using U-Pb ages, mineralization of Columbite Group Minerals in the Kibara Belt ranges in age from 1020 to ca. 930 Ma (Melcher et al., 2015 and 2017).

2.2 GEOLOGY AND STRUCTURES OF BURUNDI

The geology of Burundi is composed of rocks belonging to the Mesoproterozoic Kibaran belt known by the name of Burundian Supergroup, of Neoproterozoic Malagarasian Supergroup, and of Cenozoic sediments. The Cenozoic rocks consist of Holocene deposits (alluvium) and Pleistocene deposits (lacustrine, fluviatile and tidal deposits).

Malagarasian rocks are conglomerates, quartzites, dolomitic limestones and volcanic mafic-ultramafic rocks. Burundian Supergroup is primarily composed of arenaceous sediments of moderate to low grade metamorphic. These sediments are intruded by various generations of granites and some mafic-ultramafic rocks (Ntiharirizwa, 2013). All generation of granites are not mineralized and are categorized into four groups (G1 to G4) (De Clercq et al., 2012). Radiometric using U-Pb dating has shown that the three first generations of granites were

emplaced at 1380±10Ma, while the fourth generation was formed around 986±10 Ma (Tack et al., 2006).

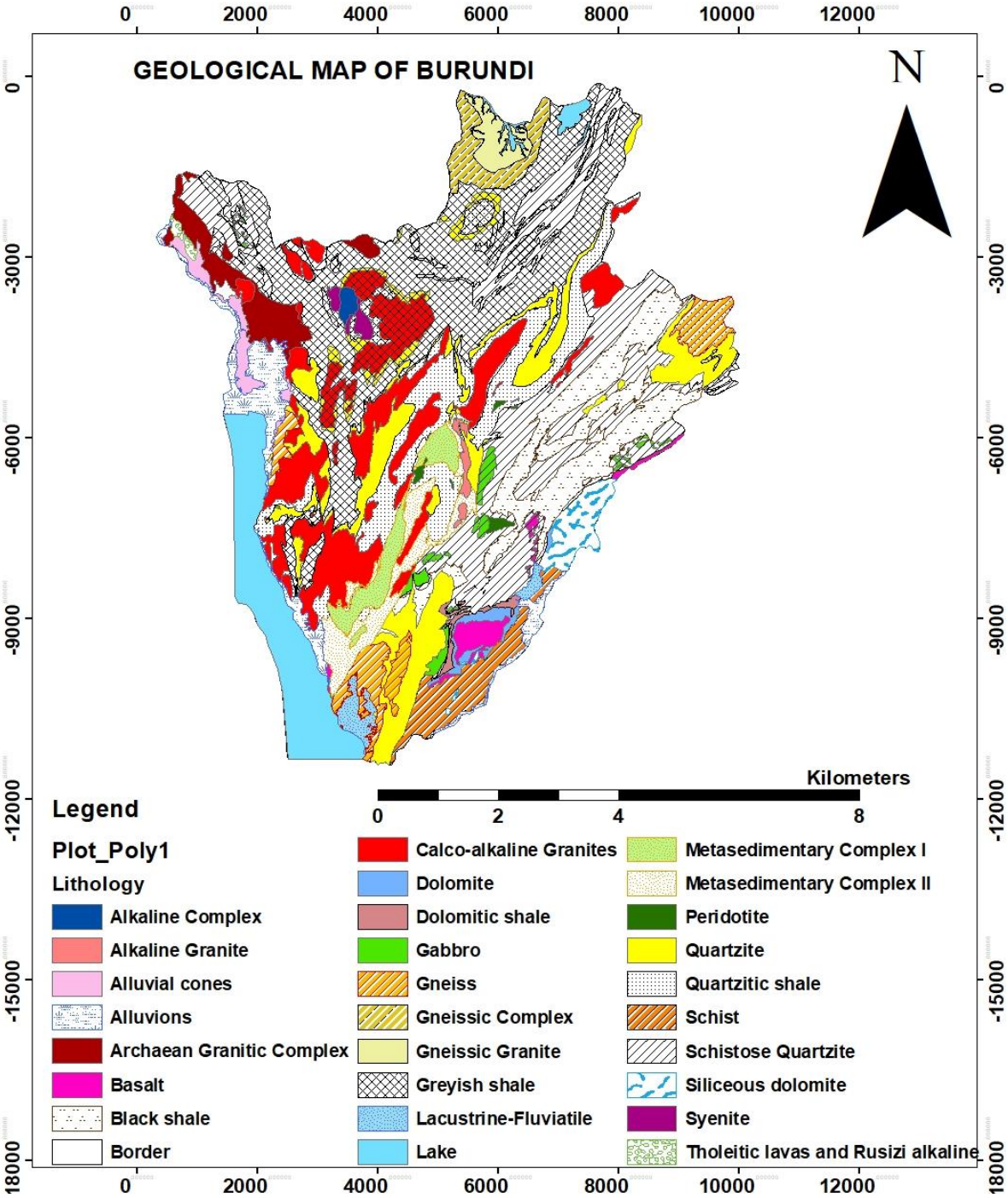

Figure 2. 2 Geological Map of Burundi (Nahimana, 2008 modified from the Ministry of Energy and Mines and RMCA, 1990).

Runyankezi is composed of Mesoproterozoic and Cenozoic rocks deposits. Cenozoic deposits are located in the valley and low lands between high hills.

Rocks belonging to the Upper Burundian Group (Mesoproterozoic) have many deformation faults caused by different intrusions of granites and basic rocks as it is stipulated above. These rocks are composed of metasedimentary rocks and intrusive rocks essentially composed of granites, pegmatites and basic rocks points, where some pegmatites are directly associated with granites case of Marangara while other pegmatites intruded existing rocks as independent igneous rocks, case of Ntega (Buvykana site). The direction, the slope of foliation and stratification vary between 20° and 87°.

2.3 GEOLOGY OF NORTHERN BURUNDI

Northern Burundi consists of sedimentary rocks that are deposits of a shallow marine area of the Karagwe-Ankole-Burundian geo-synclines. These rocks fall into three categories, namely:

2.3.1 The Lower Burundian with a thickness of about 7000m

The lower Burundian begins above the crystalline basement (Archean basement) with quartzites, in which conglomerates are interspersed, intersecting stratifications and ripple marks are frequently observed. In the Upper part of this quartzite and sandstone formation, intercalations of tufa and volcanic breccia are found. These sandstones and quartzites are surmounted by pelitic sediments, which are by far the thickest part of the lower Burundian. Between these phyllites or shales are interbedded sandstones of 10 to 100m of thick (Brinckmann et., 1986 and 1987).

2.3.2 The Middle Burundian with a thickness of about 2500m

This consists mainly of sandstone sediments. At the base of which, there is an important formation of fine-grained quartzitic sandstones with interlocking stratifications and ripple-marks; shales and schistose sandstone succeed and sometimes include interbedded quartzites (Brinckmann et al., 1986 and 1987). There are also basic volcanic intercalations at the base and acidic at the top.

2.3.3 Upper Burundian about 1350m thick:

The upper Burundian refers to coarse clastic sediments composed of quartzites, poorly graded quartzitic conglomerates and sandstone shales; in the west (NW of Burundi), with dolomitic intercalations in clastic deposits (Brinckmann et al., 1986 and 1987).

2.4 METAMORPHISM OF BURUNDIAN SEDIMENTS

The Burundian sediments, totalling about 10,000 m in thickness, have undergone regional metamorphism, from east to west. Old members are more metamorphosed than newer ones. The eastern part has arch-metamorphic rocks (Claessens and Dreesen, 1983, and field observations) while to the west (NW of Burundi), the important pelitic formations of the Burundian have undergone stronger regional metamorphism and have rocks like phyllites or garnet and muscovite schists (Theunissen, 1979). Following numerous intrusions of granitic generations, these sediments have partially undergone contact metamorphism to a very high degree (Theunissen, 1979). This overprint of contact metamorphism is manifested by the formation of staurolite and biotite. His age is that of granitic intrusions.

2.5 DEFORMATION AND FOLDING OF BURUNDIAN FORMATIONS

The Karagwe-ankole belt in Burundi shows folded structures, in eastern Burundi, a generally supra-regional NE-SW orientation is observed, and while in the NW of Burundi a clear NW-SE trend is observed. Aberrant orientations occur locally in the area of crystalline basement projections (Theunissen and Klerkx, 1980), this is the example that occurs between Kayanza and Ngozi in an EW orientation, the Ntega-Marangara circular structure**,** and the Nyambuye structure (in both cases a circular orientation around an ellipsoidal projection).

The main phase of deformation (F2) of the Karagwe-Ankole part of the entire Kibarian orogeny is preceded by a phase characterized by horizontal movements (F1). It resulted in mylonitization in the base contact zone and schistosity parallel to the bedding of Burundian sediments (Brinckmann and, 1986 and 1987, and Brinckmann et al., 2001). And this occurred around 1300 Ma and is characterized by open folds caused by different granitic intrusions evoking an overlapping tectonic regime (Deblond, 1993). The formation of faults occurred around 1275 Ma and is followed by an intrusion of stratified mafic rocks, forming an alignment of nearly 400km long in eastern Burundi (Pohl, 1994). Another phase of deformation (F3) occurs around 950 Ma when the tin granite, in other words, late granites, is put in place and is manifested by a steep tectonic regime characterized by tight isoclinal folding (Brinckmann et al., 2001). It has produced N-S oriented narrow shear zones in western Burundi, intersecting the NE-SW folded structures of the (F2) phase (Theunissen and Klerkx, 1980) (Geological map of Burundi).

2.6 THE AGE OF OROGENY AND MAGMATISM OF BURUNDIAN

The chronological sequence of the Orogeny and Magmatism of the Kibarian belt has been established on the basis of a series of radiometric dates made on rocks from Shaba, Rwanda, Burundi and Uganda (Cahen et al., 1984). In the case of Burundi, two dates on the basement have been made; this one constitutes the bedrock of Burundian sediments:

- Ledent (1979): performs U / Pb measurements on two zircon fractions as well as Rb / Sr measurements on the total Mugera granitoid gneiss rock. From there, U / Pb gave an age of 2611 Ma, while Rb / Sr provided an isochron of 2703 Ma.
- Demaffe and Theunissen (1979): provided U / PB dating measurements obtained on zircons and Rb / Sr measurements on the total rock of two types of gneiss of the Kikuka complex (Nyanza-Lac). The U / Pb measurements gave an age of 2504 ± 82 Ma, while the Rb / Sr measurements gave an age of 2600 Ma. The same exercises were carried out on ribbonized gneiss, during which the U / Pb measurements given an age of 2601 Ma at the time the Rb / Sr measurements provided an age of 2600 Ma.

The magmatism of the Burundian orogeny has been investigated by radiometric dating done on a group of syn-kinematic (syn-orogenic) granites, which is located in Shaba, Kivu, Rwanda, Burundi and Uganda. It is one of the oldest elements of Burundian magmatism and is found in two types of granite, including type A (G1) and type B (G2) (Cahen et al., 1984).

The G1 type is composed of porphyroid adamellites while the G2 type, which is well developed in the Shaba and Uganda regions, is found in biotite and muscovite granite, often with a marked gneissic texture.

For regions where the two types of granite are in association, G1 constitutes the core of the intrusive bodies, while the G2 type occupies the outer zones of the pluton having undergone stronger tectonic stress.

Granite G1 was assigned an age of 1331 ± 50 Ma at Shaba or 1370 ± 25 Ma at Rwanda and Burundi (Cahen and Theunissen, 1980, Ledent, 1979), while the same authors gave G2 granitesq an age of 1310 ± 25 Ma. This age was considered as an age of re-homogenization, which is the date of the main deformation phase in Shaba and respectively in Rwanda and Burundi thus corresponding to the establishment of intrusions.

In addition to the syn-orogenic granites, post-orogenic granites are subdivided into G3 and G4 granites. G3 is known as alkaline granite and is geochemically differentiated from the

more recent G4 tin granites. (Liegeois, 1984) suggests that the tin granites are of anatectic origin while those of G3 is of mantle origin. The G3 and G4 type granites have been attributed to age by different authors.

Alkaline granites of Kamonyi (Rwanda) were assigned an Rb / SR age of the whole rock of 1094 ± 50 Ma by Gérard and Ledent (1979) while those of Makebuko and Bururi were attributed an Rb / Sr age of the whole rock of 1125 ± 32 Ma and 1095 ± 111 Ma respectively (Liegeois, 1984). Cahen and Ledent (1979) and Cahen et al. (1984) assigned an age of 976 ± 10 Ma to G4 granites based on a series of Shaba and Rwanda dates.

2.7 GLOBAL OVERVIEW ON 3Ts

Most of the time, Niobium, Tantalum, and Tin are found mixed in the same localities or rocks except Tungsten. Tin is one of the earliest known metals among 3Ts metals, because of his use in Bronze implements as early as 3500 before Christ (BC) but the pure metal was not used until 600 BC (Kinnaird et al., 2016).

In Africa the production of Tin rose since the 1900s when the settlers promoted the mining activities and after, governments started controlling those activities. The main producers of Tin in Africa during that period were DRC, Rwanda, Burundi, Nigeria, Somaliland, Zimbabwe, and South Africa. The production of Tin in Africa decreased in 2012, about 26% related to that of 2011. In 2014, the total production was around 127,500T (USGS, 2015).

2.7.1 Geology and Occurrence of Tin

The main and commercial ore of tin is cassiterite (SnO_2), but additionally, minerals such as stannite, nigerite or Wodginite are recognized. Deposits occurred in the various style that includes disseminated and stockworks in granite cupolas, lode-style mineralization which occurred as endogranitic or exogranitic veins and that is the case of Namibia, Nigeria, Morocco, Rwanda and Somaliland, rare-metal pegmatites all over Africa over several epochs, quartz veins not associated with granites, and finally eluvial and alluvial deposits which have had huge economic viability (Kinnaird et al., 1985 and Kinnaird et al., 2016).

The enrichment and occurrence of tin in Africa have five episodes which range from Archaean pre-cambrian 2500 Ma to Mesozoic *ca.* 190 to 141 Ma (Kinnaird et al., 2016).

The Archaean deposits are found in Man Shield in West Africa, the Congo Craton, the Zimbabwe Craton, and the Kaapvaal Craton. In contrast, the Paleoproterozoic deposits are located in Birimian Province in West Africa, the Ubendian belt in Central Africa and the

Bushveld Complex in South Africa. The early Neoproterozoic (1000 to 900 Ma) deposits are known in the Kibaran Belt of Central Africa where the late Neoproterozoic to Pan-African Paleozoic belts (600 to 500 Ma) which involve the amalgamation of Gondwana and are found in most areas of Africa, with late to post tectonic intrusions of granites, pegmatites, and mineralized veins which took place around 500 to 490 Ma (Kinnaird et al., 2016).

These deposits of rare metals mineralizations associated with those intrusive rocks are mainly found in the Nubian Shield, in Ethiopia, Somalia, Sudan, Saudi, Arabia and Egypt and on the West African shield in Nigeria, in Kibaran Belt in Burundi, Rwanda, and DRC; in the Mozambique Belt of eastern Africa and the Damara Belt in Namibia. Mesozoic deposits are also known in alkaline ring complexes of the Jos Plateau in Nigeria, which form part of Niger-Nigeria complexes which date ranging from Ordovician to Jurassic (Kinnaird et al., 1985 and Kinnaird et al., 2016). The Pleistocene to Recent deposits are known. They are alluvial concentrations derived from existing mineralization which are hosted in granites and pegmatites and these occur particularly in Nigeria and the Democratic Republic of Congo.

2.7.2 Geology and Occurrence of Tungsten

2.7.2.1 Properties of Tungsten

Tungsten is a High Field Strengh Element (HFSE) is known to be dense, corrosion-resistant metal with the highest melting point among metals, hardest when combined with other metals or with carbon. Those properties make Tungsten to be considered and used by industrialized countries in metal-cutting, oil-well-drilling tools, and in specialized high-temperature items and alloys for the aerospace industry (Sinclair, 1986) .

Tungsten is recovered from two principals minerals such as Scheelite ($CaWO_4$) known as “white ore” and Wolframite ($(Fe, Mn)WO_4$), commonly known as “black ore” where the pure Scheelite contains 63.9% of tungsten by weight. In contrast, the composition of wolframite ranges from the iron-rich variety, ferberite with 60.5% of tungsten to the manganese-rich variety, huebnerite with 60.8% of tungsten. Tungsten can be substituted by molybdenum up to2.0% in Scheelite and 0.1% in wolframite (Antony et al., 2014).

2.7.2.2 Age and Types of Tungsten deposits

Tungsten deposits can be classified into seven types according to their geological accommodation, and in two groups on the basis of their interest and production (Antony et al., 2014 and Sinclair, 1986). Deposits can be in the vein (stockwork), skarn, porphyry, strata-bound, disseminated, placer, and brine (evaporite). In addition to those, pegmatite, breccia,

pipe, and hot spring deposits are added but with minor interest. Most of the production of tungsten is from vein (stockwork), skarn, porphyry, and strata-bound deposits followed by disseminated, pegmatite, breccia, and placer deposits. Brine evaporite deposits host significant content of tungsten, but those deposits are still unexploited (Antony et al., 2014).

Table 2. 1 Major types of Tungsten deposits, with their Geological environment (Sinclair, 1986).

Type of deposits	Geological setting and mineral composition	Potential production
Vein/stockwork deposits	These deposits typically consist of tungsten-bearing quartz veins or vein stockworks that occur in or near granitic intrusions. Wolframite is commonly the principal tungsten mineral; scheelite is important in some deposits. Tin, copper, molybdenum, and bismuth minerals are also present in some vein/stockwork tungsten deposits and may be economically important.	more than 50 percent of world tungsten production
Skarn deposits	Assemblage of calcium-iron-magnesium-aluminum-silicate minerals that have developed in carbonate-bearing rocks at or near contacts with granitic intrusions. Scheelite is the principal tungsten mineral in skarn deposits and occurs both as disseminated grains and in veinlets or fractures. Copper, molybdenum, and bismuth minerals are also present and may be economically recoverable.	30 percent of world tungsten production
Porphyry deposits	Consist of large, equidimensional to irregular stockwork zones of tungsten-bearing veins, veinlets, and fractures that occur in or near epizonal to subvolcanic felsic granitic intrusions. Mineralized breccia zones, either irregular or pipe shaped, may also be present. Tungsten occurs as wolframite or scheelite, and in some deposits both minerals may be present. Molybdenum is commonly present in porphyry tungsten deposits and may represent a viable coproduct or byproduct.	6 percent of world tungsten production
Strata-bound deposits	"strata-bound" refers to deposits in which the distribution of tungsten minerals is strongly controlled by bedding in the host rocks and for which a syngenetic origin may be inferred	less than 5 percent of world tungsten production.
Disseminated deposits	Most disseminated deposits consist of tungsten minerals disseminated in altered (greisenized) granite. Tungsten generally occurs as wolframite; scheelite may be important in some deposits	less than 1 percent of total world tungsten production
Placer deposits	Placer deposits consist of sedimentary concentrations of scheelite or wolframite in alluvial, eluvial, and, in some cases, marine sediments. Scheelite and even wolframite will eventually decompose upon weathering and hence, unlike cassiterite, tungsten minerals tend not to be preserved long	-

	enough to form widespread sedimentary deposits	
Brine/evaporite deposits	Tungsten-bearing brines and evaporites occur in arid regions	-
Pegmatite deposits	Tungsten is not a common constituent of pegmatites, and significant pegmatite deposits of tungsten are rare.	-
Pipe deposits	Pipe deposits range from almost perfectly cylindrical to irregular, elongated, bulbous masses of quartz that occur in the margins of granitic intrusions	-
Hot spring deposits	Tungsten occurs in hot spring deposits of calcareous tuffs or travertine. Hot spring deposits are commonly associated with bedrock tungsten deposits, from which they were probably derived by circulating hot ground water	-

Veins/stockworks deposits of tungsten are represented in every period. In contrast, skarn deposits are Proterozoic or younger, porphyry deposits are Paleozoic or younger, and strata-bound deposits are either Proterozoic or Paleozoic in age (Sinclair, 1986). The most significant production of tungsten resources is Mesozoic in age. Most of the tungsten deposits occur at a proximity of orogenic belts (Antony et al., 2014).

2.7.3 Geology and Occurrence of Nb and Ta

The abundance of Niobium and Tantalum varies according to the type of rock under consideration, and involves magmatic niobium and tantalum deposits and sedimentary niobium and tantalum deposits. Rocks associated with niobium and tantalum range in age from Precambrian to Mesozoic. Almost the total of the oxide minerals of Nb and Ta occurs in granitic rocks of orogenic affiliation, particularly in rare-element granitic pegmatites. In contrast, some are found in an orogenic alkaline igneous sequence from carbonatites and gabbros to nepheline syenites and alkaline granites. Hence, all silicates of Nb (±Ta) and (Nb, Ta)-bearing titano-silicates and zircon-silicates are related to the orogenic parageneses (Tarek, 2016).

Niobium is primarily derived from the complex oxide minerals of the pyrochlore group ($(Na,Ca,Ce)_2$ $(Nb,Ti,Ta)_2$ $(O,OH,F)_7$), which are found in some alkaline granite-syenite complexes (igneous rocks containing sodium- or potassium-rich minerals and little or no quartz) and carbonatites (igneous rocks that are more than 50 per cent composed of primary carbonate minerals). Tantalum is derived mostly from the mineral tantalite ($(Fe, Mn)(Ta,Nb)_2O_6$), which is found as an accessory mineral in rare-metal granites and pegmatites that are

also enriched in lithium and caesium (termed lithium-caesium-tantalum (LCT)-type pegmatites) (Stepanov et al., 2014).

2.7.4 Igneous rocks hosting Nb and Ta

Primary niobium and tantalum mineral deposits are found in three main types of intrusive igneous rocks (Küster and Derik, 2009, Černý and Ercit, 2005 and Schulz et al., 2017):

1. Carbonatites and associated alkaline rocks (Nb dominant).
2. Alkaline to peralkaline granites and syenites (Nb dominant), and
3. Rare-metal granites and rare-element-pegmatites of the lithium, caesium-tantalum (LCT) family where Ta dominant.

Besides, some secondary concentrations have been formed by weathering of primary deposits (laterites) and by sedimentary processes (placers).

Niobium and tantalum occur in different concentration within igneous rocks, Niobium is found in high concentration in alkali rocks, such as nepheline syenite, syenite and feldspathoidal rocks, and in alkali mafic and ultramafic rocks, and also shows a high concentration in sodic or alkali granite. In this groups lastly cited, most niobium is usually hosted in nepheline syenite and alkalic rocks (Černý and Ercit, 2005). In these rocks, otherwise, tantalum accompanies niobium.

2.7.5 Concentration of Nb and Ta in Sedimentary rocks

The enrichment of Nb and Ta deposits in the surficial and supergene environment is mainly based on the chemical decomposition of existing mineralized sources in humid environmental conditions as in case of formation of lateritic ore deposits (Tarek, 2016).

Considerable contents of niobium are found in deep-sea manganese modules and sediments and bauxites whereas tantalum contents are found in marine clays and bauxite. Because of the chemically resistant nature, high specific gravity, and hardness of some of the common niobium-tantalum minerals, as well as the similar nature of some common minerals of titanium and zirconium, these minerals commonly are locally enriched in sandstones and conglomerates.

Niobium and Tantalum placer deposits are formed by the mechanical disintegration and chemical decomposition of existing rocks hosting minerals bearing those metals like alkaline rocks, carbonatites, pegmatites and granitic rocks containing Nb and Ta mineralization and exposed to different weathering agents such chemical or physical agents (Skinner, 2005).

Table 2. 2 Major types of niobium and tantalum deposits, with key characteristics and examples. Modified from the British Geological Survey (2011).

Deposit Type	Descriptions	Grades and tonnage	Examples
Carbonatite-hosted primary deposits	Nb>Ta: Niobium deposits commonly consisting of members of the perovskite and pyrochlore mineral groups found within carbonatite intrusions in alkaline igneous provinces	Deposits show a wide range in both grade and tonnage. Morro dos Seis Lagos is the largest reported deposit; it contains about 2,900 Mt at a grade of 2.85 percent Nb_2O_5. More typical is the deposit at Niobec, which contains about 46 Mt at a grade of 0.53 percent Nb_2O_5	Niobec and Oka, Canada, Araxá, Catalão I and II, and Morro dos Seis Lagos, Brazil
Alkaline granite and syenite	Nb>Ta: Deposits containing niobium and lesser amounts of tantalum; the deposits are related to silicic alkaline granite and syenite igneous intrusions	Generally <1,000 Mt at grades of 0.1 to 1 percent Nb2O5 and <0.05 percent Ta_2O_5	Motzfeldt and Ilímaussaq, Greenland; Lovozero, Russia; Thor Lake and Strange Lake, Canada
Rare-metal granite	Ta>Nb: Deposits containing tantalum and lesser amounts of niobium; the deposits are generally found in the uppermost parts of peraluminous and (commonly) hydrothermally altered late-stage granitic plutons	Generally <100 Mt at grades of <0.05 Ta_2O_5	Yichun, China; Abu Dabbab and Nuweibi, Egypt
LCT-type pegmatite	Ta>Nb: Deposits containing tantalum and lesser amounts of niobium; the deposits are LCT-enriched-type pegmatites	Generally <100 Mt at grades of <0.05 Ta_2O_5	Greenbushes and Wodgina, Australia; Tanco, Canada; Volta Grande, Brazil; Kenticha, Ethiopia
Secondary (regolith) deposits	Niobium and (or) tantalum ore minerals concentrated in zones of intense weathering above carbonatite and granite or pegmatite intrusions, or in sedimentary placer deposits derived from such intrusions	Lateritic deposits generally have <1,000 Mt at grades of up to 3 percent Nb_2O_5. Placer deposits, such as the deposit at Tomtor, can have very high grades of up to 12 percent Nb_2O_5	Araxá and Catalão, Brazil; Tomtor, Russia; Greenbushes, Australia

2.7.6 Geochemistry of Nb and Ta

Niobium (Nb) and Tantalum (Ta) are usually associated in nature. They are the two essential rare-metal accessories in granite-pegmatites, forming a large number of transported minerals and are major constituents in the mineral columbite-tantalite (Schulz et al., 2017).

In additional to granite-pegmatite, these elements are also prominent in some alkali granite, alkaline complexes proper-nepheline syenites and nepheline syenite pegmatites and in numerous carbonatites. The rate of Niobium and Tantalum differs from one type of rock to another and from mineral one another, with a large concentration of Nb-Ta minerals in granite pegmatites rocks. That preponderance of one element over the other occurs in certain types of rocks such as nepheline syenites (niobium-rich) and lithium-bearing pegmatites (tantalum-rich) or in some rocks modified by metasomatic processes. In nature those elements consist entirely of single isotopes, Niobium has one isotope Nb^{93},and Tantalum has two isotopes, Ta^{181} and Ta^{180}, but the last accounts for only 0.01% of the element (Parker and Fleischer, 1968).

These elements form a pair of aspects with strong geochemical coherence; they are closely associated and found together in most rocks and minerals in which they occur both are lithophile and show a strong affinity for oxygen. They are high-field-strength elements (HFSEs); their ions are relatively small and have intense electrostatic fields (Schulz et al. 2017).

Their potential to substitute for more common elements in most rock-forming minerals is reduced by their HFSE characteristics. It makes them virtually immobile under most natural conditions which lead to a low concentration of those elements in the surface environment (Wood, 2005 and Schulz et al. 2017).

The reason of this coherence is the similar ionic radii and the same valance states and similar ionic radii of the two elements, Nb^{+5} = 0.69 A° and Ta^{+5} = 0.68 A°, which make fundamental parameters controlling the accommodation of an element into crystal structures (Parker and Fleischer, 1968).

Columbite (Fe, Mn)(Nb, $Ta)_2O_6$ is the most typical member of the Nb-Ta minerals in pegmatites with Niobium (Nb) predominant over the Tantalum, as it is shown in his chemical formula, it can be Manganocolumbite (Mn,Fe)$(Nb,Ta)_2O_6$ with a high proportion of Manganese or Ferrocolumbite (Fe, Mn)$(Nb,Ta)_2O_6$ with a high percentage of Iron-Tantalite

$(Fe,Mn)(Ta,Nb)_2O_6$ this includes rare members of the columbite-tantalite series with Ta predominating over Nb (Stepanov et al., 2014).

Manganocolumbite is a typical mineral of the Li-rich pegmatites. It is found as black, tabular, striated crystals, with vitreous to submetallic lustre and yellowish-green to dark brown streak. In contrast, Ferrocolumbite is a rather rare mineral occurring mostly in non-Li pegmatites or in Li-free units of Li-pegmatites. It is found as black, platy crystals with a submetallic lustre and has a reddish-brown streak.

Manganotantalite $(Mn,Fe)(Ta,Nb)_2O_6$ members of the columbite-tantalite series with Ta and Mn in excess of Nb and Fe have been classified as manganotantalites. They are more widespread than the tantalites and may be regarded as the type of minerals of Ta mineralization in the highly fractionated Li pegmatites. This type contains minerals such as:

- Tapiolite (Fe) (Ta, $Nb)_2O_6$ generally occurring in Li-poor pegmatites. Still, in places, it is closely associated with the Li pegmatites, although it may occur in the Li-poor units of these pegmatites.
- Microlite $(Ca,Na,U)_2(Ta,Nb,Ti)_2(O,OH,F)_7$, is an important source of Ta and is closely associated with Li-pegmatites.
- Wodginite, $(Ta,Nb,Sn,Mn,Fe)_{16}O_{32}$ This rather rare Ta mineral is usually found in a cleavelandite-muscovite unit marginal to the quartz core in a pegmatite.

Table 2. 3 Major minerals of Nb-Ta (British Geologic survey, 2011)

Mineral name	Mineral group	Formula	Nb_2O_5 (%)	Ta_2O_5 (%)
Columbite	Columbite-tantalite	$(Fe,Mn)(Nb,Ta)_2O_6$	78.72	n.a.
Tantalite	Columbite-tantalite	$(Fe,Mn)(Ta,Nb)_2O_6$	n.a.	86.17
Pyrochlore	Pyrochlore	$(Na,Ca)_2Nb_2O_6(O,OH,F)$	75.12	n.a.
Microlite	Pyrochlore	$(Na,Ca)_2Ta_2O_6(O,OH,F)$	n.a.	83.53
Tapiolite	Tapiolite	$(Fe,Mn)\ (Ta,Nb)_2O_6$	1.33	83.96
Ixiolite	Ixiolite	$(Ta,Nb,Sn,Mn,Fe)_4O_8$	8.30	68.96
Wodginite	Wodginite	$(Ta,Nb,Sn,Mn,Fe)O_2$	8.37	69.58
Loparite	Perovskite	$(Ce,La,Na,Ca,Sr)(Ti,Nb)O_3$	16.15	n.a.
Lueshite	Perovskite	$NaNbO_3$	81.09	n.a.
Euxenite	Euxenite	$(Y,Ca,Ce,U,Th)(Nb,Ti,Ta)_2$	47.43	22.53
Struverite	Rutile	$(Ti,Ta,Fe)O_2$	11.32	37.65
Ilmenorutile	Rutile	$Fex(Nb,Ta)_{2x4}Ti1\text{-}xO_2$	27.9	n.a.

2.7.7 The behaviour and formation of Nb-Ta during magma crystallization

The magmatic-hydrothermal transition in granitic systems separates a purely magmatic system dominated by a crystal-melt interaction from a system dominated by a crystal-melt-magmatic fluid phase interaction. From these hydrothermal activities, result pegmatites or quartz veins, or, pervasive, leading to significant element mobility and to the formation of greisen (Pirajno., 2013 and Ballouard et al., 2016). These hydrothermal alterations occur during the sub-solidus stage of granitic magma emplacement, and most of the cases lead to the formation of economic mineralization such as Tin (Sn) and Tungsten (W).

In granites and pegmatites rocks, Nb and Ta are mainly hosted by Columbite and Tantalite minerals. Temperature is the major condition to control the solubility of these minerals in the presence of granitic melt, that increases with the temperature but decrease as the aluminium saturation index (ASI) increases (Stepanov et al., 2014). At high-temperature, in the case of lithospheric granites (anatexis) Nb/Ta ratios is high in melts, and that reflect the complete consumption of biotite and the high abundance of titanium (Ti)-bearing oxides in the residue leading to the incorporation of Ta over Nb. In contrast, the rations decrease with low-temperature partial melt because residual biotite preferentially incorporates Nb over Ta.

The crystallization of Ti-bearing oxides (rutile, titanite and ilmenite) decreases Ti content and Ta/Nb of the melts, in other words, the consummation of Ti yields the formation of Nb over Ta and lead to the enrichment of Nb in the melt. Still, in some cases, magnetite can reduce Ti content without fractionating Nb and Ta, amphibole produces mild Ta/Nb fractionation, but leaves Ti in the melt (Stepanov and Hermann, 2013). Besides, the fractionation of the biotite and the muscovite increases the Ta/Nb ratio and decreases Ti content in the melt.

Niobium and tantalum are present in the lattice of the micas in isomorphous substitution for titanium and aluminium (Parker and Fleischer, 1968). For preserving electrostatic equilibrium, niobium and tantalum substitute for titanium with simultaneous substitution of lithium in biotite:

$Mg^{+2}+Ti^{+4}<=>Li^{+1}+(Nb,Ta)^{+5}$

But with muscovite which contains minor titanium that substitution in the mineral occurs between aluminium and lithium, niobium, and tantalum:

$2Al^{+3}<=>Li^{+1}+(Nb,Ta)^{+5}$

2.7.8 Primary and secondary resources of Nb-Ta for industries

2.7.8.1 Primary resources

It is known and common to find tantalum and niobium together in the same type of mineral deposits or the mineral of similar characteristics. They are usually found in solid solutions, and that is the case of columbite-tantalite represented by the formula $((Fe,Mg,Mn)(Nb,Ta)_2O_6$, or minerals from the pyrochlore group. Commonly Niobium/Tantalum is extracted from mineral deposits associated with specific igneous rocks (Bourgeois et al., 2017). The weathering of these deposit types can result in other kinds of niobium-tantalum mineral deposits such as laterites concentrating pyrochlore, and alluvial deposits (Placers).

2.7.8.2 Secondary resources

In the secondary stage, niobium can be extracted as a by-product of tin smelter waste or extracted from sludge, from the cemented carbide tool industry or mill scrap from alloyed and unalloyed metal fabrication and scrap from industrial alloys and superalloys. According to end-of-life products, Niobium is found in electronic waste equipment, vehicles and mostly in steels (Bourgeois et al., 2017).

Tantalum also can be extracted as a by-product of Tin smelter waste. That smelter waste typically contains 8 to 10 per cent Tantalum oxide but can be as high as 30%. Low-grade smelter waste can be upgraded by electrothermic reduction yielding a synthetic concentrate with up to 50% Tantalum and Niobium (Bourgeois et al., 2017).

2.7.9 Use of Niobium and Tantalum

Niobium and Tantalum are rare metals and constitute only about 20% and 1.7 parts per million, of the material contained within the earth's crust (Richard et al., 1993). The crustal abundance of Niobium is higher than that of lead and Tin, and even tantalum is present at a geochemical concentration that is comparable to that of Tin.

2.7.9.1 Use of Niobium

Niobium is principally used as an alloying element in high-strength low-alloy (HSLA) steels and superalloys; the leading use of Niobium is in ferrous metallurgy. The steel industry uses about 75 per cent of world niobium production for the production of a variety of steel alloys that contain small amounts of other metals to improve corrosion resistance strength,

toughness, and other properties such as mechanical strength and high-temperature strength (Schulz et al., 2017). Manufactured steels are used in pipelines, transportation, and

structural applications. The HSLA steels are currently used in oil and gas pipeline steels, in lighter and more fuel-efficient automobile, and significant contraction such as skyscraper bridge and nuclear reactors. Niobium is also used as a carbide stabilizer in stainless steels to improve their resistance to corrosion when used in exhaust manifolds, firewalls, and pressure vessels (Richard et al., 1993). In addition to those applications, niobium is contained in cobalt, nickel, and iron-base superalloys used for high-temperature applications such as jet engine components, gas turbines, rocket subassemblies, turbocharger systems, and heat-resisting and combustion equipment. These can be extended to the manufacturing of superconducting magnets used in Magnetic Resonance Imaging (MRI) and Nuclear Magnetic Resonance Instruments (NMRI) (Schulz et al., 2017).

2.7.9.2 Use of Tantalum

The principal use of Tantalum is in electronics industries that include rectifiers, amplifiers, oscillators, controls, signal devices, alarm systems, and timing devices in which the ability of tantalum to conduct alternating current in only one direction and the high electrical resistance of some tantalum alloys are utilized (Schulz et al., 2017). It is also used in aerospace and other transportation applications, because of its high melting point of 2,996°C, strength at elevated temperatures, and corrosion resistance, is combined with cobalt, iron, and nickel to produce refractory superalloys (Richard et al., 1993).

2.7.10 Processing and Mining of Nb-Ta

2.7.10.1 Mining

Mining is a set of techniques for extracting ores from their accommodation or where they are located. That takes in consideration several factors such as size and grade of the ore the depth and distribution of the ore minerals (disseminated or concentrated) and the geotechnical properties of the rock to determine the type of mining method which is adequate for a given ore deposit. It may be open-pit or underground (Bourgeois et al., 2017). Almost all mines in carbonatites and other steeply-dipping intrusive rock structures are mined in open pits whereas underground mining is restricted to deep deposits mainly in pegmatitic ores. It is essential to know that primary minerals involve blasting and crushing, while secondary minerals require excavation.

2.7.10.2 Processing

Processing consists of a combination of several operations including crushing (jaw, cone or impact crusher), Grinding (ball or rod milling) and classification (screens and hydrocyclones) in closed circuit, conventional (jig, shaking table), centrifugal (spiral) and enhanced gravity separation (MGS, Falcon concentrator) depending on the size of liberated particles, selective reverse flotation to concentrate the finest material, normally at controlled pH, regular and high magnetic separation to remove companion magnetic phase, and thickening circuit to recycle the process water (Bourgeois et al., 2017).

The niobium producers process the ore to make ferroniobium (FeNb) or niobium pentoxide (Nb_2O_5), which is then shipped to consumers. Others ship niobium mineral concentrates to processing companies. The ore is crushed, beneficiated by flotation and magnetic separation for iron minerals removal to produce a pyrochlore $(Na,Ca)_2Nb_2O_6(O,OH,F)$ mineral concentrate grading 55 to 60 percent of Nb_2O_5 (Schulz et al., 2017).

Gravity and flotation are main methods that are used to separate heavy minerals that contain tantalum from the bulk ore. The concentrate is then subject to electrical (electrostatic and/or electromagnetic) separation and other methods used to separate tantalum minerals from other heavy minerals.

After a breakdown treatment which includes operation such as reduction, chlorination, alkaline fusion and leaching, the obtained mixed oxides of tantalum ($Ta_2O_{5)}$ and niobium (Nb_2O_5) are subjected to chemical processing step (Olushola and Folahan, 2011).
First of all is the reaction between oxides and hydrofluoric acid (HF) but H_2SO_4 can be used, the reactions are as following:

$Ta_2O_5 + 14\ HF \rightarrow 2H_2(TaF_7) + 5H_2O$

$Nb_2O_5 + 10HF \rightarrow 2H_2(NbOF_5) + 3H_2O$

The following step is the dissolution of dipotassium oxypentafluoroniobate monohydrate ($K_2[NbOF_5]\cdot H_2O$) and dipotassium heptafluorotantalate ($K_2[TaF_7]$) in water. The two are extracted separately from the organic solvent with water, followed bay the addition of potassium fluoride to produce a potassium fluoride complex or precipitated with ammonia as the pentoxide (Olushola and Folahan, 2011):

$2H_2(NbOF_5) + 2HF \rightarrow\ K_2[NbOF_5]\downarrow + 2\ HF$

or

$2H_2[NbOF_5] + 10\ NH_4OH \rightarrow Nb_2O_5\downarrow + 10\ NH_4F + 7\ H_2O$

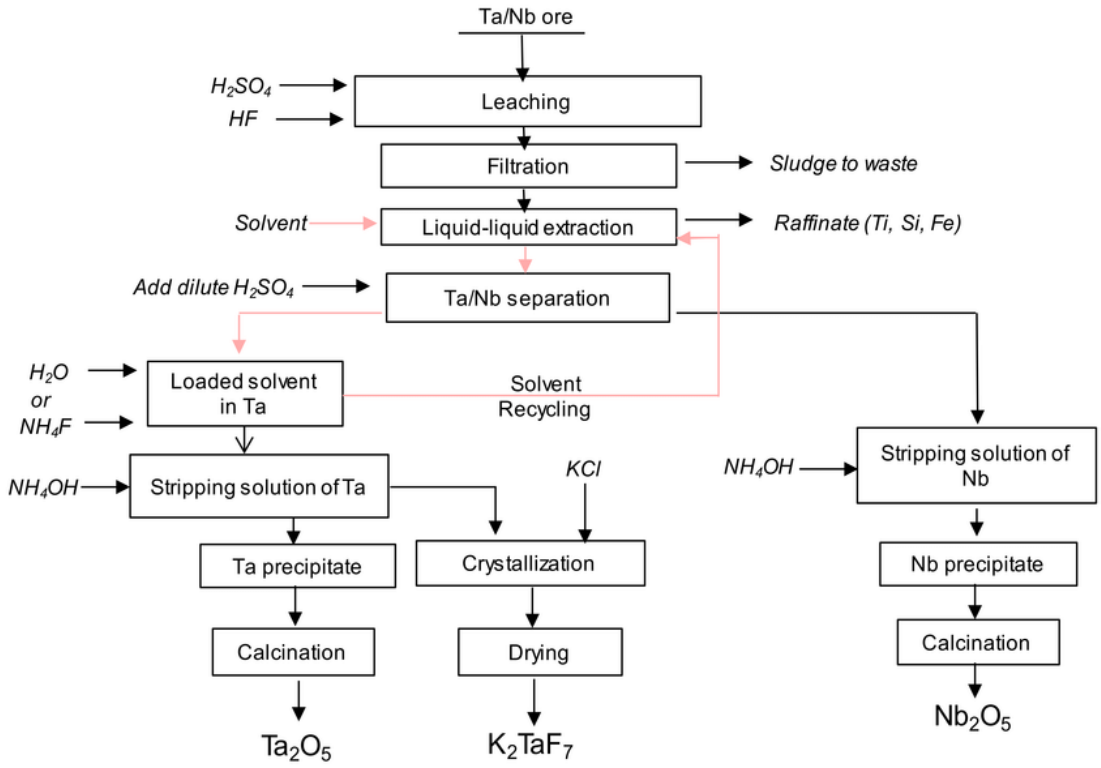

Figure 2. 3 Process scheme for Nb and Ta production (Arrachart et al., 2015)

The tantalum compounds are then subjected to smelting operations to make tantalum metal products (Roskill Information Services Ltd, 2012).

More than a half of all tantalum production in the world consists of tantalite ore $(Fe,Mn)(Ta,Nb)_2O_6$, and the remainder comes from tin slag, from other minerals such as strüverite and columbite-tantalite $(Fe,Mn)(Nb,Ta)_2O_6$ and from recycling and synthetic concentrates (Bourgeois et al., 2017). Historically the global supply of tantalum has been 70 per cent from concentrates, 10 per cent from tin slag, and 20 per cent from recycling and synthetic concentrates (Schwela, 2010).

2.7.11 Reserve of Niobium-Tantalum in the World

The important Niobium resources in the World identified are located predominantly in Brazil with about 95 per cent and Canada with about 3.5 per cent of which we add resources located in Angola, Australia, China, Greenland, Malawi, Russia, South Africa, and United States (Sto-Viruet et al., 2013; British Geological Survey, 2011; Papp, 2013b; and Schulz et al., 2017).

Carbonatites complexes host the largest niobium resources, but resources in alkaline granites or syenite complexes are widespread and large, and they are generally lower in grade than

carbonatite-hosted deposits. The deposits tend to have more complex geology and mineralogy than do carbonatites, which can affect the ease with which the niobium could be recovered (British Geological Survey, 2011; Papp, 2013b).

Resources of tantalum are more widespread than those of niobium. On the top comes Brazil with 106,000 metric tons of tantalum which represent approximately 40 per cent of the World resources. The remaining 60 per cent of identified tantalum resources can be classified in decreasing order of tonnage as follows:

Table 2. 4 World Tantalum producers (Schulz et al., 2017)

Name	**Metrics Tons**
Australia	54,000
China and Southeast Asia	27,000
Russia and the Middle East	26,000
Central Africa	23,000
other Africa	17,500
North America	4,500
Europe	1,900

These tantalum resources are principally associated with large pyrochlore deposits in carbonatite complexes and in pegmatite districts for Brazil, whereas in Australia and United States are principally hosted by LCT-type pegmatites (Schulz et al., 2017).

2.8 MINING ACTIVITY AND ITS EVOLUTION IN BURUNDI

2.8.1 Mining potential in Burundi

Burundi is a small country member of the East African Community located in the north-east of the Kibarian chain in the Karagwe-Ankole segment with an area of approximately of 27,843 km^2. This strategic position, from the regional geology point of view, explains its varied mineral potential. Research carried out in Burundi since the 1960s until today has revealed the existence of mineralized deposits in various mineralizations such as Lateritic and sulphurized nickel, Rare Earth, Iron-Titanium-Vanadium, Group of Columbite minerals, Cassiterite and Wolframite, Platinoids, Gold, Minerals and Industrial Rocks (Phosphates, Carbonatites, Limestones, Kaolin, Feldspar). To these mineralizations are added mineral fuels such as peat, Hydrocarbons and geothermal indices.

Table 2. 5 Mining potential of Burundi (OBM, 2019)

Name of ore	Location	Minimum reserves
Lateritic nickel	Musongati (Rutana)	150 MT
	Nyabikere (Karuzi)	46 MT
	Waga (Gitega)	35 MT
Sulphide nickel	Muremera (Cankuzo)	Not evaluated
	Rutovu-Bukirasazi-Buhoro (Bururi-Gitega)	Cibles intéressantes identifiées
Vanadium	Mukanda (Gitega)	9,7 MT Primary ore 2,1 MT secondary ore
Gold	Provinces Cibitoke,	Under evaluation
	Province Muyinga,	Being evaluated
	Les provinces de Ruyigi, Bururi, Kirundo,Bubanza, Kayanza,	Not evaluated
Cassiterite, Columbite-tantalite, Tungsten	Provinces Cibitoke, Bubanza, Ngozi Kayanza, Muyinga, Kirundo	Not evaluated
Rare earth	Gakara (Bujumbura)	186.000 T but under evaluation to increase reserves
	Minago (Bururi)	but under evaluation
hydrocarbons	Basin of Rusizi Lake Tanganyika Basin	Not evaluated
Phosphates	Matongo (Kayanza)	270.000T
Carbonatite	Matongo (Kayanza)	9,44 MT
Kaolin	Mvumvu (Kayanza) Vyerwa (Ngozi)	2,7 MT 632 MT
Quartzite	Mukinya (Ngozi)	5,13 MT
Feldspars	Kanyaru-Haut (Kayanza)	Not evaluated
Peat	Nyamuswaga (4,3MT), Ndurumu (14,4MT), Buyongwe (20MT), Nyavyamo (17,6MT)	56,3 MT
Limestone	Cibitoke-Busiga (Ngozi)	Not evaluated

2.8.2 History and evolution of the mining activity of rare metals in Burundi

Mining activities began in Burundi in the 1920s and focused primarily on the extraction of tin, niobium-tantalum and alluvial and eluvial gold in northwestern Burundi. One of the many centres of mining activity was at Muhokore and Mulehe for Cassiterite ores. From the 1940s and 1950s, the establishment of small-scale mining in the Kirundo regions was born. The first documents from the Mulehe mine date back to 1948, when the Corem Company began the exploitation of eluvial cassiterite. During this early phase, primary mineral extraction was also undertaken, and the company also owned the Nemba mine in Rwanda. It was located immediately north of Mulehe in Kirundo Province. From the late 1960s until 1978, Sobumines, which had taken over the Mulehe concession, mainly exploited the vein mineralization and undertook extensive tunnelling and other underground mining for this purpose.

Wolframite has been mined at Nyabisaka since the 1950s. There are several small-scale mining operations here, in which primary ore has been excavated from vein outcrops and secondary ore from slope debris. Documents from the 1950s indicate the existence of a small launderette near the Nibenga River. The ore from the Nyabisaka was pre-concentrated by manual sorting and dry sieving and then processed into final concentrate at the Mulehe mine. Alongside these mechanized operations, artisanal cassiterite was also mined in many small mineralized points in northern Burundi; these activities were concentrated in the mountainous region of northwestern Burundi, which produced about 80% of gold and 60% of tin, mainly from alluvial deposits.

According to the Ministry of Public Works, Energy and Mines, until 1984 production was:

3,000 t of cassiterite, 150 t of Wolframite, 56 t Colombo-tantalite, and 6 t of gold

With the advent of Burundi's independence, Belgian companies have gradually withdrawn. After their departure, the organized artisanal mining activity should stop to give way to the uncontrolled exploitation carried out by the craftsmen, without technical supervision and inadequate mining equipment.

Following this anarchic exploitation, the phenomena of environmental degradation, ore fraud, the loss of public revenue and the fall in production followed. As an indication, the table below shows the evolution of artisanal mining production from 1933 to 1979, sixteen years after independence.

Table 2. 6 The production of artisanal mining from 1933 to 1979 (OBM, 2019)

Nature of the ore	Period	Cumulative production in kg	Average per year in kg
Gold	1933-1961	5,324	183.6
	1962-1965	0.5	0.125
	1966-1979	66.4	4.7
Cassiterite	1934-1961	2,465.700	88,060
	1962-1965	106,000	26,500
	1966-1979	985,000	75,770
Columbite-tantalite	1935-1961	82,500	3,056
	1962-1975	Statistics not available	Statistics not available
		11,700	2,930
	1976-1979		
Tungsten	1974-1977	8,430	2,108

After 1979, the Government of Burundi decided to stop the artisanal mining activity for a geological exploration campaign. This campaign started in the early 1980s with the help of German cooperation. The artisanal mining activity resumed during the year 1988 with the COMEBU Company and the 2000s with the counters. The table below shows the evolution of artisanal mining production from 1989 to 2018.

Table 2. 7 Mining production from 1989 to 2018 (OBM, 2019)

year	Gold in kg	Cassiterite in kg	Columbite-tantalite in kg	Tungsten in kg
1989	18.850	103,823	-	-
1990	5217	97,900	-	-
1991	3613	106,090	-	-
1992	5592	182,645	8527	-
1993	6024	71,977	45911	-
1994	2279	-	29166	9558
1995	3819	14,654	42167	27492
1996	2556	23,528	36856	12065
1997	-	20,935	45921	-
1998	-	8,980	30480	-
1999	-	18,408	42149	-
2000	-	9,978	31175	-
2001	415	5,398	122537	-
2002	483	-	72441	-
2003	2854.753	8767	24382	32788
2004	3229.163	18612	23356	23857
2005	3904.6031	8100	25400	294505
2006	4312.5989	78898	16177	668184
2007	2422.7521	50600	51550	443400
2008	2170.2396	96384	116586	560136
2009	979.63393	28250	44523	333207
2010	309.79101	28700	67365.4	336723.1
2011	1051.9267	51844.2	158781.7	505105
2012	2146.85948	116720.2	258578.1	564769.6
2013	2823.23835	3132.2	73518.3	115212.7
2014	649.725	-	105546.7	48909.3
2015	548.50	31757.20	44479.50	77847
2016	396	22243.50	31687.10	131432.00
2017	953.0281	161534.50	74481.40	259768.50
2018	601.705	159249.6	21915.95	194390

2.9 LEGAL FRAMEWORK AND TRANSPARENCY OF THE MINING SECTOR IN BURUNDI

2.9.1 Legal framework of the mining sector in Burundi

To strengthen the mining sector in Burundi and make it legal according to global standards, many reforms have been made mainly in the regulation. The mining sector of Burundi has:

- A Mining Code responding to regional standards since 2013;
- A Mining Regulation dating from June 2015 which is the application text of the Mining Code;
- A Mining Policy document to harmonize mining legislation with the Burundi 2025 vision, the PRSP, the VMA and other regional and international instruments;
- An investment code of Burundi;
- Public-Private Partnership Law (PPP).

2.9.2 Transparency of the mining sector

1. Burundi has officially declared its intention to join the Extractive Industries Transparency Initiative (EITI);
2. The EITI Membership Action Plan has been developed;
3. The EITI National Champion has been decreed;
4. The ore traceability mechanism is operational for coltan, wolfram and cassiterite ores commonly referred to as 3Ts ores;
5. ICGLR certificate

Since 2014, under this legal framework, the artisanal mining activity has changed structure, it has gone from individualization to an organization into cooperatives of national law constituted the people themselves and that to facilitate the traceability of minerals of Coltan, Cassiterites and Wolframite in the first situation. Today, research companies are operational for discovery of exploitable deposits, and there are two for 3Ts including NTega Holding Burundi and Burumine companies.

CHAPTER THREE: MATERIAL AND METHODS

This chapter highlights the materials and methods used in a different stage of research. This work involved both field investigations and laboratory analyses. The acquirement of various data in this research included methods such as geological survey and geochemical survey.

Data collection was carried out in the year 2019 from January to March in Runyankezi area in collaboration with Ntega Holding geologists. Laboratory analyses were done in the ALS Chemex ("ALSC"), an independent and internationally accredited (ISO 17025) laboratory in Johannesburg, South Africa.

3.1 GEOLOGICAL ASSESSMENT

3.1.1 Geological fieldwork

Geological fieldwork was carried out to confirm different lithologies using an existing geological map. It assisted in identifying lithologies hosting 3Ts mineralisations, and various intrusive rocks. During this assessment, vertical stratigraphy was investigated. The vertical investigation aimed to map micro-structures, boundary relationships, and lithology variations (Fig.3.1).

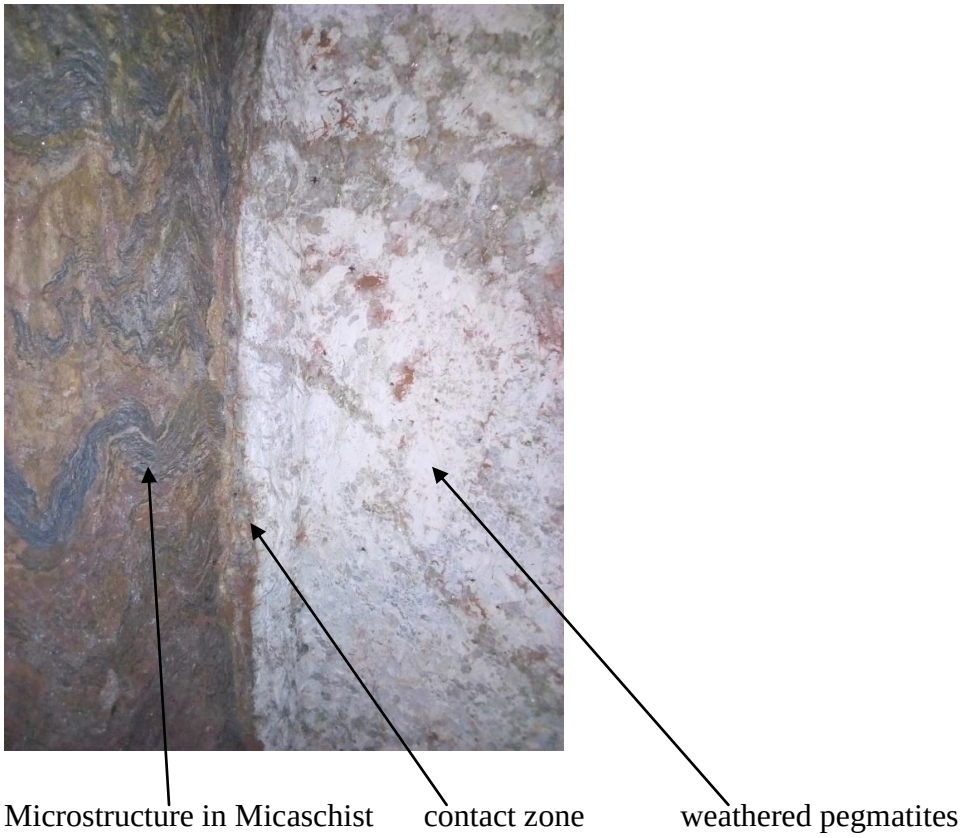

Figure 3. 1 Contact between host rocks and pegmatites (field investigation)

Samples were collected from different locations (Fig.3.2) for petrological and geochemical analysis. Those samples were collected from hard outcrop rocks while others were obtained from underground rocks after digging, but those rocks are highly weathered.

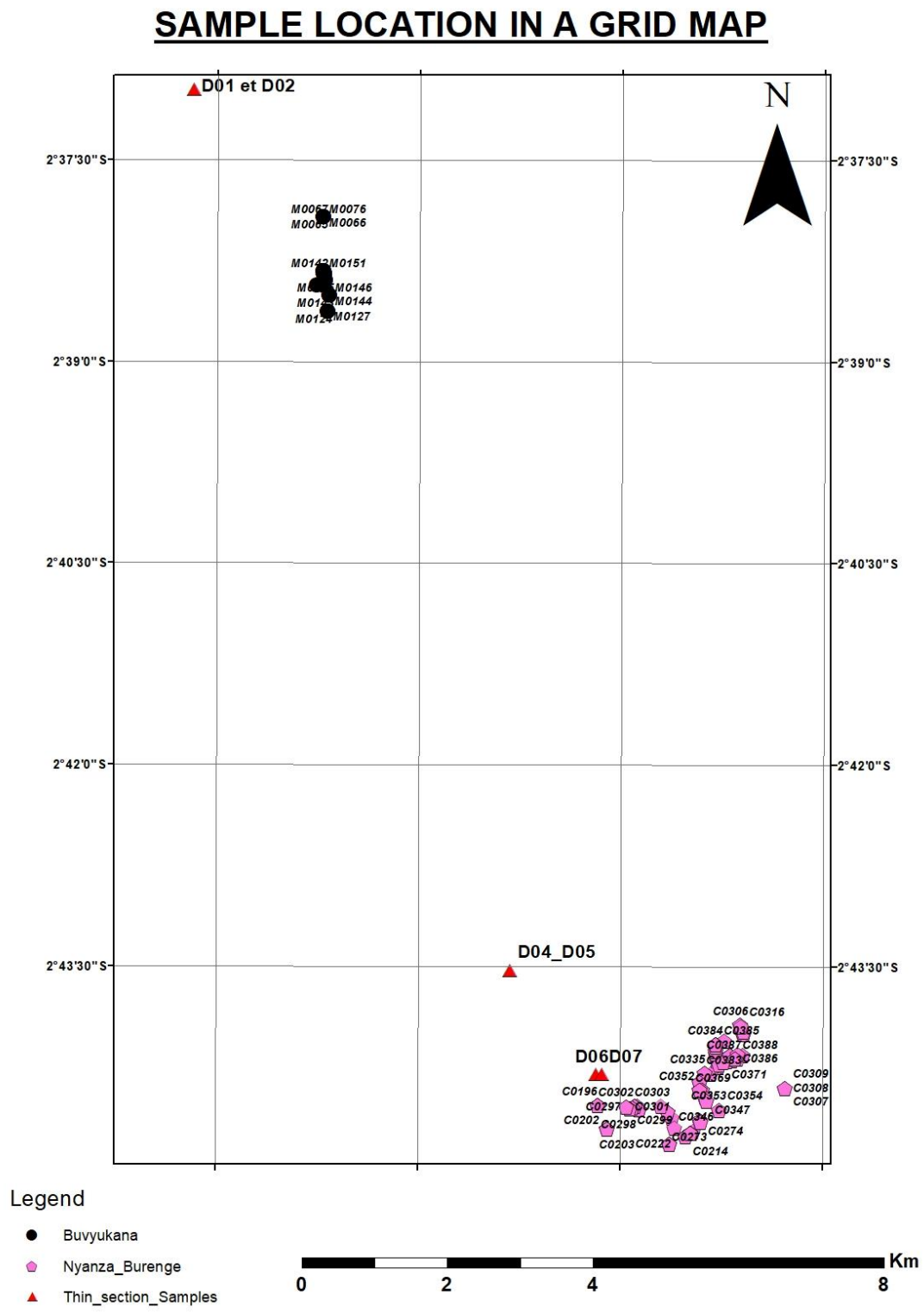

Figure 3. 2 Sampling map

3.1.2 Petrology investigation

About 20 thin sections and 12 polish sections were prepared from hard and weathered rock samples collected during fieldwork.

Thin section, polish section, and their detailed petrographic analysis were carried out at the Burundian mining and Quarry Office (OBM). The preparation of the thin sections and the polished sections require a series or a series of operations up to obtaining a microscopically analyzable slide.

3.1.2.1 Thin section

The first step was rock identification. Structural data like foliations and lineations were noted. The rock also has to be hard enough to be cut. That was followed by rock cutting with the aid of a suitable saw followed by grinding of the part to be glued on the glass of the thin section after polishing with the abrasive powder of variable granulometry of 80, 400, 1400 and 2000 where 2000 was used for the final polishing to have a smooth part facilitating the attachment on the blade. The blade was polished so that the rock and the blade can bond. After polishing the glass and rock were glued with Araldite, but it should be noted that only one drop of Araldite is sufficient and a press release for 24 hours follows this. The thin section was subjected to Petrothin machine up to a thickness of 100 Microns then returned to manual polishing using abrasive powder to a thickness ranging between 30 to 40 Microns, and the best size was of 30Microns.

The micrometre and a microscope were used to know if the minerals were well-cut. It was manifested by the sharpness of the colour and the shape of the minerals.

3.1.2.2 Polished sections

The polished section involved friable rocks that were not hard, and for this, the sample must contain between 5 and 6 grams of grain. A mould was prepared, which was the mixture of Araldite, and its hardener in a proportion of 100 grams of Araldite and 30 grams of Araldite hardener and the mixture left for 3 minutes. Then it was put in an empty pot (castable vacuum system) where 5 grams of the mixture was systematically poured in each mould containing 5 grams of ores or rock. The container was connected to a compressor to drive out air bubbles in the polished sections. The drying lasted 9 hours in an oven at 50 ° C or 24 hours in the open air. Then the section was put in a grinding and polishing machine (grinder-polisher)

grinding discs (75 Microns and 35 Microns) and pre-polishing 9 Micron and 3 Microns, even 1Micron is possible and usable.

3.2 GEOCHEMICAL ASSESSMENT

3.2.1 Digging, Sampling and Standards Operating Procedures (sops)

Sampling programs conducted followed carefully-established protocols that are in line with international standards industry practice.

3.2.1.1 Pit, Trench and Gallery digging

Pits sampling was done in collaboration with Ntega Holding field geologists. Digging was supervised by well-experienced technicians. Layers were separated according to the change of lithology and meter-by-meter. Topsoil, red earth and mica schists were not interesting for sampling. The minimum depth was 5m if there was no pegmatitic body, and the maximum was 10m. After the log description of at least one of the walls, channel sampling was performed immediately to avoid possible contaminations and leaching. Two cross-lines of the width of 20 cm and depth of 5-10cm were made, and sampling was from bottom to top to avoid contamination. The sample was homogenised on-site and then divided several times to obtain a representative quantity of 2 to 3kg intended for laboratory analyses. The sample is packed in a plastic bag and labelled and the description form completed. The file was verified, and the geo-technician prepared a dispatch form, which was sent with the samples to the preparation laboratory after re-verification.

Trenches were dug, based on the results of pits or compiled previous data implemented, and the technician kept track of excavating. After logging of trench and sampling, a log file was prepared. Channel samples are taken by technicians in the perpendicular direction to the pegmatitic body dip using cleaned utensils (plastic plate and chisel or geological hammer) and packed in plastic bags and labelled to give field number. The technician prepared a dispatch form to send the samples to the preparation after verification.

For a gallery and adit, targets selected and its parameters studied. The parameters investigated included; the properties of the layers to cross, direction and dip, length of the gallery, and the lithology. Geo-technicians supervised every step of the work, including the logistics, wooden supports, the lighting within the adit and the ventilation in collaboration with the geologist and mining engineer.

Figure 3. 3 Gallery (Adit) with Wooden Support

Sample locations were selected, and then the geo-technician took the bulk sample over the entire height of the gallery, 1m wide and 20 cm deep. After homogenization, the litho-geochemistry sample was taken and was of 2 to 3 kg, packed in plastic backed and labelled. The remaining material was considered as a bulk sample. The geo-technician prepared the dispatch form for litho-geochemistry samples to be sent to the laboratory for preparation after verification. The bulk sample carried a field number.

Figure 3. 4 Sampling and description within the gallery at 26 m of the depth

3.2.1.2 Standard Operating Procedures (SOPs)

Wells (Pits)

The grid of 50m X 50m was designed except for barren areas. The size of these pits was 1.50 x1.00 m. Layers were logged according to the lithology boundaries at every meter depth. Topsoil, red earth and mica schists areas were not taken into consideration; in other words, were note sampled. Depth was 5 m if no pegmatite or 10 m if the pegmatite is available and photos were taken where necessary.

Trenches

Based on the results of wells (pits) or other historical data, trenching was implemented. Trenches were designed in the north-south direction. The geo-technician supervises the digging operation by separating the topsoil from the material to be sampled. The length of the channel may vary depending on the thickness of the pegmatite. The depth reached 3.50 m if the pegmatite is not crossed. Otherwise, it could reach 10m deep. The mining engineer ensured the stability of the structure if the depth is greater than 3.50 m. Log description of the trench made on a wall and defined the areas to be sampled. The strike and the dip of the pegmatitic body were taken if possible as well as photographs.

Galleries (Adit)

The target was selected and investigated. The parameters in the gallery to be investigated are location, the natures of the layers to cross, direction and dip, length and width of the gallery.

In collaboration with the mining engineer, the position of the gallery was defined. The mining engineer supervised the execution of the works of the opening of the gallery.

3.2.1.3 *Sampling*

Without delaying, to avoid possible contaminations or leaching, the geo-technician came to sample for the geochemistry analysis on two contiguous walls indicated, by cutting two cross-lines (width 20cm, penetration/or depth 5-10cm); The height of the drawing cross is 1 m to 2 m depending on the lithology in place;

Sampling was from bottom to top to avoid current contamination. The channel sample was first homogenised and then split several times to obtain at the end of the process, a representative quantity of weight of 2-3kg for laboratory preparation and analysis. A clear reference sampling plan must be available that shows numbers, so that will be allocated to the samples and the control quality protocol to be used (Normally, every ten samples). The samples were packed in a clean, labelled and a description form completed by a geo-technician (an excel sheet) attached by geo-technician.

The geologist manager checked and approved the dispatch form. Litho-geochemical samples were sent from Kirundo to Bujumbura laboratory for preparation and analysis. The same procedures were used again in the case of trenches and gallery.

3.2.2 Analytical Methods

3.2.2.1 Sample preparation and dispatch

Rock and soil sample collected from pits, trenches and tunnels were prepared and performed mainly by Burundian Mining and Quarry office Laboratory (LOBM). A few samples were prepared using the Ntega laboratory that was set up in Kirundo Company's field camp and at its Bujumbura office. This included drying operations; crushing using a jaw crusher, grinding with mortar and pestle made of laboratory porcelain and metal sample splitter insuring used utensils are thoroughly washed with water and dried after each use.

As mentioned above, most of the samples were prepared at LOBM where they are oven-dried at 110°C, crushed to 85% passing 2mm, then homogenised and divided to get two samples of 250g, samples that are ground to 85% passing 75microns; one has been used for analysis, the other for the archive. The ground material is packed in craft paper with exact sample number as delivered. Drying, crushing, grinding, and quartering are done according to a well-defined protocol submitted at the same time as the samples.

After, Samples were packed in plastic buckets with a range of sample numbers, and the number of samples clearly mentioned in a paper inserted in the bucket. They are accompanied with a sample submission form provided by ALS with sample details and analytical instructions and are delivered to a commercial shipping agency in Bujumbura ("Brucargo") and carried to ALS Chemex ("ALSC"), an independent and internationally accredited (ISO 17025) laboratory in Johannesburg, South Africa. Shipping documentation and sample submission sheets were sent to ALSC.

At ALSC, samples are weighted, and their status checked. If a sample is not well prepared or delivered as rock or mineral sample, it is finely crushed to 70 % passing a 2 mm screen, riffle-split and pulverised in a swing mill to 85 % passing 75 microns. Depending on the required analysis method, samples were couriered by ALSC to their analytical facilities in Vancouver, Canada ("ALSC-V").

3.2.2.2 Sample Analysis

ALSC South Africa checked and recorded the sample numbers and assigned a job number in their laboratory information management system ("LIMS"). Sample receipt verification is then e-mailed to Ntega Holding's senior project geologist.

Soil samples, with inserted Certified Reference Material and coarse blank in the sample, were received in ALSC South Africa and sent to ALSC-V Canada. Due to low 3T concentration, they are analysed by Ultra Trace Aqua Regia inductively coupled plasma mass spectrometry ("ICP-MS") method code ME-MS41 for Ag, Al, As, Au, B, Ba, Be, Bi, Ca, Cd, Ce, Co, Cr, Cs, Cu, Fe, Ga, Ge, Hf, Hg, In, K, La, Li, Mg, Mn, Mo, Na, Nb, Ni, P, Pb, Rb, Re, S, Sb, Sc, Se, Sn, Sr, Ta, Te, Th, Ti, Tl, U, V, W, Y, Zn, Zr.

Pulp rock samples (including 10% QA/QC samples) were received in different batch in ALSC South Africa and sent to ALSC-V Canada to be analysed using inductively coupled

plasma mass spectrometry ("ICP-MS") (method code ME-MS81d: a combination of method ME-MS81, elements by lithium borate fusion and ICP-MS and method ME-ICP06: all elements by lithium metaborate or tetraborate fusion, followed by the dissolution of the melt and ICP-AES analysis) for Ba, Ce, Cr, Cs, Dy, Er, Eu, Ga, Gd, Hf, Ho, La, Lu, Nb, Nd, Pr, Rb, Sm, Sn, Sr, Ta, Tb, Th, Tm, U, V, W, Y, Yb, Zr, SiO2, Al2O3, Fe2O3, CaO, MgO, Na2O, K2O, Cr2O3, TiO2, MnO, P2O5, SrO, BaO.

Rock and mineral samples (including 20% QA/QC samples) were received in a batch in ALSC South Africa then couriered to ALSC-V for Wavelength Dispersive X-Ray Fluorescence Spectrometry (WDXRF spectrometry) on a pressed pellet for Ta, Nb and Sn elements (method code ME-XRFO5), due to concentration levels beyond the upper detection limit, all elements by lithium borate 50:50 flux are analysed by XRF spectrometry (method code ME-XRF10) for Ta, Nb and Sn.

3.2.2.3 Sample Security

Written standard operating procedures ("SOP") were used for the handling of samples to ensure a secure and auditable chain-of-custody from the field to Kirundo Ntega Holding's field camp and Bujumbura office's sample preparation and different laboratory analyses. Local sample transport was exclusive done by Rainbow staff, and Brucargo was responsible for shipment to ALSC-SA and Shandong Xinhai Mining Technology & Equipment Inc.

3.2.2.4 ***Quality Assurance and Quality Control***

For samples dispatched to ALSC, in total 85 certified standards (twelve GTA01, twenty-three GT03, sixteen AMIS0338, twenty AMIS0339 and fourteen AMIS0340), 84 blanks and 16 duplicates have been inserted by Ntega Holding employee with their sample numbers. In their turn, ALSC inserted 287 certified standards (Thirty-three AMIS0085, twenty-six AMIS0167, twenty-one AMIS0185, seventeen AMIS0286, twenty-five AMIS0304, twenty-one CDN- W-4, three MRGeo08, five OGGeo08, twenty-five OREAS- 105, twenty-two OREAS 146, three OREAS 905, five OREAS 920, seventeen SARM- 43, thirty-two SRM88B, thirty-two SY-4), 119 certified blanks and 94 duplicates as part of their internal quality assurance and quality control ("QA/QC") process. ALSC inserted certified reference material ("CRM") and duplicated into all batches of samples for ICP-MS, ICP-AES and WDXRF analysis.

Standards

Geo stats Pty Ltd in Australia produced certified Pulp Tantalum Reference Material GTA01 and GTA03 and African Mineral Standards ("AMIS") in Johannesburg, South Africa, manufactures Li, Ta Pegmatite ore AMIS0338, AMIS0339 and AMIS0340 are used as Certified Reference Material ("CRM"). The results for Ta, Nb and Sn were assessed and found to be within the accuracy limits specified by Geostats and AMIS. The performance of Ta on AMIS0338 and Sn on AMIS0339 is shown in (Fig.3.5) and (Fig.3.6), respectively. The results for certified standards (AMIS0085, AMIS0167, AMIS0185, AMIS0286, AMIS0304, CDN- W- 4, MRGeo08, OGGeo08, OREAS- 105, OREAS 146, OREAS 905, OREAS 920, SARM- 43, SRM88B, SY- 4) inserted and analysed by ALSC, as part of their internal QA/QC process, show acceptable accuracies for Ta, Nb and Sn elements.

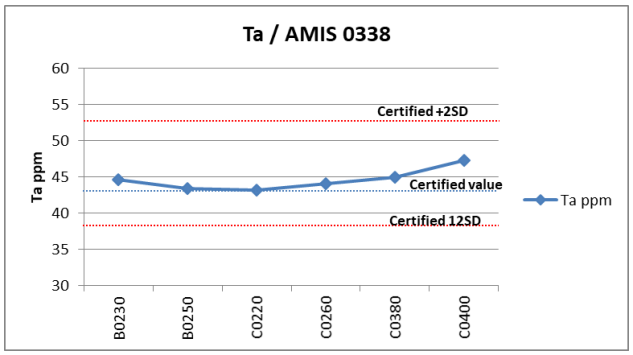

Figure 3. 5 Control chart for AMIS0338 for Tantalum

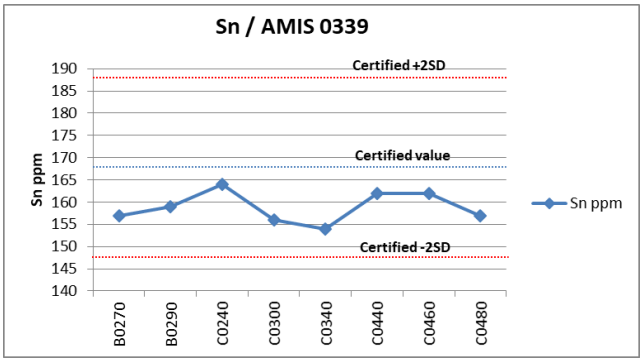

Figure 3. 6 chart for AMIS0339 for Tin

3.6 USE OF GIS DURING THIS WORK

During this research, various software was used, such as ArcGIS and Excel. The Runyankezi Area was referenced in WGS 84. The most important maps used for geo-referencing are existing topographic and geological maps covering the area of the Runyankezi taken from Burundian Mining and Quarry office. The primary objectives of the GIS work were to record and combine all the technical data collected during fieldwork, to provide the working map, and to create final maps such as sampling map, and geological map. Sample location data was controlled by Garmin GPS units and recorded in Lat/Long coordinates using the WGS 84 datum.

CHAPTER FOUR: RESULTS AND DISCUSSION

4.1 MINERALIZATION AND OCCURRENCE OF (Nb-Ta, Sn, W) BEARING ROCKS IN RUNYANKEZI

According to this research, Runyankezi can be subdivided into two main sites (targets) such as Buvyukana in Ntega and Nyanza-Burenge in Marangara, and that reflects the mineralized zones in that area, which are the main focus of this research. The lithologies in those all sites are similar except some differences concerning the size of the rock grains (granulometry).

4.1.1 Occurrence of specific 3Ts bearing lithologies and their classification

The mineralization of the Runyankezi region is often associated with pegmatitic lithologies, which appear in several aspects.

In the northern part of the study area, on the border with Rwanda, some granites can be described as a granite belt or a granite alignment flush with SW-NE defining brecciated areas. They are observed on the hills of Kigufi, Kigari, Nyaruhengeri and Mpindo-Kigaga. On Kigufi and Kigari summits outcrops unmineralized quartzites and hard pegmatites while granites outcrop on the western franc to Rwanda at the boundary defined by Kanyaru valley.

It is evident that the mineralization of Coltan and Cassiterite is found in the pegmatites dispersed in this region, but not all of these pegmatites are mineralized. These pegmatites are directly associated with granites, sometimes independent in host rocks or as a result of the intrusion of granite defining a halo marking the contact zone.

There are three categories of pegmatites:

- Those that appear in direct association with granite (Mpindo-Kigaga);

- Those who are independent of these granites (Buvyukana) and;

- Those derived from the emplacement of granites (Nyanza-Burenge).

Significant mineralization of 3Ts are found in independent pegmatites, or more evolved pegmatites located in Buvyukana followed by those derived from the emplacement of granite but with low concentration, and are located in Nyanza-Burenge. In contrast, pegmatites directly associated with granite are not fertile or barren (Mpindo-Kigaga).

4.1.2 Rock description and location of mineralization in the rock

Some pegmatites are intimately associated with the granites, and they are hard and phaneritic, they are observed at the level of the hill Mpindo-Kigaga (Ntega) in association with the foliated granite, aphanitic and flush with block joints (fig.4.1). The same type of pegmatite is also exposed at the Ndurumu River (Marangara), and these pegmatites are not mineralized.

Figure 4. 1 Outcrop Granite together with pegmatite in the north part of Runyankezi

The independent pegmatites not directly associated with the granites intrude host rocks such as Mica schists, defining a stratigraphy beginning by the Mica schists at the base and ending with a layer of cultivable land or laterite. The stratigraphy is as follows:

Mica schist (bottom) - tourmaline layer-Greisen (muscovite+Qz) -pegmatite (feldspars + quartz) -laterite-cultivable land (top).

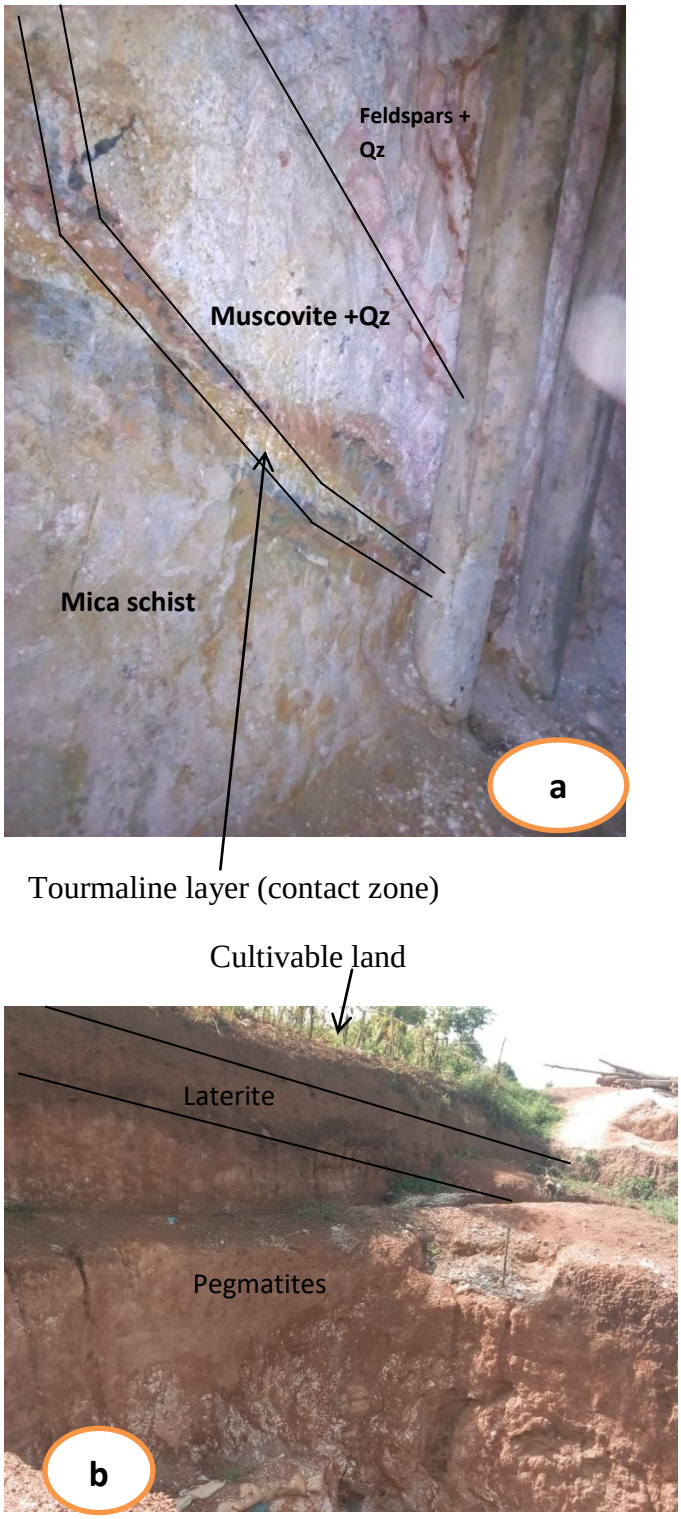

Figure 4. 2 Profile of the rock unit in the study area

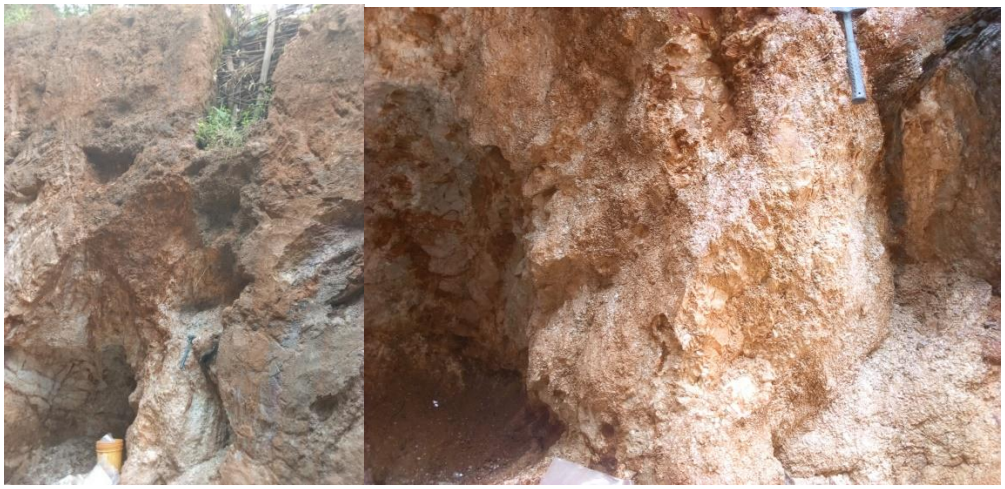

Figure 4. 3 High weathered pegmatites at Buvyukana site

These pegmatites are deeply weathered, meteoric alteration leading to kaolinization of the pegmatite. They show traces of veins marking the zones of the weakness of these pegmatites. These veins are intertwined (stockworks) testifying the hydrothermal alteration before the weathering of these pegmatites. Enclaves of granites and other rocks are remarkable testifying that crystallization of these pegmatites involved melting of pre-existing rocks. This reflects the mineralogy composition of these pegmatites, which is much more similar to that of their mother granites.

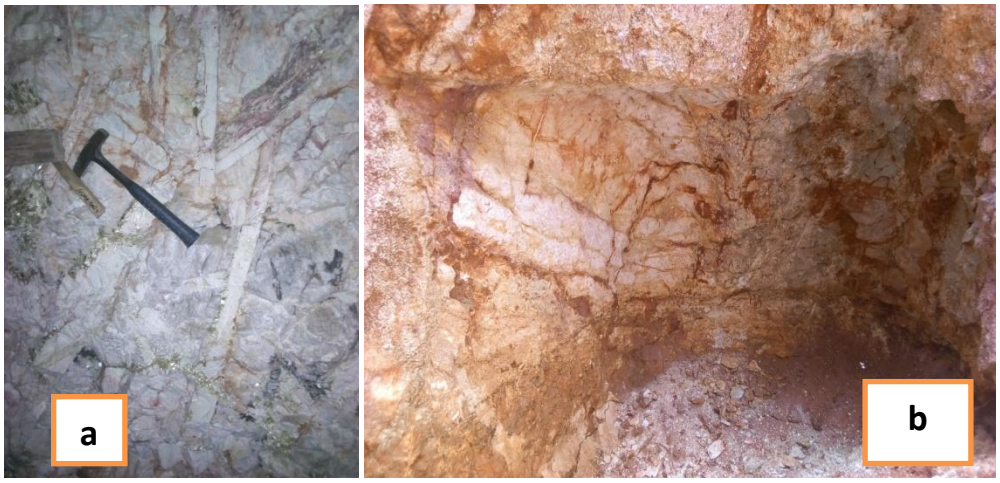

Figure 4. 4 Stockworks veins in weathered pegmatite (a) and diaclases (b)

These pegmatites are strongly mineralized in coltan and cassiterite, which is the characteristic of Buvukana pegmatites occurrence. The mineralization in these pegmatites is not homogeneous, the strong mineralization is found in the highly weathered parts and rich in muscovite part of pegmatite while the rest of the pegmatite is a bit hard. The predominant minerals are: quartz,

feldspar, muscovite and tourmaline which appear according to the layers defined in the stratigraphic unit considered (Fig.4.2).

As for the pegmatites which derive from the emplacement of the granites, they are presented in two parts; the first part comes from the granites at depth which means that the fluids are derived from the granite which subsequently intrudes the country rock (mica schist) through structural features (lineaments). Thus forming the second part where the mineralization of exploitable coltan is concentrated. And this is observed at Nyanza-Burenge site. These pegmatites have undergone meteoric weathering, and the stratigraphy resembles that of the granite-independent pegmatites with quartz and muscovite as dominant minerals, but they differ in places where these pegmatites are accompanied by granite in the form of migmatite or metamorphosed granite (Fig.4.5).

Figure 4. 5 Contact between Granite and Pegmatite

The pegmatites closest to the granite are sterile and show plagioclase enrichment, which is contrary to the distant pegmatites which are rich in feldspars. Significant mineralization is observed at the level of pegmatites that are not associated with granites, that is, independent pegmatites.

4.2 INVESTIGATION OF MINERALOGY, PETROLOGY, AND GEOCHEMISTRY OF NIOBIUM-TANTALUM, TIN AND TUNGSTEN BEARING ROCKS IN RUNYANKEZI

This part of work concern the identification and description of minerals that constitute rocks carrying 3T's mineralization, investigation of whole-rock geochemistry, the tectonic setting as well as the rock group belonging in the study area. Note that the bearing rocks of these mineralizations were subjected to an intense weathering, taking samples to make thin sections was completely difficult or even impossible. The samples used during the making of the thin sections were taken from the granite rocks and their associated pegmatites.

4.2.1 Mineralogy investigation

4.2.1.1 Mineralogy of Mpindo-kigaga Granite and its associated Pegmatite

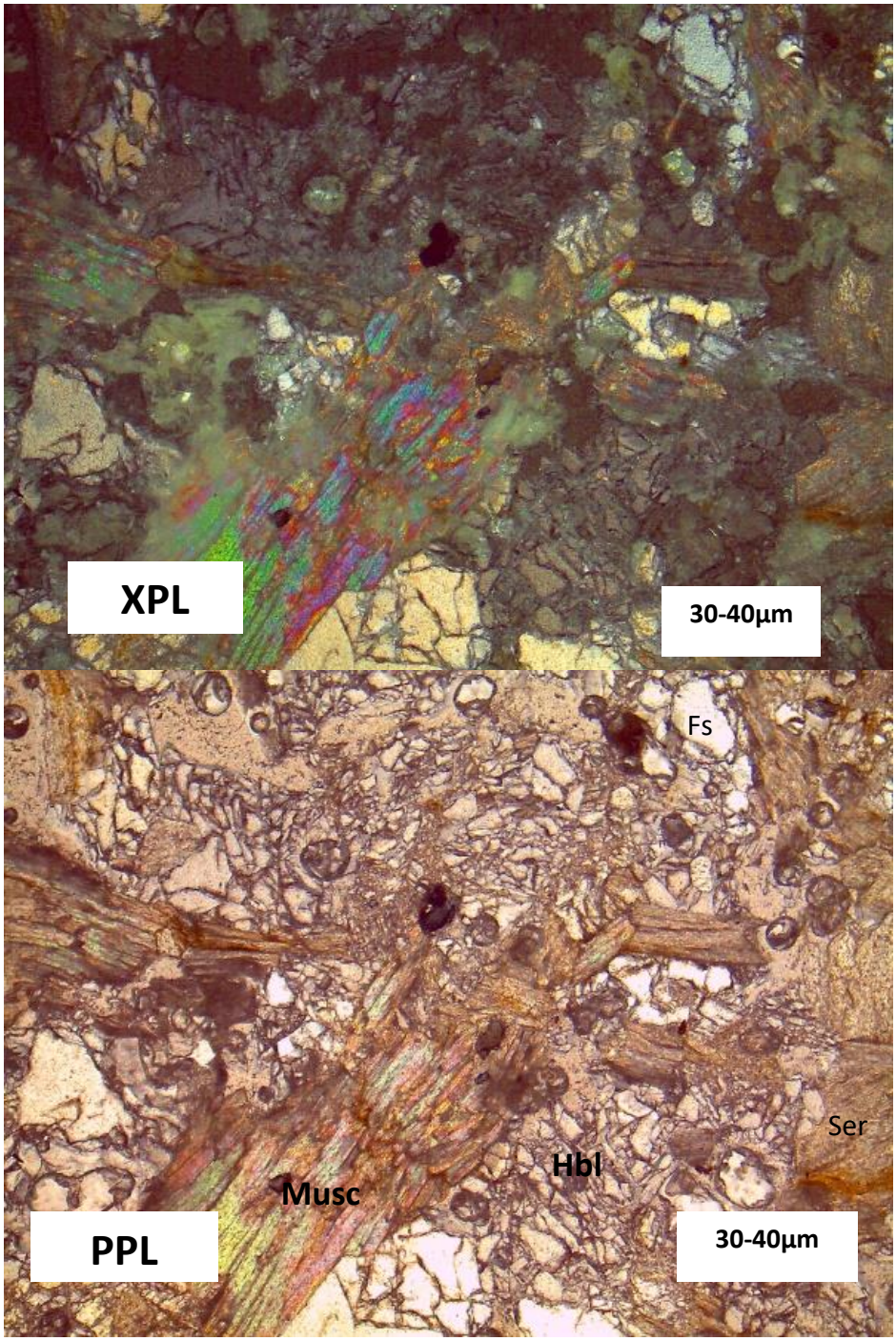

Figure 4. 6 Photomicrographs of foliated granite from Mpindo-Kigaga. Fs=Feldspar, Hbl=Hornblende, Musc=Muscovite, Ser= Sericite, Waypoint: X: 29.94712; Y:-2.6163.

This granite appears almost on the border with Rwanda in the northern part of the study area in the commune of Ntega where the Buvyukana site is located. It is gneissic granite, finely

grainy and foliated of greyish colour which is in association with a pegmatite. Under microscopy, this granite shows minerals such as muscovite, feldspar, hornblende and sericite.

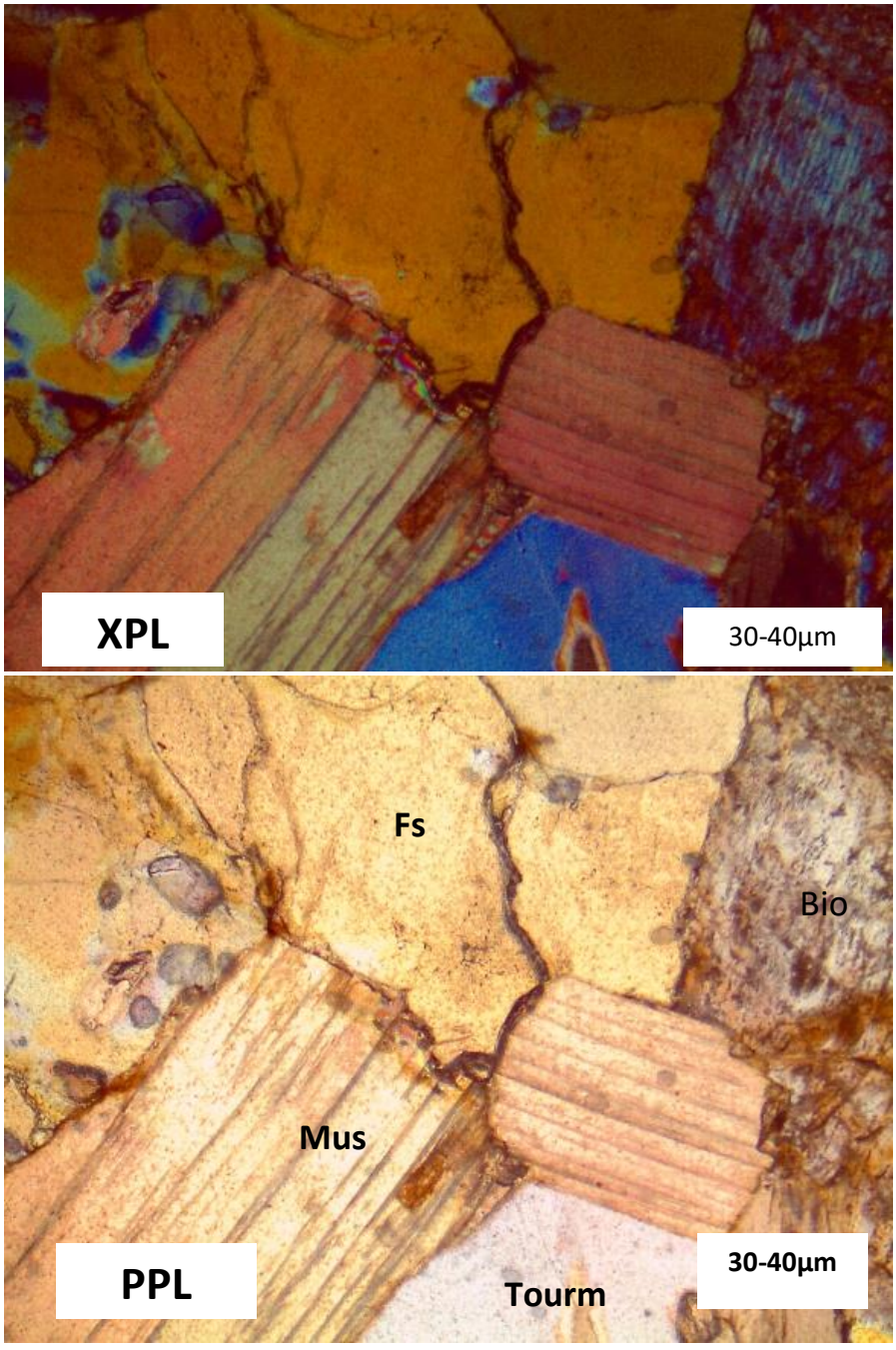

Figure 4. 7 Photomicrographs of Pegmatite from Mpindo-Kigaga. Fs=Feldspar, Musc=Muscovite, Tourm= Tourmaline, Bio= Biotite. Waypoint: X: 29.94712; Y:-2.6163.

This pegmatite outcrops directly in association with granite; it is coarsely grained and unaltered. Microscopy shows an association of biotite, muscovite, Tourmaline and feldspar. Biotite has a strong alteration as can be seen in the image above.

4.2.1.2 Mineralogy of Granite from Ndurumu River and its associated Pegmatite

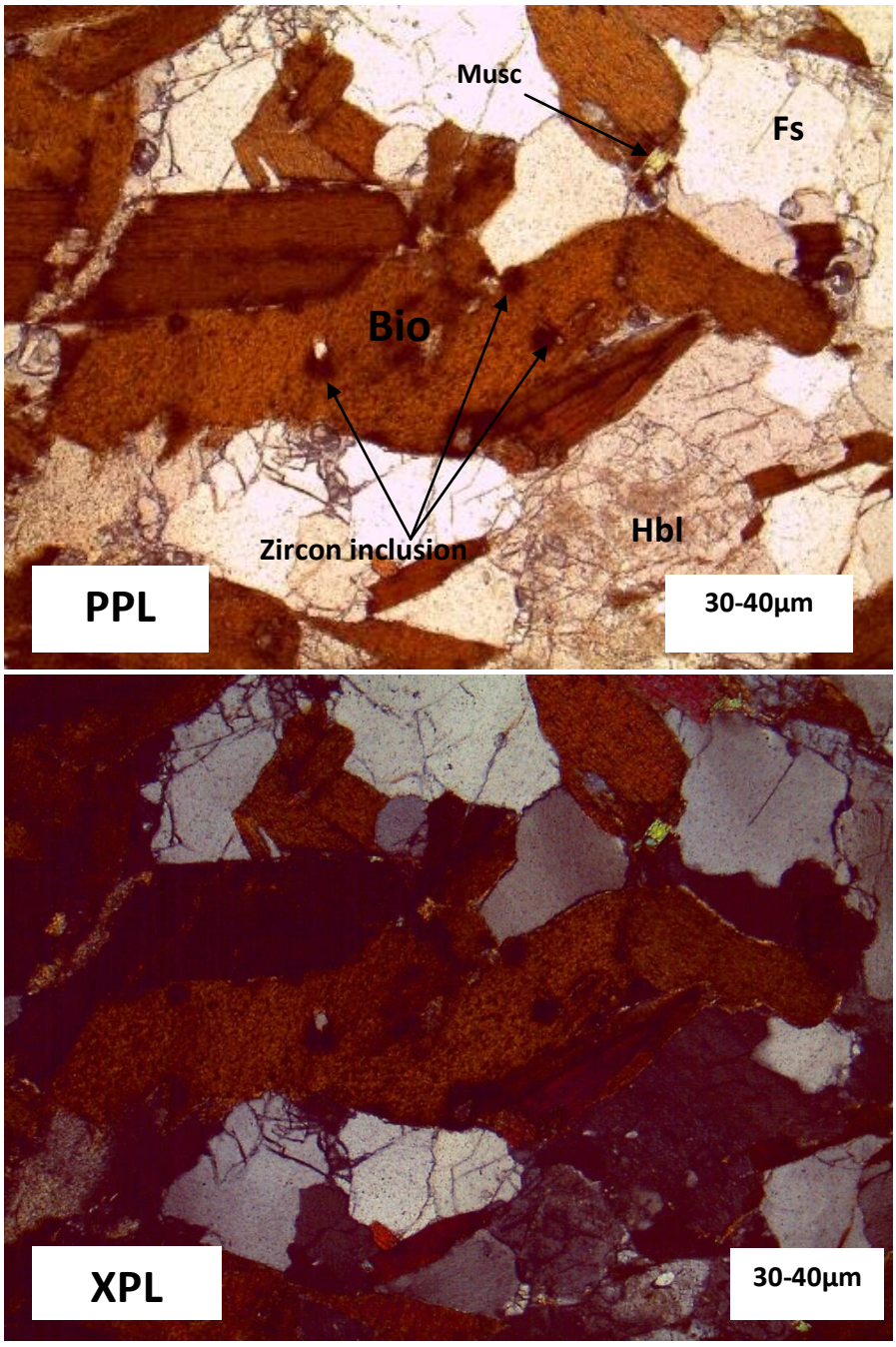

Figure 4. 8 Photomicrographs of granite from Ndurumu River. Fs=Feldspar, Musc=Muscovite, Hbl=Hornblende, Bio= Biotite, Waypoint: X: 29,98636; Y:-2,72552.

This granite outcrops in the southern part of the study area in the Commune of Marangara where the Nyanza-Burenge site is located. This granite resembles that of Mpindo-Kigaga, it is finely grainy and foliate and associated with a coarsely grained unaltered pegmatite. Microscopy shows that this granite is enriched in biotite and feldspar, but hornblende and

muscovite are present. In addition to what is mentioned above, biotite has inclusions of zircon marking its alteration.

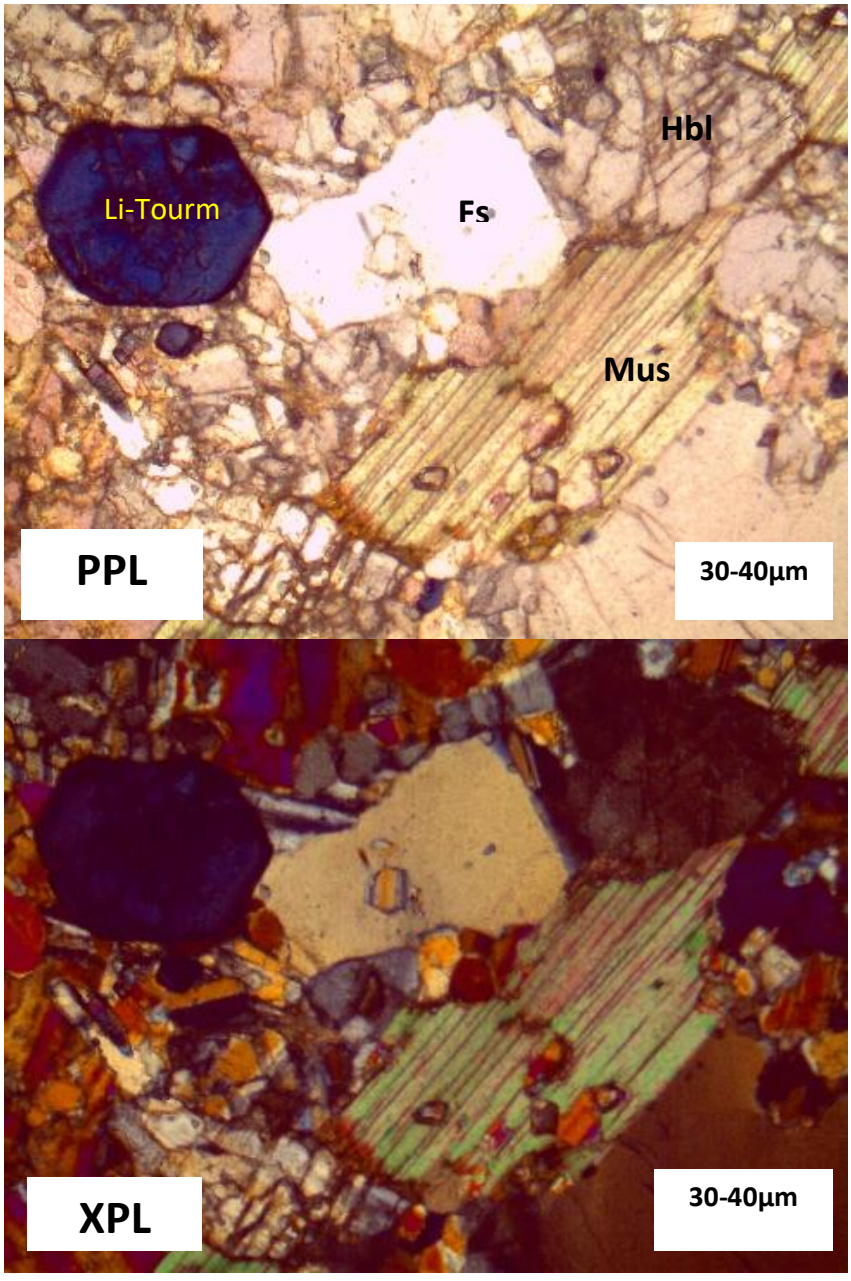

Figure 4. 9 Photomicrographs of pegmatite from Ndurumu River. Fs=Feldspar, Musc=Muscovite, Hbl=Hornblende, Tourm=Tourmaline. Waypoint: X: 29,98636; Y:-2,72552.

This pegmatite outcrops directly in association with granite; it is coarsely grained and unaltered. Microscopy shows an association of muscovite, Tourmaline rich in lithium (Elbaite), Hornblende and feldspar. The left part below the tourmaline (elbaite) shows the interpenetration of feldspars.

4.2.1.3 Mineralogy of Granite from Rurambo-Nyanza (South part of the study area)

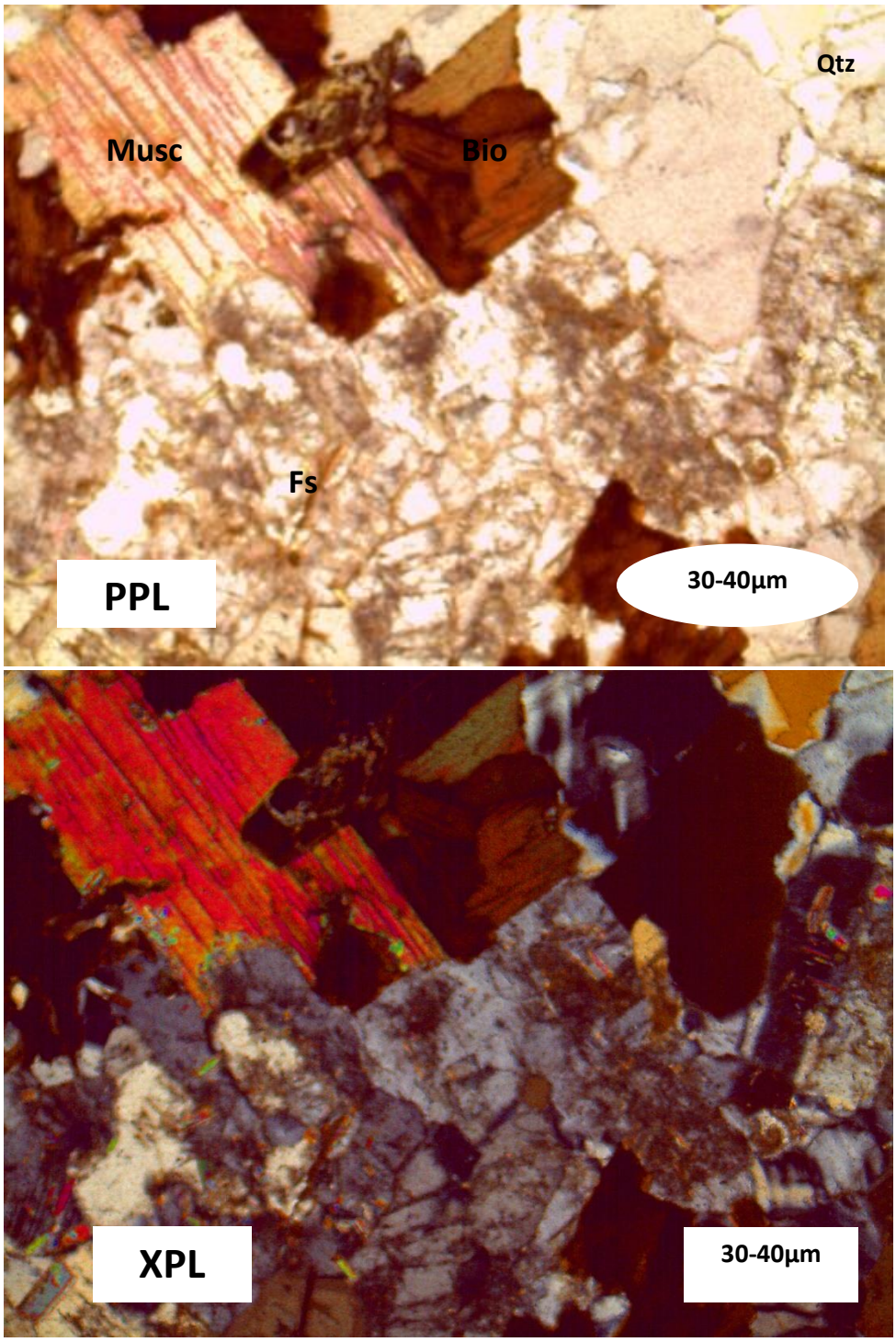

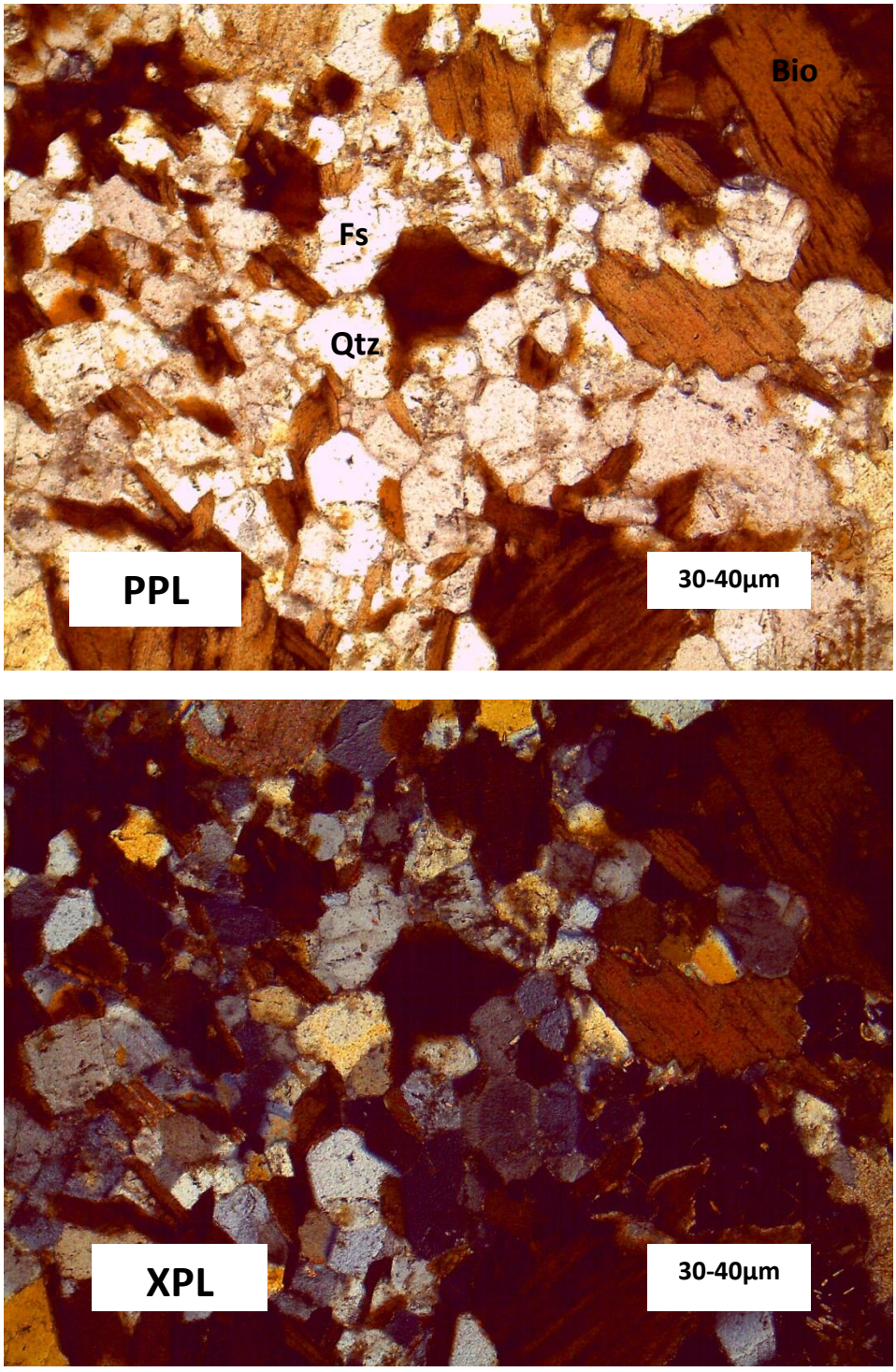

Figure 4. 10 Photomicrographs of granite from Rurambo-Nyanza. Fs=Feldspar, Musc=Muscovite, Qtz=Quartz, Bio= Biotite. Waypoint: X: 29,99773; Y : -2,73845.

This granite outcrops in the locality of the Nyanza-Burenge. It is moderately grainy granite, including quartz, biotite and feldspar visible to the naked eye. In addition to that, microscopy shows the presence of muscovite, it is granite with two micas.

4.2.2 Composition and classification of sampled rocks in burenge-nyanza using major elements

The purpose of this section is to classify rocks using their chemical composition especially major elements, in order to infer the identified rocks and groups in which they belong, the tectonic setting, and the composition of the liquid which gave sampled rocks. Different bivariate diagrams and ratios were used, such as variation diagrams commonly known as Harker variation diagrams for both major elements and trace elements and total alkalis- silica diagram (TAS). In the first case (Fig.4.11.b) silica (SiO2) is compared with other oxides which highlight the trend/patterns in the chemical data, whereas in the second case (Fig.4.11.d) the silica (SiO2) is compared with the sum of K_2O+Na_2O. The used ratios are based on Alumina saturation, such as A/CNK= $Al_2O_3/(K_2O+Na_2O+CaO)$, and A/NK= $Al_2O_3/(K_2O+Na_2O)$.

Table 4. 1 Chemical analysis of twenty samples from Nyanza-Burenge and their normalized values.

SAMPLE	C0191	C0192	C0195	C0196	C0199	C0206	C0207	C0212	C0213	C0231
SiO2	68,2	68,5	63,5	63,4	51,7	76,5	68,3	75	78,9	64,5
SiO2 (N)	73,11	73,43	69,23	69,25	57,11	79,82	73,33	79,29	81,58	68,28
Fe2O3+MgO	4,245	4,363	6,81	6,67	12,67	2,52	3,98	1,71	1,56	10,09
Al2O3	19,35	18,95	20,7	20,9	23,8	14,85	19,3	16,8	14,7	17,85
Al2O3 (N)	20,74	20,31	22,57	22,82	26,29	15,49	20,72	17,76	15,20	18,89
TiO2	0,18	0,14	0,53	0,52	0,82	0,17	0,28	0,07	0,06	0,33
TiO2 (N)	0,19	0,15	0,57	0,56	0,90	0,17	0,30	0,07	0,06	0,34
Al2O3/TiO2	**107,5**	**135,35**	**39,05**	**40,19**	**29,02**	**87,35**	**68,92**	**240**	**245**	**54,09**
Fe2O3	3,9	4,02	6,07	5,93	10,1	2,38	3,65	1,6	1,49	9,25
Fe2O3 (N)	4,18	4,30	6,61	6,47	11,15	2,48	3,919	1,69	1,540	9,79
MnO	0,03	0,11	0,03	0,02	0,06	0,03	0,03	0,02	0,03	0,03
MnO (N)	0,03	0,11	0,03	0,02	0,06	0,03	0,03	0,02	0,03	0,03
MgO	0,06	0,05	0,18	0,18	1,37	0,04	0,06	0,02	0,02	0,29
MgO (N)	0,06	0,05	0,19	0,19	1,51	0,04	0,06	0,02	0,02	0,30
CaO	0,01	0,01	0,01	0,01	0,26	0,01	0,01	0,01	0,01	0,05
CaO (N)	0,01	0,01	0,01	0,01	0,28	0,01	0,01	0,01	0,01	0,05
Na2O	0,08	0,08	0,06	0,05	0,95	0,11	0,1	0,06	0,08	0,21
Na2O (N)	0,08	0,08	0,06	0,05	1,04	0,11	0,10	0,06	0,08	0,22
K2O	1,42	1,37	0,55	0,47	1,25	1,7	1,37	0,96	1,38	1,76
K2O (N)	1,52	1,46	0,59	0,51	1,38	1,77	1,47	1,01	1,42	1,86
P2O5	0,03	0,02	0,05	0,05	0,1	0,02	0,01	0,02	0,02	0,12
P2O5 (N)	0,03	0,02	0,05	0,05	0,11	0,02	0,01	0,02	0,02	0,12
Cr2O3	0,03	0,03	0,02	0,02	0,04	0,03	0,02	0,03	0,03	0,05
Cr2O3 (N)	0,03	0,03	0,02	0,02	0,04	0,03	0,02	0,03	0,03	0,05
SrO	0,01	0,01	0,01	0,01	0,02	0,01	0,01	0,01	0,01	0,01

SrO (N)	0,01	0,01	0,01	0,01	0,02	0,01	0,01	0,01	0,01	0,01
BaO	0,01	0,01	0,01	0,01	0,05	0,01	0,01	0,01	0,01	0,02
BaO (N)	0,01	0,01	0,01	0,01	0,05	0,01	0,01	0,01	0,01	0,02
K2O+Na2O (N)	1,6	1,5	0,66	0,56	2,43	1,88	1,57	1,07	1,50	2,08
CaO+K2O+Na2O (N)	1,61	1,56	0,67	0,57	2,71	1,89	1,58	1,08	1,52	2,13
A/CNK	12,81	12,97	33,38	39,43	9,67	8,15	13,04	16,31	10	8,83
A/NK	12,9	13,06	33,93	40,19	10,81	8,20	13,12	16,47	10,06	9,06
LOI	7,34	7,23	8,37	9,01	3,63	4,51	6,6	6,03	4,91	6,56
Total	100,62	100,51	100,08	100,56	94,15	100,35	99,73	100,61	101,62	101,02
Total-LOI	93,28	93,28	91,71	91,55	90,52	95,84	93,13	94,58	96,71	94,46

SAMPLE	C0256	C0257	C0258	C0305	C0306	C0321	C0335	C0337	C0338	C0351
SiO2	70.7	69.2	67.2	66,7	65,2	73,8	67,6	76,9	68,1	71,8
SiO2 (N)	75,27	73,34	70,58	72,87	71,83	77,77	71,79	80,38	72,34	75,77
Fe2O3+MgO	3,46	4,12	4,97	3,49	3,83	5,39	2,46	4,82	5,05	1,95
Al2O3	16,55	18,45	19,95	20	20,5	14,25	21,3	12,85	19,05	18,7
Al2O3 (N)	17,62	19,55	20,95	21,85	22,58	15,01	22,62	13,43	20,23	19,73
TiO2	0,14	0,19	0,22	0,46	0,46	0,35	0,07	0,34	0,3	0,04
TiO2 (N)	0,14	0,20	0,23	0,50	0,50	0,36	0,07	0,35	0,31	0,04
Al2O3/TiO2	**118,21**	**97,10**	**90,68**	**43,47**	**44,56**	**40,71**	**304,28**	**37,79**	**63,5**	**467,5**
Fe2O3	2,99	3,76	4,61	3,01	3,31	4,94	2,29	4,53	4,66	1,82
Fe2O3 (N)	3,18	3,98	4,84	3,28	3,64	5,20	2,43	4,73	4,95	1,92
MnO	0,04	0,04	0,04	0,01	0,01	0,02	0,04	0,02	0,02	0,03
MnO (N)	0,04	0,04	0,04	0,01	0,01	0,02	0,04	0,02	0,02	0,03
MgO	0,26	0,13	0,13	0,19	0,17	0,18	0,03	0,09	0,1	0,03
MgO (N)	0,27	0,13	0,13	0,20	0,18	0,18	0,03	0,09	0,10	0,03
CaO	0,01	0,01	0,01	0,01	0,01	0,03	0,01	0,01	0,01	0,01
CaO (N)	0,01	0,01	0,01	0,01	0,01	0,03	0,01	0,01	0,01	0,01
Na2O	0,09	0,1	0,13	0,04	0,03	0,14	0,16	0,07	0,11	0,1
Na2O (N)	0,09	0,10	0,13	0,04	0,03	0,14	0,16	0,07	0,11	0,10
K2O	3,09	2,39	2,81	0,99	0,98	1,11	2,62	0,78	1,69	2,2
K2O (N)	3,29	2,53	2,95	1,08	1,07	1,16	2,78	0,81	1,79	2,32
P2O5	0,02	0,04	0,05	0,05	0,04	0,03	0,02	0,03	0,04	0,02
P2O5 (N)	0,02	0,04	0,05	0,05	0,04	0,03	0,02	0,03	0,04	0,02
Cr2O3	0,02	0,03	0,04	0,04	0,02	0,04	0,03	0,04	0,04	0,02
Cr2O3 (N)	0,02	0,03	0,04	0,04	0,02	0,04	0,03	0,04	0,04	0,02
SrO	0,01	0,01	0,01	0,01	0,01	0,01	0,01	0,01	0,01	0,01
SrO (N)	0,01	0,01	0,01	0,01	0,01	0,01	0,01	0,01	0,01	0,01
BaO	0,01	0,01	0,01	0,03	0,03	0,01	0,01	0,01	0,01	0,01

BaO (N)	0,01	0,01	0,01	0,03	0,03	0,01	0,01	0,01	0,01	0,01
K2O+Na2O (N)	3,38	2,63	3,08	1,12	1,11	1,31	2,95	0,88	1,91	2,42
CaO+K2O+Na2O (N)	3,39	2,64	3,09	1,13	1,12	1,34	2,96	0,89	1,92	2,43
A/CNK	5,18	7,38	6,76	19,23	20,09	11,13	7,63	14,94	10,52	8,09
A/NK	5,20	7,40	6,78	19,41	20,29	11,4	7,66	15,11	10,58	8,13
LOI	4,74	6,04	6,38	7,6	7,65	5,4	6,45	5,26	6,81	5,63
Total	98,66	100,39	101,58	99,13	98,41	100,29	100,61	100,93	100,94	100,39
Total-LOI	93,92	94,35	95,2	91,53	90,76	94,89	94,16	95,67	94,13	94,76

4.2.2.1 Rock classification: Total alkalis- silica diagram (TAS) and SiO_2 vs K_2O diagram

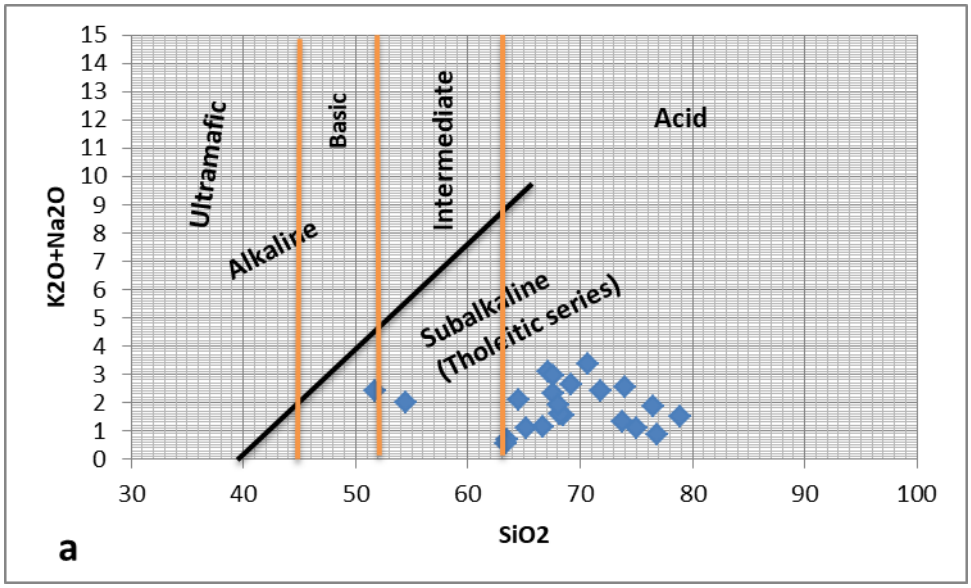

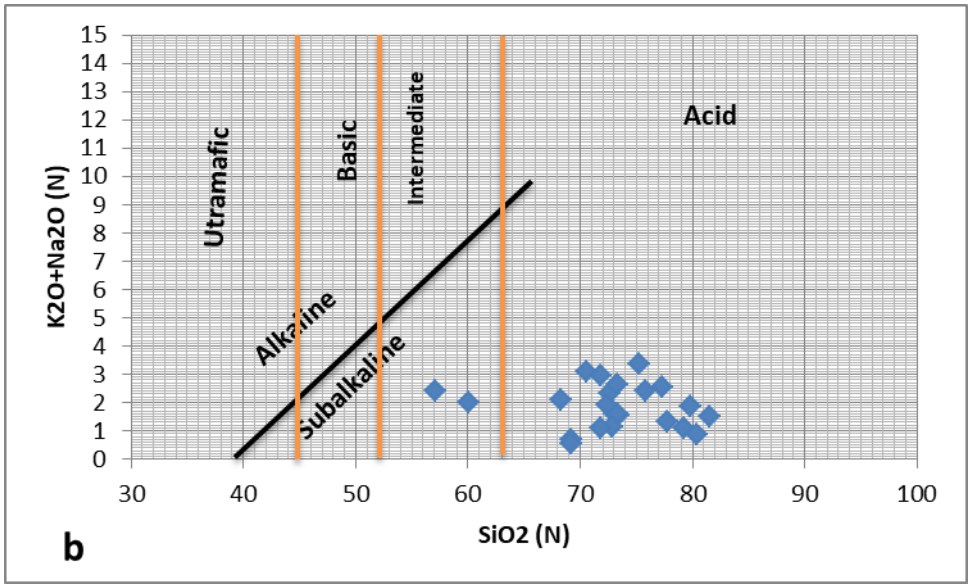

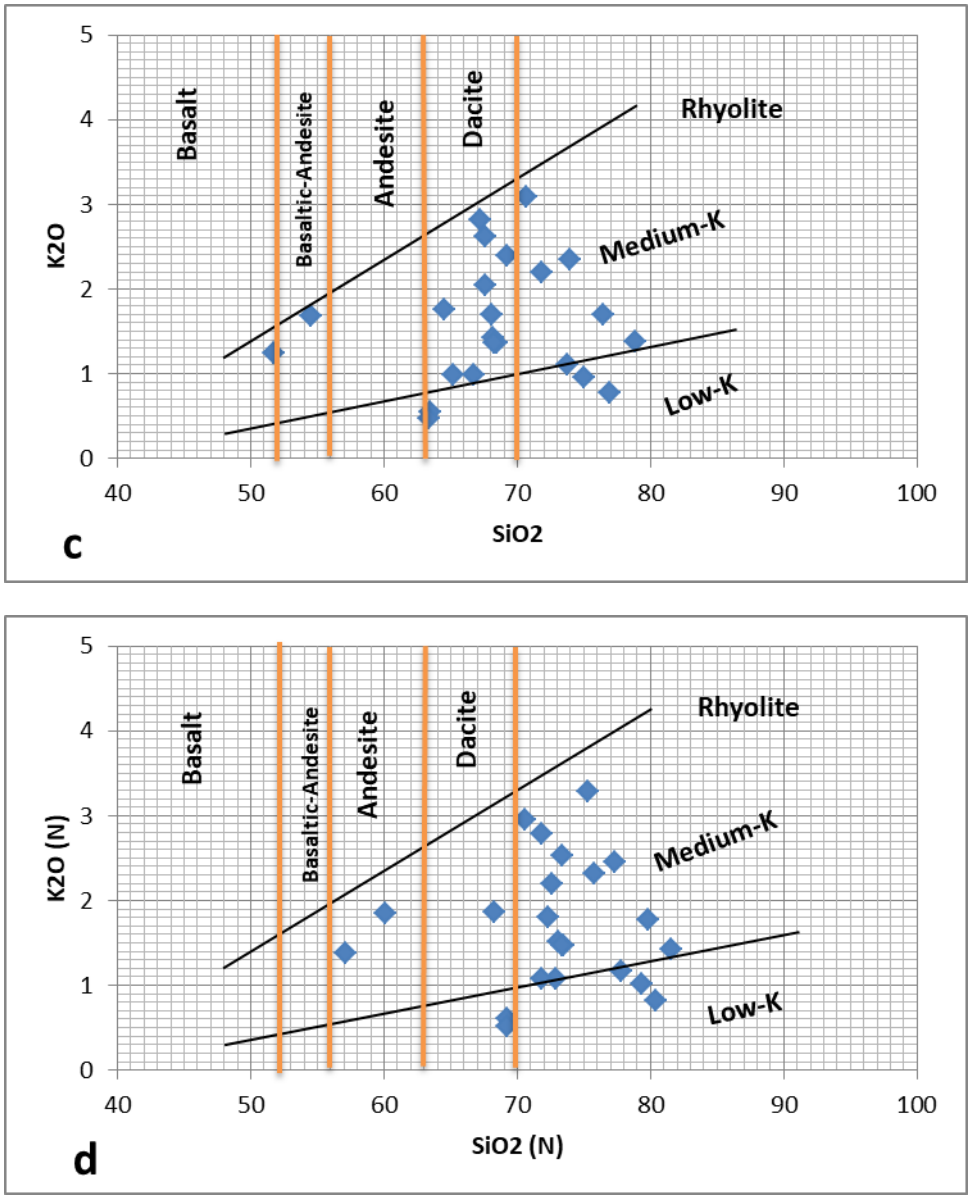

Figure 4. 11 a-b.Composition and classification diagram of Nyanza-Burenge rocks (MackDonald, 1968 and Le Maitre et al., 1989), **c-d**.Subdivision of subalkaline rocks of Nyanza-Burenge using the K_2O vs SiO_2 (Le Maitre et al., 1989).

Diagrams **a** and **c**, are same respectively with diagrams **b** and **d** after removing LOI and normalization. The valuable diagrams for this section are b and d as it is shown that the LOI has an effect on results once they are plotted. The silica composition of plotted samples range from 57wt% to 82wt% (Fig.4.11.b), which interval corresponds to intermediate to acid rocks, and the represented rocks are sub alkaline (Fig.4.11.b)**.** The plot of the same samples in SiO_2 vs K_2O diagram highlights that those rocks are low-K to medium-K (calc-alkaline) (Fig.4.11.d) which correspond to increasing thickness of the continental crust. Those rocks range from Andesite to Rhyolite and most of the plot in rhyolite interval.

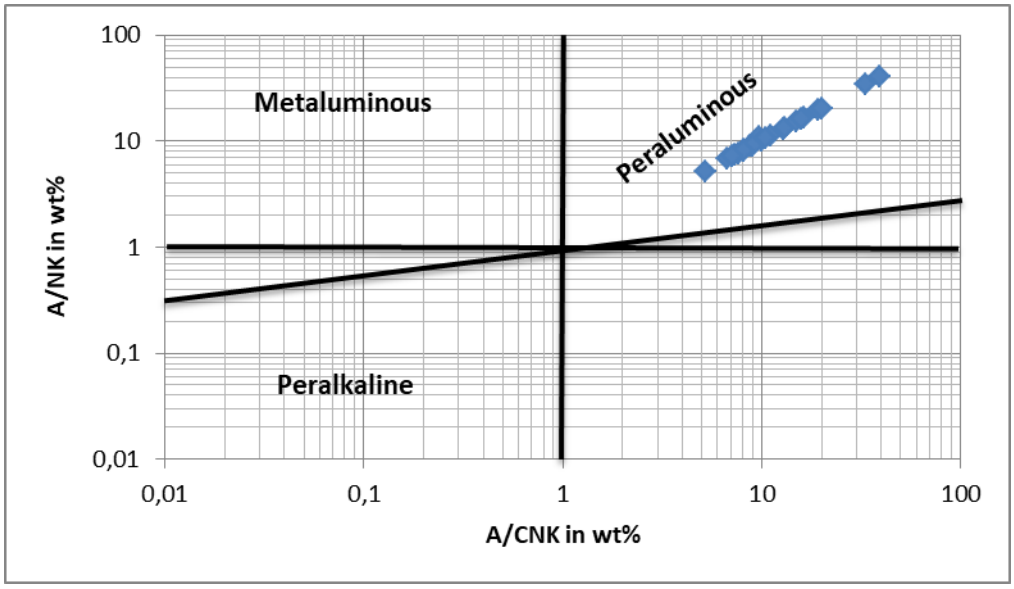

Figure 4. 12 Classification diagram of Nyanza-Burenge rocks based on Alumina saturation (Shand, 1943)

The check of Alumina Saturation shows that all samples have A/CNK= $Al_2O_3/(K_2O+Na_2O+CaO)$ and A/NK= $Al_2O_3/(K_2O+Na_2O)$ ratios which are greater than one (A/CNK>1, and A/NK>1) (Tab. 4.1), that implies that the sampled rocks are **alumina-oversaturated** and correspond to **peraluminous** rocks. The excess alumina is related mainly to micas, especially muscovite, in addition to Al-rich biotite, and aluminous accessory minerals such as tourmaline and others (Le Maitre et al., 1989). This evidenced the attributed minerals to the rocks from the study area in section **4.2.1**.

4.2.2.2 Tectonic Setting

To deal with the tectonic setting, bivariate diagrams were used, especially TiO_2 vs Al_2O_3, and TiO_2 vs (Fe_2O_3+MgO).

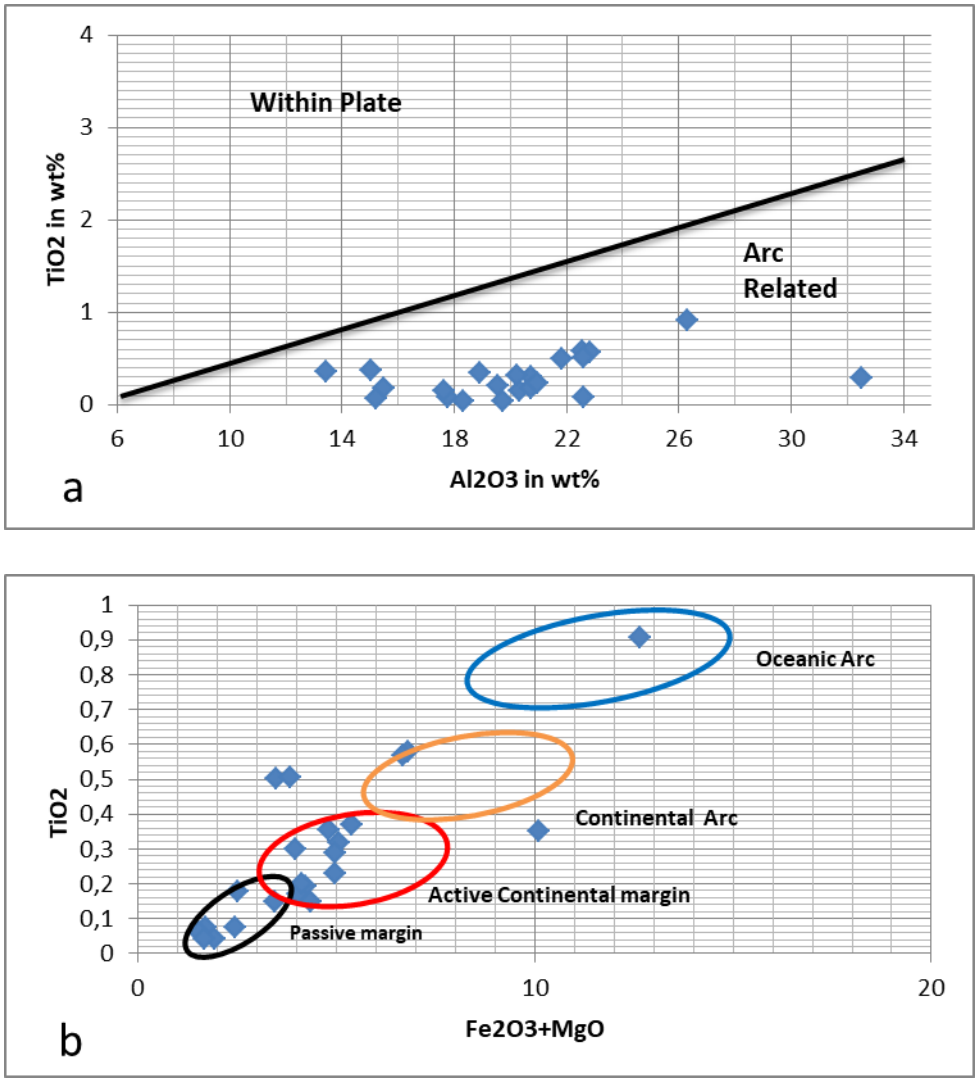

Figure 4. 13 a.Bivariate plot of Al_2O_3 versus TiO_2 showing environment related to different Geological fields (After Muller et al., 1992), **b**.Bivariate plot of Fe_2O_3+MgO versus TiO_2 showing geological fields (After Bhatia, 1983).

All plotted samples showed that the environment of the study area is related to arc (Fig.4.13.a)**,** where most of them show active continental margin and passive margin as main geologic fields (Fig.4.13.b)**,** the passive margin is explained by the fact that the fluid is from the melting of prexisting rocks and those rock are sedimentary, it implies that their origin is related to passive margin**.** Al_2O_3/TiO_2 ratio indicates the source of rock composition, it between 3 and 8 for mafic igneous rocks, 8 and 21 for intermediate rocks, and between 15

and 70 and above for acid igneous rocks (Hayashi et al., 1997). All samples have Al_2O_3/TiO_2 ratios which are far greater than 15 (Tab.4.1), which indicate that the liquid source of those rocks is felcic or acidic.

4.2.2.3 Harker variation diagrams

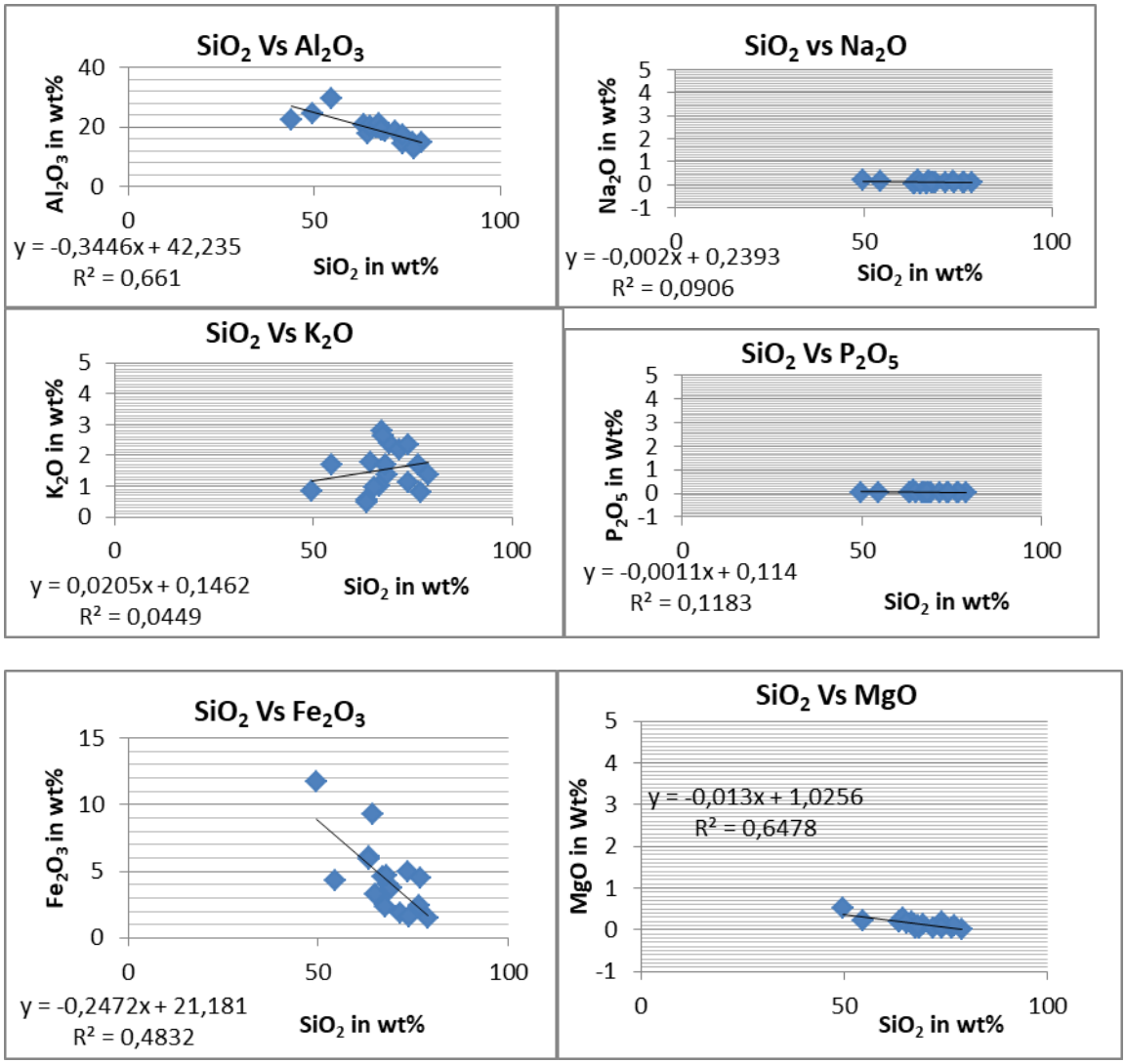

Figure 4. 14 Harker variation diagram for major elements in Nyanza-Burenge site

In these diagrams, silica (SiO_2) is correlated with oxides such as Al_2O_3, K_2O, Na_2O, MgO, P_2O_5, and Fe_2O_3. These diagrams highlight that SiO_2 is not correlated with Al_2O_3, Na_2O, MgO, P_2O_5, and Fe_2O_3 oxides (Fig.4.14)**.** This seems to be right because the concentration of SiO_2 is too high regarding that of compared oxides, which is to say that the incorporation conditions were not the same. In contrast, SiO_2 is correlated with K_2O (Fig.4.14), which

means the same conditions during their incorporation. That positive correlation confirms that the sampled rocks are felsic rocks (Feldspar and Silica).

4.2.3 Whole-rock geochemical of sampled rocks in runyankezi

This sub-section highlights the geological conditions at which rocks have been subjected using trace elements. It is based on the use of ratios and plotted diagram. In addition, it highlights what happened during crystallization-fractionation and after crystallization-fractionation such as hydrothermal alteration.

4.2.3.1 Use of Nb/Ta and/or Ta/Nb ratios in Genetic setting of 3Ts minerals

Melts formed during high-temperature anatexis tend to have high Nb/Ta ratios, as a result of the complete consumption of biotite and the high abundance of titanium (Ti)-bearing oxides in the residue, which preferentially incorporate Ta over Nb. In contrast, low-temperature partial melting generates melts with low Nb/Ta ratios because residual biotite preferentially incorporates Nb over Ta (Stepanov et al., 2014 and Ballouard et al., 2016).

As biotite and Ti-bearing minerals are also involved during the differentiation of granitic melts, fractional crystallization also changes the Nb/Ta ratios:

- Nb/Ta increases in the presence of high-temperature fractional crystallization of Ti-rich melts due to the preferential saturation of Ti-oxide minerals over biotite,
- Nb/Ta ratios decrease during low-temperature differentiation of granitic melts due to the fractionation of biotite and muscovite (Stepanov et al., 2014).

Magmatic-hydrothermal processes account for the decrease of the Nb/Ta ratio in peraluminous granites.

Peraluminous granites that show significant evidence of interaction with fluids systematically display Nb/Ta ratios <5. That reflects that Nb/Ta ratio of the value of 5 represents a threshold between a purely magmatic system with Nb/Ta > 5 and a magmatic-hydrothermal one with Nb/Ta < 5 (Ballouard et al., 2016).

Besides, the decrease of the Nb/Ta ratios to values <5 in peraluminous granites reflects the concomitant effect of fractional crystallization and sub-solidus hydrothermal alteration, likely by F-rich acidic reduced fluids of magmatic origin (Stepanov et al., 2014 and Ballouard et al., 2016).

4.2.3.2 Analysis and Discussion of plotted Diagrams

This part of the project will talk about the geochemistry of the rocks which have been sampled during the sampling campaign otherwise rocks hosting 3Ts bearing minerals as it appears in the frame of this project. This includes a correlation diagram between Sn, Nb, Ta, W, and others trace elements, normalized multi-element diagram. Petrogenesis and magmatic differentiation were evaluated using Zr/Hf ratio plotted against the Nb/Ta ratio, and K/Rb ratio plotted against the Nb/Ta ratio. In addition to those diagrams quoted above, Ta has been plotted against the Ta/Nb ratio to highlight the type of deposit is available. The evaluation of post-magmatic alteration and availability of mineralization has been done using Rb/Sr and Ba/Rb ratios.

The use of Nb/Ta, Zr/Hf, Ta/Nb, K/Rb, Rb/Sr, and Ba/Rb ratios were with high significance during this geochemical characterization based on different diagrams plotted. The use of Nb/Ta ratio compared to various ratios such as K/Rb, and Zr/Hf showed different situations during rocks formation. Where:

- The higher or lower value of the Nb/Ta ratio is a function of the temperature, where high-temperature anatexis tend to have high Nb/Ta ratios because of the total consumption of biotite instead of titanium bearing oxides whereas low-temperature partial melting generates melt with low Nb/Ta ratios because residual biotite preferentially incorporates Nb over Ta (Stepanov et al., 2014).
- The ratio between Nb/Ta and K/Rb, granites with low Nb/Ta display K/Rb values less than 150, and that reflect the character of pegmatite-hydrothermal evolution (Shaw, 1968 and Ballouard et al., 2016);
- The comparison Nb/Ta ratio and Zr/Hf ratio, where Zr/Hf is considered as a marker of either magmatic-hydrothermal interaction or fractional crystallization (Linnen and Keppler, 2002; Claiborne et al., 2006 and Ballouard et al., 2016), is also a geochemical indicator of the fertility of granitic rocks, in the diagram where Nb/Ta is compared to Zr/Hf, barren granites plot in the field defined by $26<Zr/Hf<46$ and $5<Nb/Ta<16$ whereas peraluminous granites associated with Sn, W and/or U deposits have Zr/Hf ratios between 18 and 46 where Nb/Ta ratios are less than 5. But rare metals granites are characterized by lower Zr/Hf ratios less than 18 with Nb/Ta ratios that are under 5 (Ballouard et al., 2016).

- Peraluminous granites that show significant evidence of interaction with fluids show Nb/Ta ratios less than 5.
- Rb/Sr ratio shows high values where alteration is most intense, and mineralization is available, while Ba/Rb ratio shows low values in the area.

4.2.3.2.1 Buvyukana Site

1 Spider Diagram

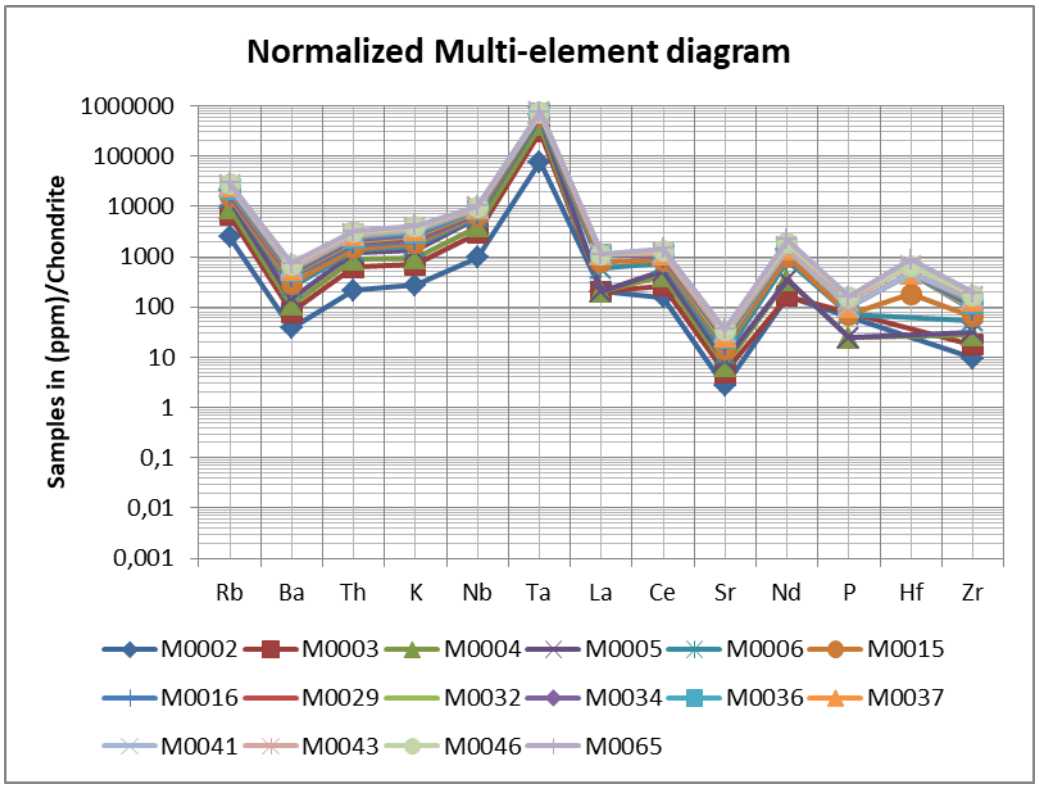

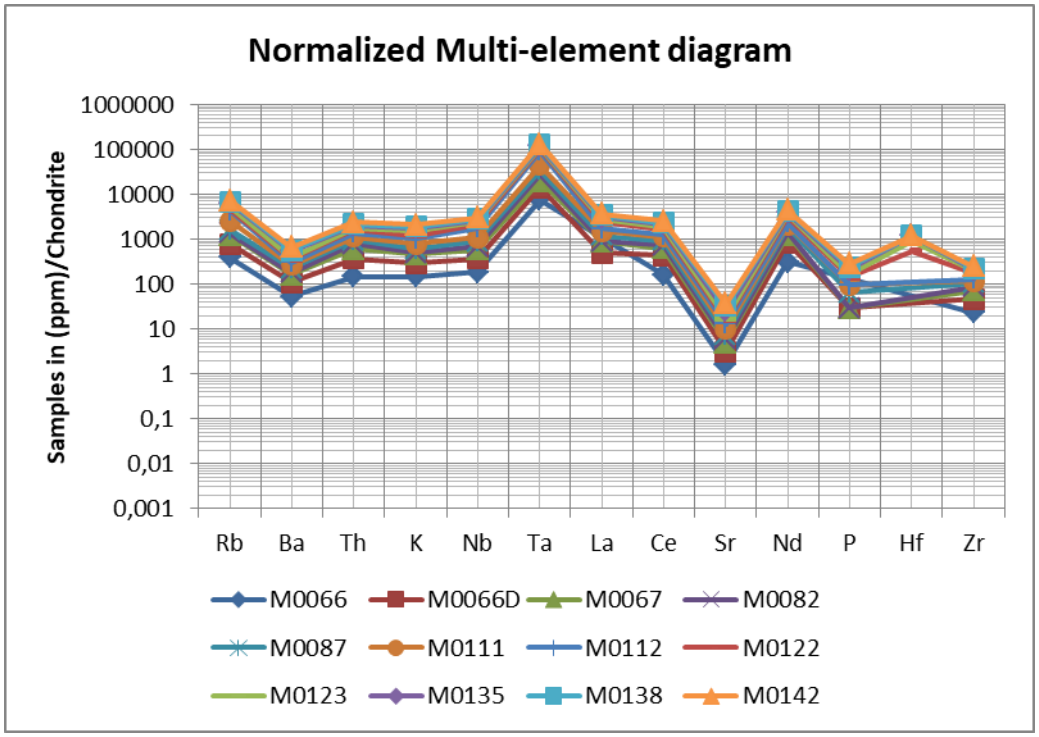

Figure 4. 15 Rare Earth element abundances in Buvyukana pegmatites and granites, normalized to Chondritic values after Thompson (1982).

Buvyukana site displays a high depletion in an element such as Mg, Ca, Cr, Ni, Ti, V, REE and Y but a high concentration in iron over 40,000 ppm, that concentration of iron is related to mica-schist in which the peraluminous granitic-pegmatites are intruded, and that explains the significant enrichment in Nb and Ta as High field Strength Elements (HFSE) (Zaraisky et al., 2009 and Ballouard et al., 2016) which is observed in Buvyukana site.

The above diagram displays a lack or a very low concentration in REE, with a negative anomaly of Ba and Sr. The negative anomaly of Sr paired with the absence of Ca imply the removal of plagioclase and the hydrothermal alteration which affected the rocks, hence, it indicates that the phenomena happened under low temperature in the upper crust where the formation of feldspars, Biotite, muscovite and quartz was favoured, in addition, Zr/Hf ratio is also too low. In contrast, the site shows enrichment in Large Ion Lithophile (LIL) group such as Rb at which K is with high concentration indicating feldspars fractionation. The negative anomaly of Sr and Ba, the low Zr/Hf ratio, and the high concentration of Rb and Th indicates peraluminous rocks (Imeokparia, 1985).

Above information reflect the crustal contamination of magma which occurs in the orogenic setting in association with crustal shortening where ore formation procedure is hydrothermal

processes. All those pieces of information correspond to the continental crust and are indicators of more differentiated/evolved and mineralized rocks which are associated with late magmatic differentiation (Jamali, 2016).

2 *K/Rbvs Nb/Ta Diagram*

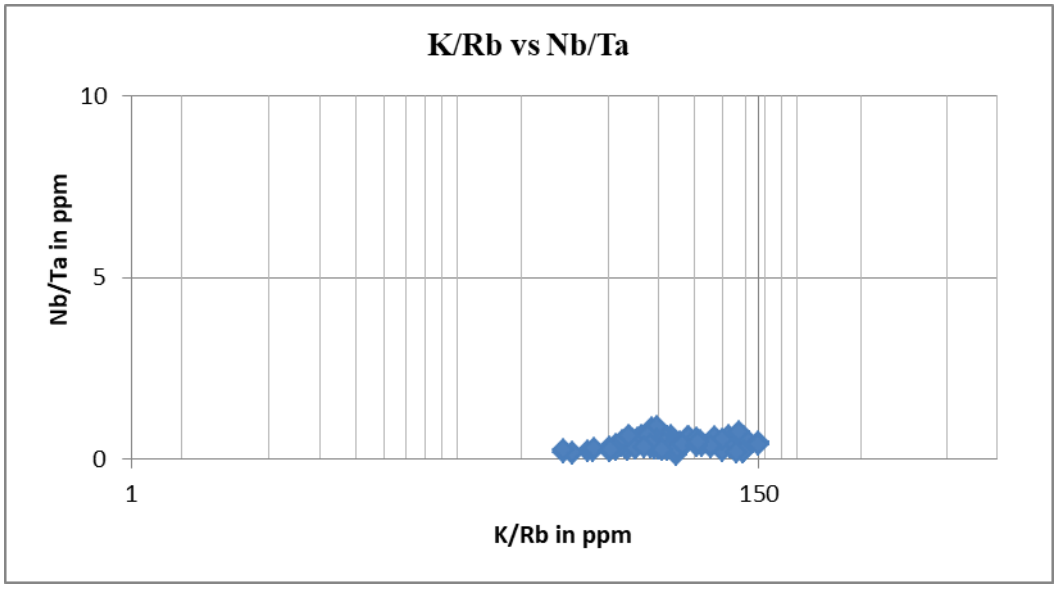

Figure 4. 16 Plot of K/Rb vs Nb/Ta highlighting pegmatite-hydrothermal evolution (Shaw, 1968 and Ballouard et al., 2016).

In this diagram (**K/Rb vs Nb/Ta)** almost all samples are plotted in the field defined by low Nb/Ta ratio < 5 and K/Rb < 150, which reflects that those samples are from rocks which their formation involves hydrothermal evolution, and subjected to post-magmatic alteration, in addition, the low Nb/Ta ratios which are less than 5 imply that the sampled rocks have been formed during low-temperature partial melting.

3 Correlation between Elements

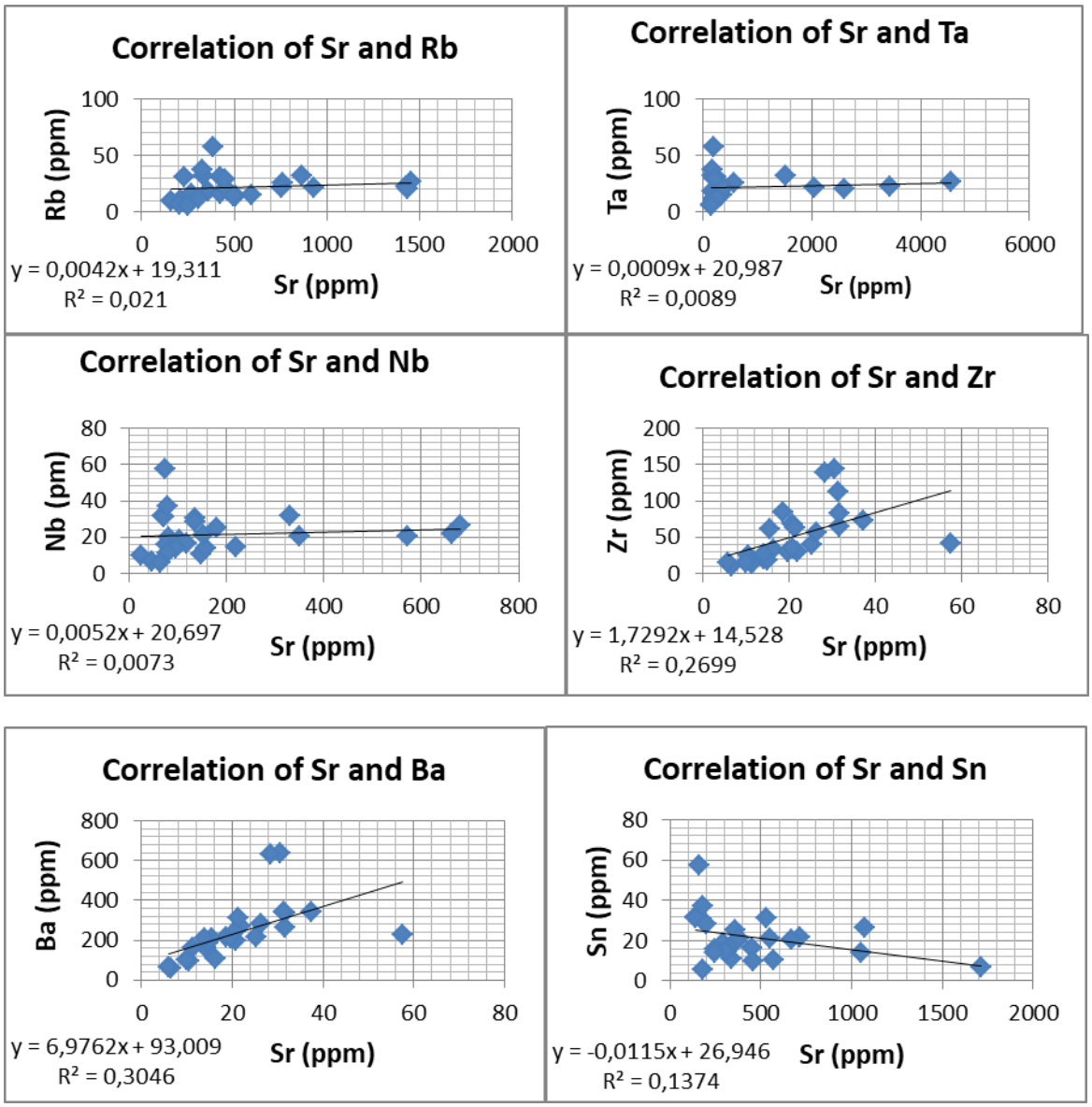

Figure 4. 17 Correlation of Sr with: Rb, Nb, Ta, Zr, Ba, and Sn in Pegmatite.

Correlation between Sr and Rb is too weak because, during hydrothermal alteration, Rb resists to the alteration while Sr is highly mobile. Sr is not correlated with Ta, Nb, and Sn because those elements (Ta, Nb, and Sn) are concentrated during a hydrothermal alteration in contrast of Sr which is leached/ transported during that process. Sr and Ba are correlated, both are LILE and mobile during hydrothermal alteration as feldspars fractionate (Imeokparia, 1985), but the positive correlation with Zr is that Zr is shifted from the melt as the crystallization evolves giving place to Hf, then it is removed in final phase where hydrothermal alteration is with high significance.

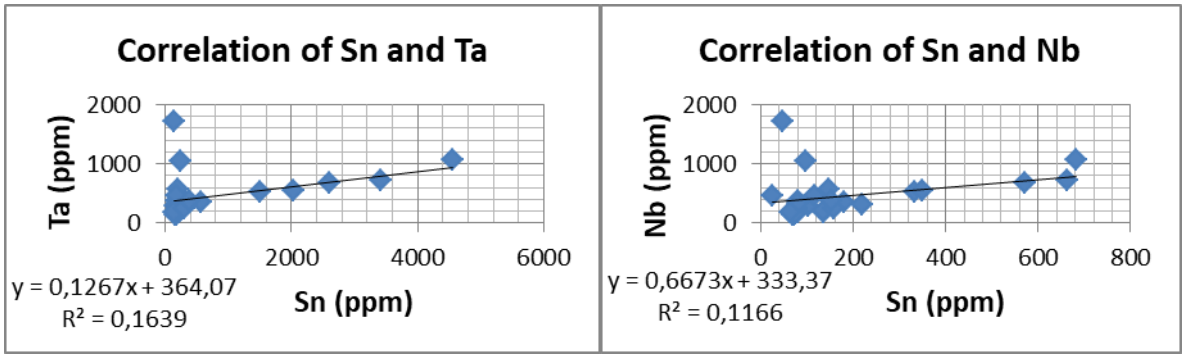

Figure 4. 18 Correlation of Sn with: Nb, and Ta in Pegmatite.

Sn shows positive correlation with Nb, and Ta, that indicates that they have been subjected to the same conditions during their crystallization and setting.

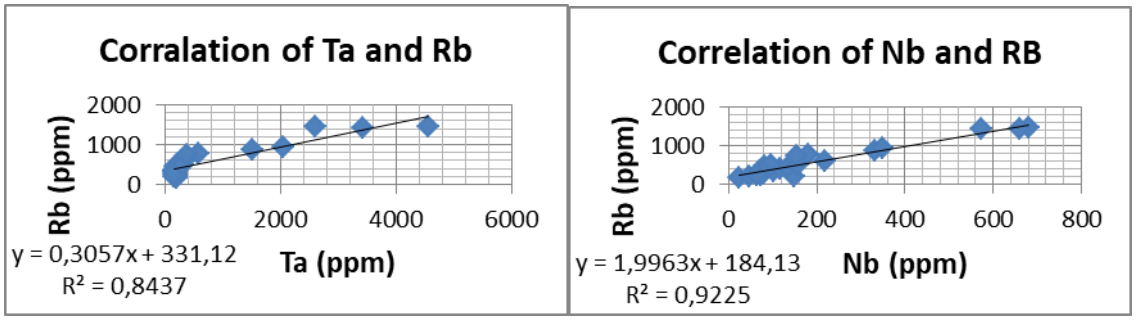

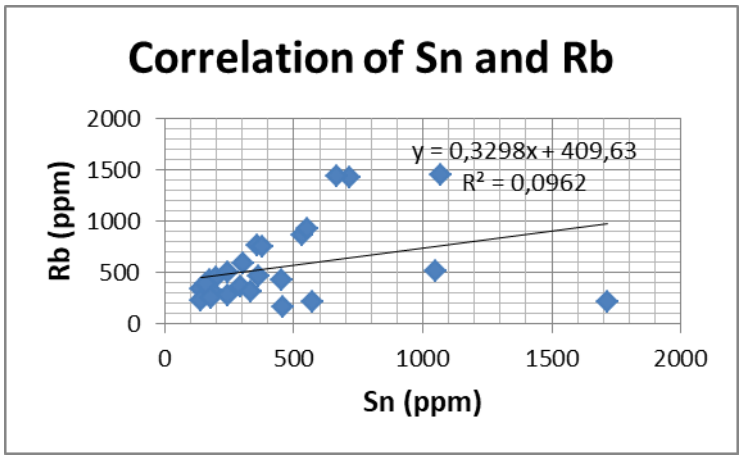

Figure 4. 19 Correlation of Rb with: Nb, Sn, and Ta in Pegmatite.

Rb is correlated with Ta, Nb, and Sn, and those elements are enriched in the crust where the concentration of Nb, Ta, and Sn is controlled by hydrothermal-alteration during which Rb is not mobile.

4 *Zr/Hf vs Nb/Ta Diagram*

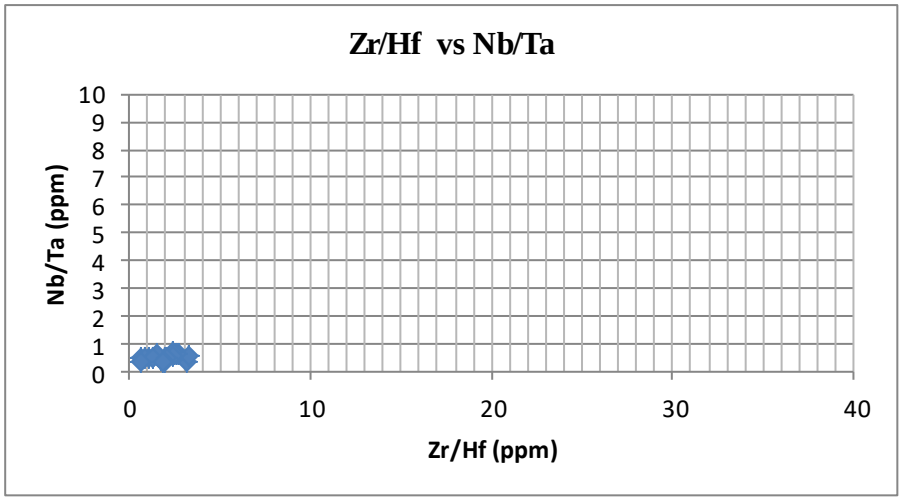

Figure 4. 20 Plot of Zr/Hf vs Nb/Ta as geochemical indicator of the fertility of granitic rocks (Linnen and Keppler, 2002; Claiborne et al., 2006 and Ballouard et al., 2016)

In this diagram (Zr/Hf vs Nb/Ta) all samples plotted in the field which falls between 0 and 1 as a value of Nb/Ta ratios and 0 and 4 as value of Zr/Hf ratios where this field answers to rare metals related granites such as Ta-Cs-Li-Nb-Be-Sn-W, and this corresponds to the LCT-pegmatite type related to S-type granite. The low Zr/Hf ratios indicate the high degree of fractionation and high evolutionary state of those rocks, and their formation took place at low temperature (Zaraisky et al., 2009; .0Stepanov et al., 2014 and Jamali, 2016).

5 *Rb/Sr vs Ba/Rb Diagram*

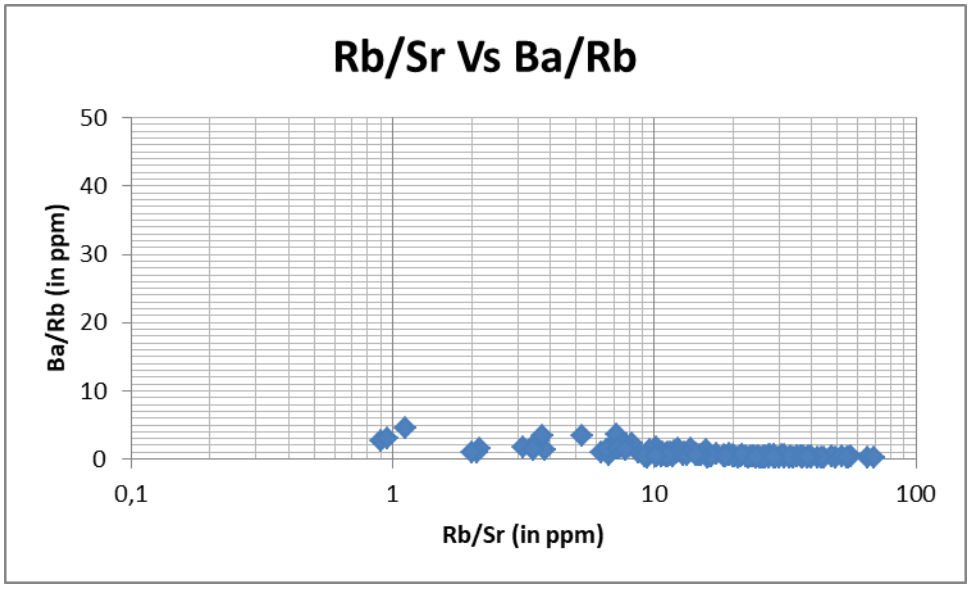

Figure 4. 21 Plot of Rb/Sr Vs Ba/Rb to test post-magmatic alteration (Imeokparia, 1981).

The plotted diagram shows high values of Rb/Sr ratio to that of Ba/Rb ratio, in such situation, the rocks, where those samples were collected display an increasing in Rb/Sr ratio in same time decreasing of Ba/Rb ratio. The above result shows that those rocks have been subjected to several alterations events such as sericitization, albitization, tourmalinization, muscovitization, kaolinization, and greisenization which are the prominent cause of occurrence of mineralization of the 3T's in the investigated area. Thus, magmatic-hydrothermal fractionation was followed by post-magmatic alteration (hydrothermal alteration).

4.2.3.2.2 Nyanza-Burenge Site

1 Spider Diagram

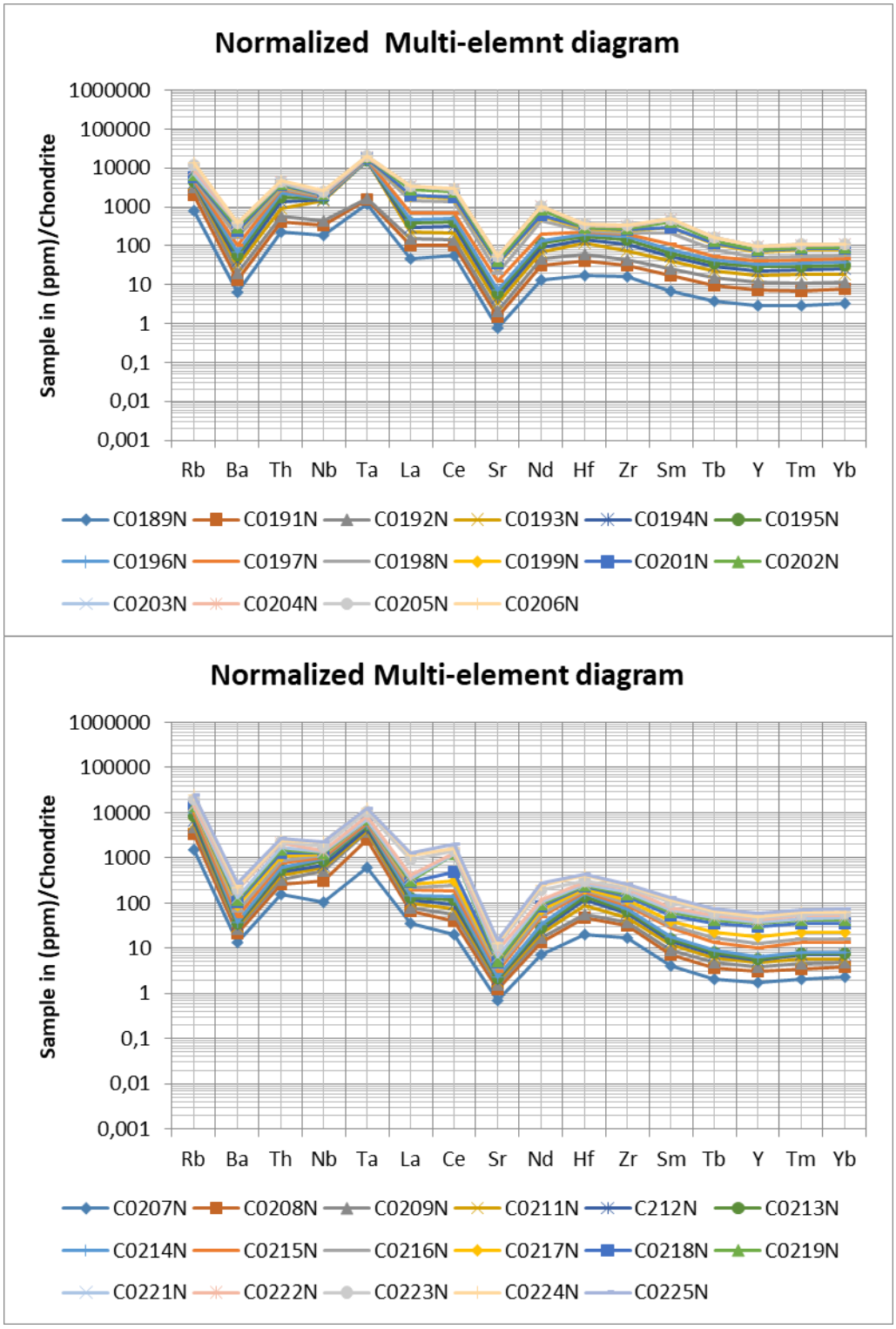

Figure 4. 22 Rare Earth element abundances in Nyanza- Burenge pegmatites and granites, normalized to Chondritic values after Thompson (1982).

Nyanza-Burenge site displays a slight depletion in an element such as Fe, Mg, Ca, Cr, Ni, Ti and V. High Field Strength Emelent (HFSE) such as Nb, and Ta with a high concentration of Nb to that of Ta, and in addition to that, other HFSE are present including W, Zr, and Hf. The above diagram displays the presence of Rare Earth Element either HREE or LREE are all present with a high concentration of LREE to that of HREE. Besides, the diagram shows a high concentration of Rb element as Large Ion Lithophile (LIL). Always the diagram shows a negative anomaly of Sr and Ba which means the removal of plagioclase, hydrothermal alteration, fractionation of feldspar, and indicates peraluminous rocks. With the above information, high concentration of Nb to that of Ta and the presence of REE imply that the sampled pegmatite belongs to NYF-pegmatite type related to I-type granite, and in addition, high concentration of Rb indicates that granites that gave liquids from which those pegmatites crystallized are generated from the crust, they correspond to sub alkaline rocks. The abundance of both Zr and Hf and high Zr/Hf ratios which are observed implies the less degree of differentiation and low evolutionary state of these rocks (Jamali, 2016). Consequently, those rocks were formed in a condition where the temperature is high compared to that of Buvyukana pegmatites.

2 *Zr/Hf vs Diagram*

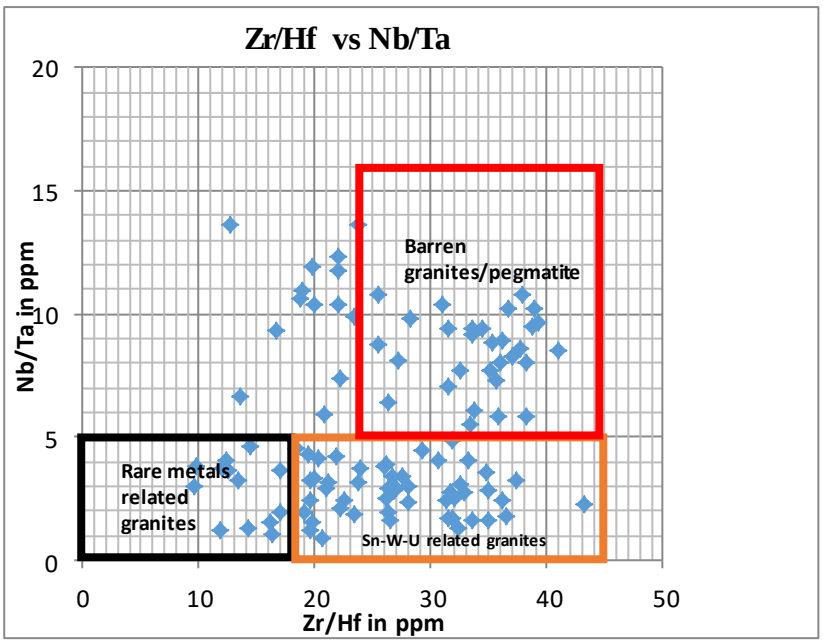

Figure 4. 23 Plot of Zr/Hf vs Nb/Ta as geochemical indicator of the fertility of granitic rocks (Linnen and Keppler, 2002; Claiborne et al., 2006 and Ballouard et al., 2016)

In this diagram (Zr/Hf vs Nb/Ta) all plotted samples are scattered and can be divided into three fields according to their position in the above diagram,

- A field defined by 0 to 18 as the value of Zr/Hf ratios and Nb/Ta<5, this field counts very little samples and corresponds to **rares metals related granites such as Ta-Cs-Li-Nb-Be-Sn-W**
- A field defined by 18 to 46 as the value of Zr/Hf with Nb/Ta<5 and correspond to peraluminous granites associated with Sn, W, and/or U deposits;
- Field defined by 26 < Zr/Hf <46 and 5 < Nb/Ta < 16 and correspond to the Barren granite (Stepanov et al., 2014)**.**

The above sub-groups indicate three environments; one is for high temperature and corresponds to pure magmatic pocessus and gave raise to barren granites field while the others display the magmatic-hydrothermal to hydrothermal with moderate temperature which corresponding to the peraluminous granites field (Sn-W-U) and **rares metals related granites with depletion in** Large Ion Lithophile (LIL)**.**

3 ***Rb/Sr vs Ba/Rb Diagram***

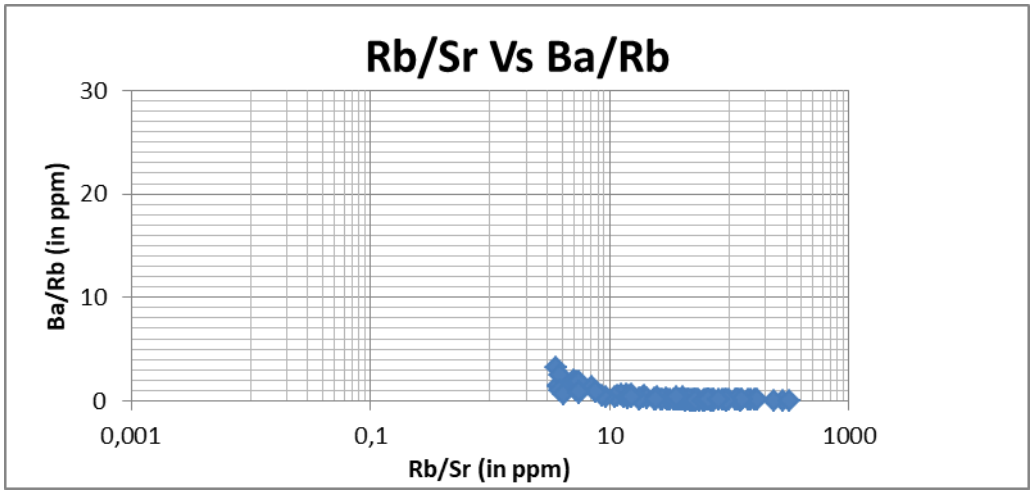

Figure 4. 24 Plot of Rb/Sr Vs Ba/Rb to test post-magmatic alteration (Imeokparia, 1981)

In this diagram, samples show high values of Rb/Sr ratio to that of Ba/Rb ratio. That implies that the sampled rocks have been subjected to a number of alterations events but no significant because the site displays a low concentration of 3Ts ores. Hence kaolinization and sericitization were significant, and however, greissenization, tourmalinization, and muscovitization also took place. The no significant hydrothermal-alteration is evidenced by the low concentration in mineralization of 3 Ts which is observed in that area.

4 *Correlations between Elements*

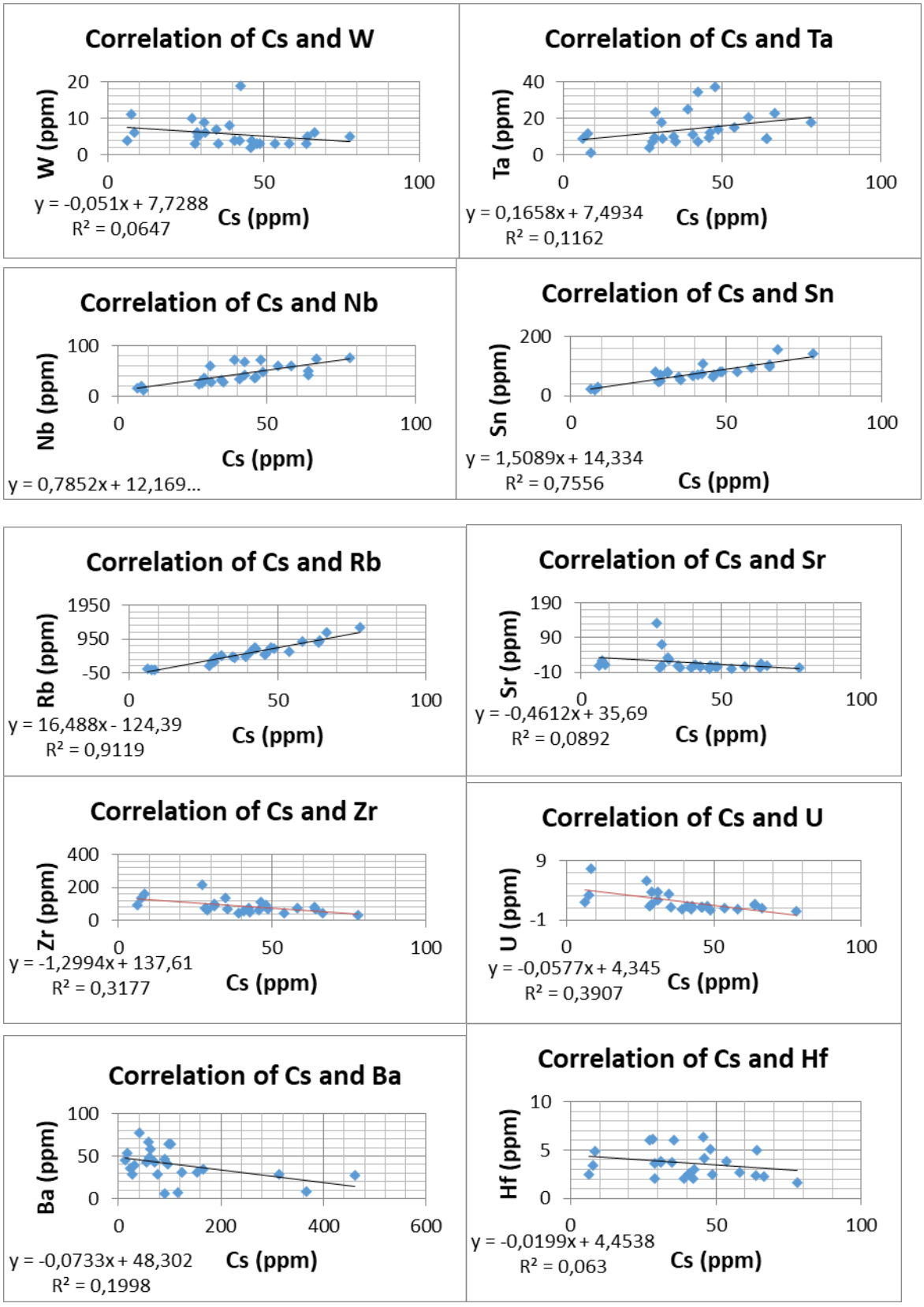

Figure 4. 25 Correlation of Cs with Nb, Sn, Ta, Rb, Zr, Ba, U, Sr, W, and Hf in Pegmatite

Cs is an element which characterized the more evolved and differentiated suites associated minerals. It is evident to have a positive correlation with elements such as Nb, Ta, Sn, and Rb, in contrast, Cs shows negative correlation with W, Sr, Zr, U, Ba and Hf remember that the analyzed rocks display an environment with high temperature, not more evolved and less differentiated, Cs is not compatible in such conditions in contrast of above elements.

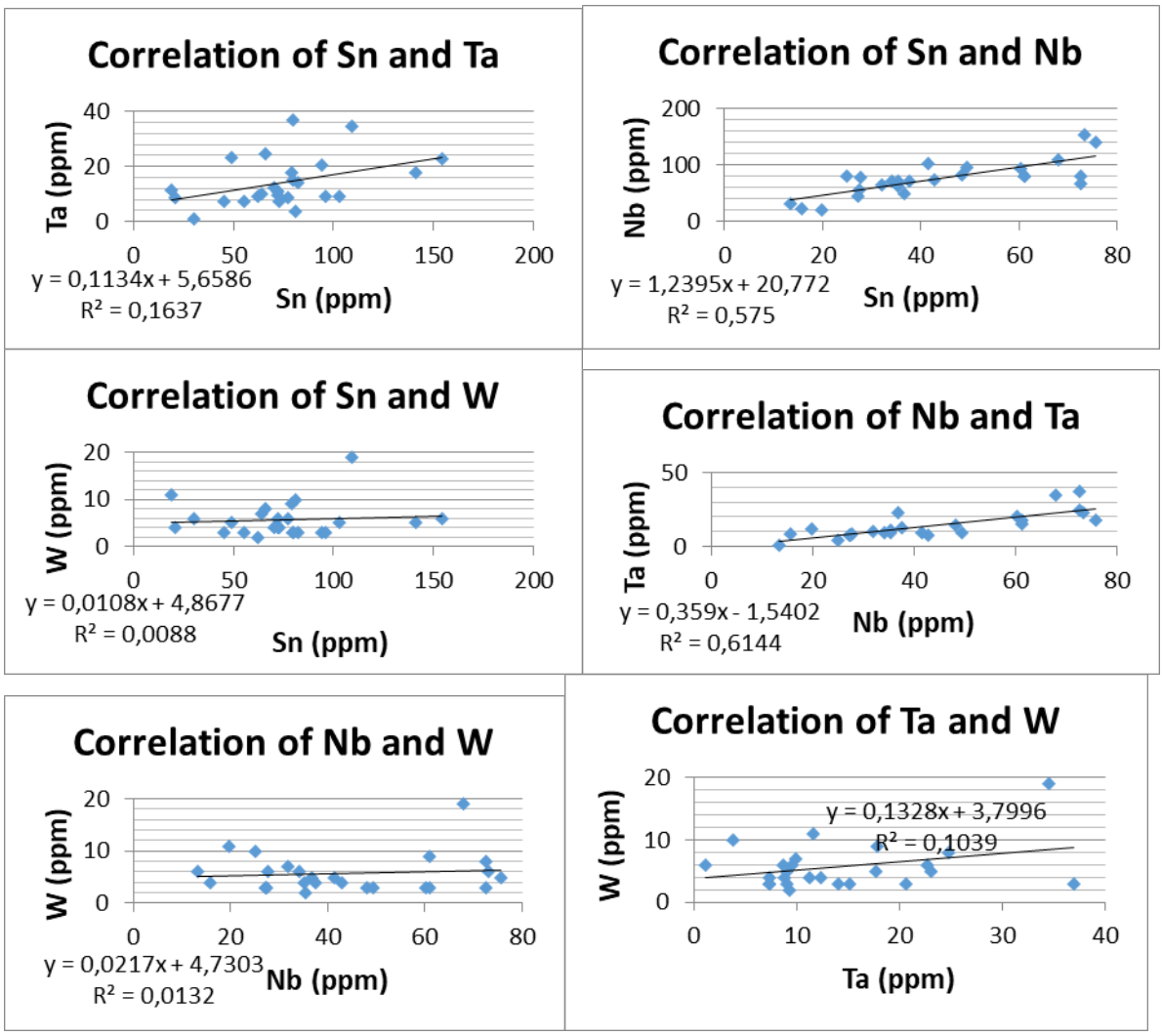

Figure 4. 26 Correlation of Sn with Nb, Ta, and W in Pegmatite; Correlation of Nb with Ta, and W in Pegmatite; and Correlation of Ta with W in Pegmatite

In the above diagrams, almost all elements are correlated except Nb vs W, and Sn vs W wich display weak correlations.

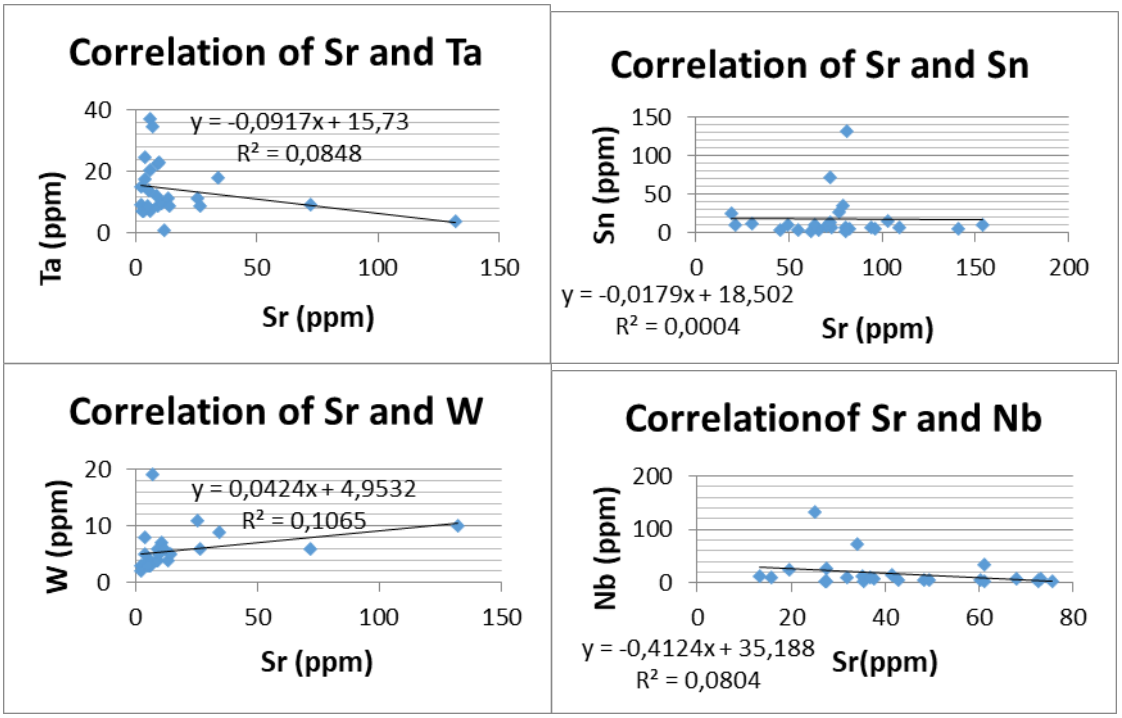

Figure 4. 27 Correlation of Sr with: Nb, Sn, Ta, and W in Pegmatite

Sr shows negative correlation with Ta, Nb, and Sn, as long as these three elements are controlled by hydrothermal alteration Sr is affected and leached. The positive correlation with W shows a similar condition during their incorporation.

4.3 CHARACTERIZATION OF 3T'S MINERALIZATION IN THE RUNYANKEZI AREA, NORTHERN BURUNDI

Rare-elements (Nb-Ta, Sn, and rarely W) rather are associated with carbonatites, peralkaline granites and feldspathoid-bearing rocks, or peraluminous granites and pegmatites. Rare-elements pegmatites have long been recognized as having two characteristic suites of rare elements.

There is a correlation between these pegmatites and different suites of granites. From that, peralkaline rare-element granites have an NYF affinity, whereas peraluminous rare-element granites have LCT affinity. But all those have a common feature to be enriched in fluxing elements, particularly F (Linnen and Cuney, 2005).

Carbonatites are well known for their LREE enrichment with a high concentration in La, Ce, Nb and Zr with depletion in Ta and Hf (Barker, 1996). Peralkaline granites are more enriched in trace-element such as REE, La, Yb, Nb, Zr and depleted in Ta and Hf while peraluminous granites in particular high phosphorus granites have very low REE concentration including Zr and Nb. By contrast, those granites are highly enriched in Ta and Hf (Linnen and Cuney, 2005 and Linnen and Ontario, 2014).

4.3.1 Overview on pegmatites rocks and nb-ta deposits

Pegmatites are exceptional coarse-grained igneous rocks with interlocking grains. They are found as irregular dykes, lenses, pods or veins within or near the margins of batholiths, plutons, or in surrounding country rocks (Simandl et al., 2018). Pegmatites are with chemical composition as that of granites, and individual pegmatites bodies may be simple or complexly zoned. They are usually associated with aplites (*Intrusive igneous rock in which the mineral composition is the same as granite, but in which the grains are much finer, less than 1 mm across. Quartz and Feldspar are the dominant minerals*) and Ta mineralizations are commonly associated with them (London, 2014 and Simandl et al., 2018).

The main primary Ta resources are found in pegmatite-related deposits, rare element-enriched granites, and in peralkaline granites complexes. Other important resources are also found in weathered crusts overlying mentioned hard-rock deposits types and in placer deposits where Ta may be a co-product of tin (Linnen et al., 2014 and Simandl et al., 2018). In contrast, most Nb is mined from Carbonatites complex-related deposits and peralkaline

intrusion, where Nb is in association with rare earth element (REE) mineralization (Simandl et al., 2018).

4.3.2 Classification of pegmatites

Based on the depth of crystallization, combined with textural, geochemical and mineralogical attributes, granitic pegmatites can be divided and subdivided into classes, subclasses, and subtypes. Pegmatites are in five distinguished categories that may contain Ta-Nb and Sn mineralization. They are abyssal, muscovite, muscovite-rare-element, rare-element, and miarolitic classes (Cerný et al., 2012 and Melcher, 2017 and Simandl et al., 2018). Rare-element pegmatite dykes derived from a fertile granite intrusion and are typically distributed over 10 to 20 km^2 area within 10 km of the fertile granite (Selway et al., 2006). Those fertile granites are characterized by more massive plutons or batholiths, typically greater than 10 km^2 in outcrop area, they are also poor in Fe, Mg, and Ca (Selway et al., 2006).

Among those various classes, the rare-element class is the most economical with respect to Ta mineralization. This class contains subclasses such as **REE subclass with Be, REE+Y, U, Th, F and Nb with Ta** as the minor element is known as NYF pegmatite; another **class is Li subclass with Li, Rb, Cs, Be, Ga, Sn, Hf, Nb-Ta, B, P and F** known as LCT pegmatite (Melcher, 2017). LCT pegmatites are concentrically but irregularly zoned, and typically have a thin border zone, a wall zone, an intermediate zone, an albite zone, and a core zone where most of the time, Tantalum **mineralization is found in the intermediate zone and albite zones** (Schulz et al., 2017).

NFY pegmatites are associated with the A-type granites, subaluminous to metaluminous (Al-Poor), quartz-poor granites or syenites (Selway et al., 2006). The said granites have an enormous quantity of K+Na, F, and Zr, low Al and high Fe/Mg. In these granites, Nb enrichment is extreme but Ta/Nb varies little.

In contrast, LCT pegmatites are associated with S-type granites which derived from sedimentary protolith and those pegmatites are from hydrous granitic magmas which derived from S-type. Those pegmatites and the granites they derived share the following characteristics (Stepanov et al., 2012 and Stepanov et al., 2014):

- Element compositions are close to the granite eutectic, with low mafic composition such as Mg, Fe, and Ca;
- High content in Li, Cs, Rb and low concentration in Sn and Be;
- Very low concentrations of Ti, Zr and LREE, with LREE depleted relative to HREE, negative Nd anomalies;
- High contents in Nb and Ta with high Th/Nb.

4.3.3 Origin of pegmatites

After crystallization of fertile granite, pluton residual fractionated granitic melt that remains, generally concentrates at the roof of the pluton, and can intrude along fractures and faults in the host rock to form pegmatite dykes (Selway et al., 2006). As the distance from the parent fertile granite intrusion increases, these dykes increase in the degree of fractionation, rare element content, volatile content, the complexity of internal zoning, and extent of alteration such as albitization of K-feldspar.

Pegmatite dykes with the greatest economic potential, hosting Li, Cs, and Ta are located at the greatest distance around 10 km from the parent granite because of their abundant volatiles content which increases the mobility of the melt (Schulz et al., 2017).

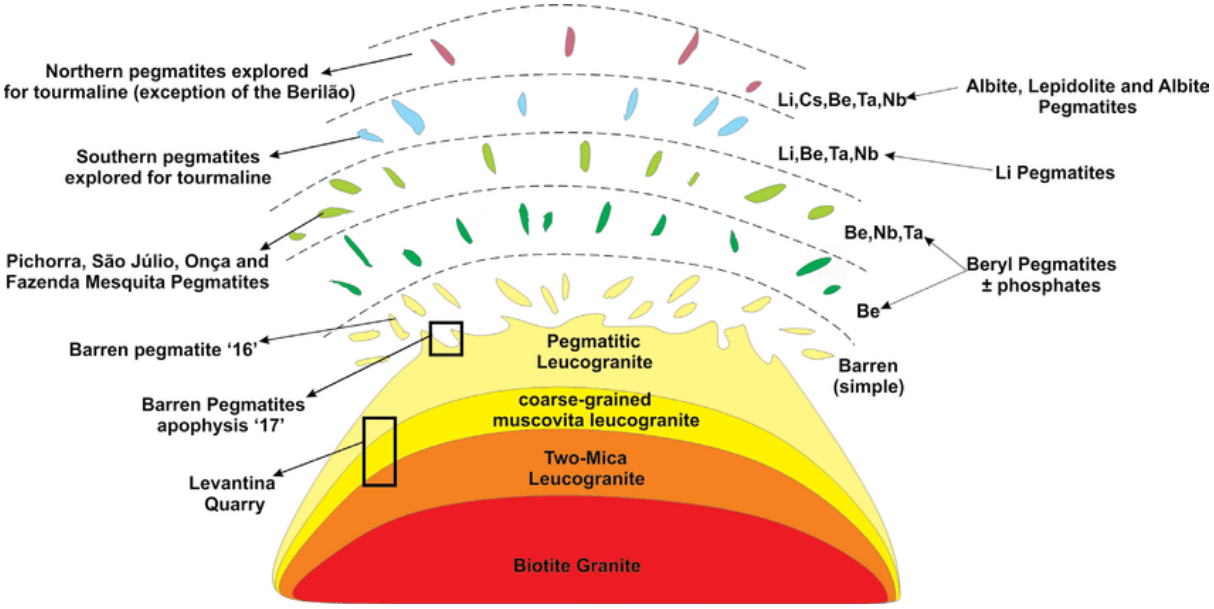

Figure 4. 28 Schematic representation of regional zoning and evolution from a simple biotite granite to a complex pegmatite, applied to the studied pegmatites (Modified from Trueman and Cerny, 1982 and London, 2008)

4.3.4 Style of mineralization in runyankezi area

Mineralizations of 3Ts in Runyankezi are found in pegmatites where their location does not follow a random emplacement. It is in altered and more evolved pegmatites that those mineralizations are found. Those pegmatites, together with their host rocks, define a well-known stratigraphy.

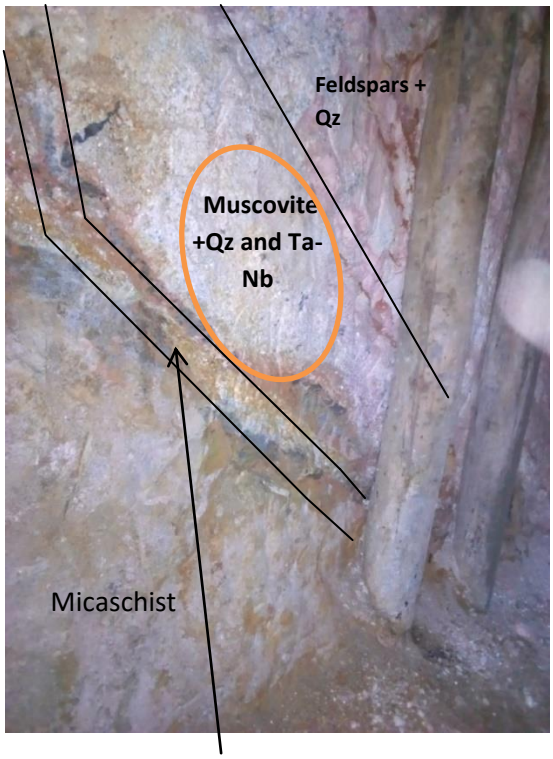

Tourmaline layer (contact zone)

Figure 4. 29 Location of the mineralization

The mineralizations are located at the greisen (muscovite-Rich) portion and decrease as the core of the pegmatite approaches (Fig.4.29), which is to say that these mineralizations are closely related to the conversion of muscovite.

It should be noted that the mineralizations in these pegmatites increase as the distance from the granite generating fluids that gave rise to these pegmatites increases. Pegmatites close to the granite are sterile/barren.

4.3.5 Association and type of deposits in runyankezi

In an area where 3T's occur, define association among them that ranges from single ore to mixed ore. Among single ore can be found Nb-Ta (always together), Sn, and W. Mixed ores are only Nb-Ta-Sn. Runyankezi accounts only single association such as Nb-Ta, and Sn but W is not present.

The type of deposit was investigated on the base of Ta vs Ta/Nb diagram in both Buvyukana and Burenge-Nyanza sites. The comparison between Ta/Nb ratio and Ta, was used to differentiate the type of deposits, from that, Ta deposits related granites-pegmatites have Ta value between 100-1000 ppm and Ta/Nb value between 1-10 ppm, Nb deposits related carbonatites have Ta value between 10-1000 ppm and Ta/Nb value between 0.001-0.1 ppm whereas upper crust is defined by Ta > 1 and Ta/Nb > 0.1 (Stepanov et al., 2014).

1 Ta vs Ta/Nb diagram in Buvyukana

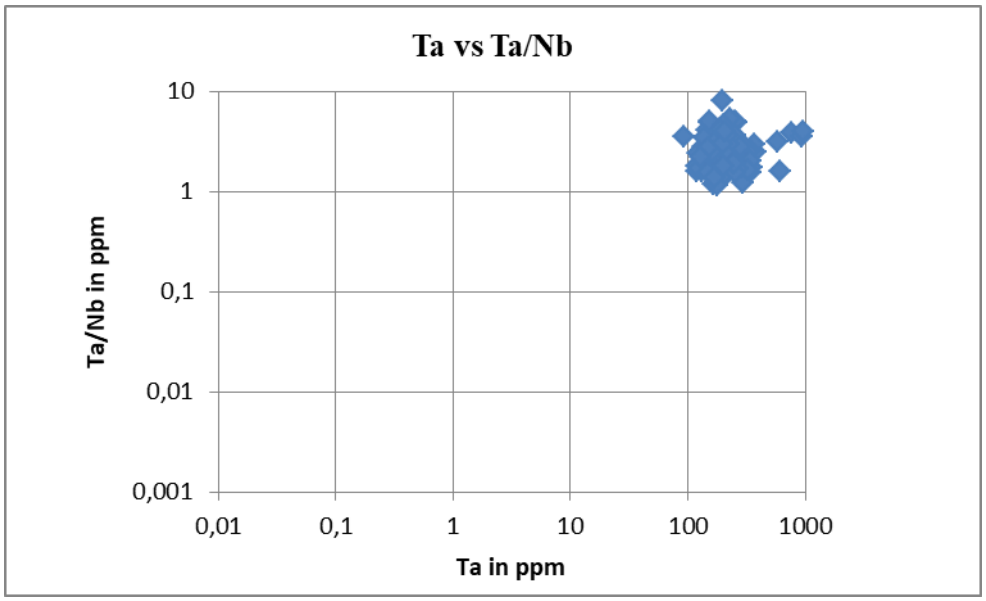

Figure 4. 30 Plot of Ta vs Ta/Nb highlighting the type of deposit (Stepanov et al., 2014)

In this diagram (Ta vs Ta/Nb) almost all samples plotted in the field defined by the value of Ta/Nb ratio comprise between 1 and 10, whereas the value of Ta is located between 100 and 1000, this position highlights and corresponds to the Tantalum deposits in granitic-pegmatites.

2 Ta vs Ta/Nb diagram in Nyanza-Burenge

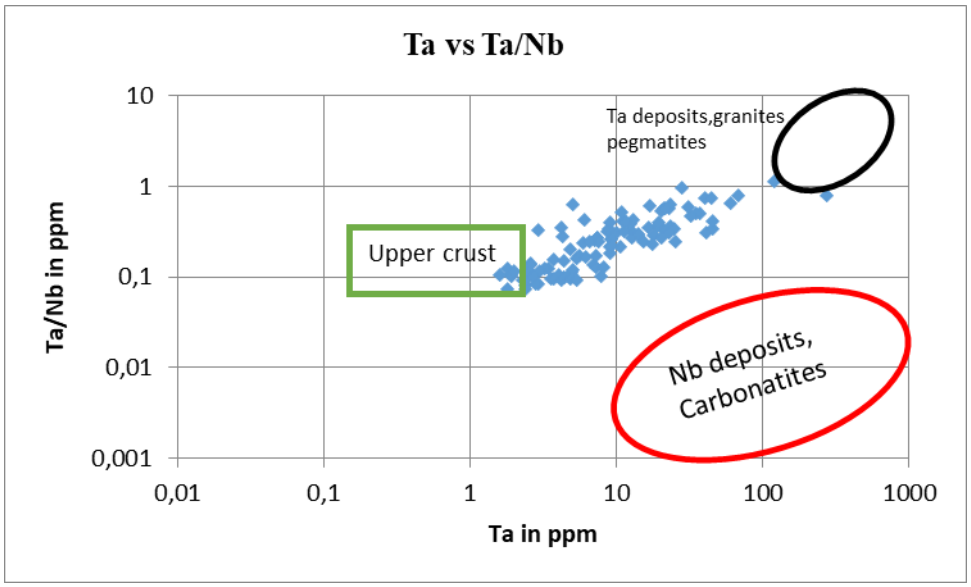

Figure 4. 31 Plot of Ta vs Ta/Nb highlighting the type of deposit is (Stepanov et al., 2014)

In this diagram (**Ta vs Ta/Nb)** almost all samples plotted in the field defined by the value of Ta/Nb ratio comprise between 0.1 and 1, whereas the value of Ta is located between 1 and 100, this position highlights and corresponds to the complex situation. The plotted samples show a transition between niobium (Nb) deposits related carbonatites to Ta deposits related granites-pegmatites, the results show a magmatic-hydrothermal in an upper-crust environment where Nb, Ta, Sn, and W are present.

These two diagrams show that Runyankezi area is dominated by Ta deposits related to granites-pegmatites.

4.4 DISCUSSION

In fact, Runyankezi accounts two types of pegmatites which appear in Buvyukana and Nyanza-Burenge sites.

In Buvyukana, pegmatites are highly evolved with a high concentration of Ta comparing to the remain of the 3Ts. Those pegmatites show very low concentration in Rare Earth Element, low ration of Zr/Hf, and a low ratio of Rb/Sr while the ratio of Ba/Rb is increasing regarding to that of Rb/Sr. Zr/Hf ratio indicates that Buvyukana pegmatites are evolved while Rb/Sr and Ba/Rb ratios indicate that those pegmatites have been subjected to hydrothermal alterations which are on the base of the high concentration of Ta, those pegmatites are far from granitic batholith and are for LCT-type. The Nb/Ta ratio is less than five, which

indicates that their formation took place at low temperature. They display rare metals related granites as type of deposit such as Ta-Cs-Li-Nb-Be-Sn-W and correspond to pure hydrothermal deposits.

In contrast, Nyanza-Burenge pegmatites are not evolved and are close to granite batholith. The site displays a very low concentration of 3Ts with a high concentration of Niobium to that of Tantalum. Those pegmatites show a high concentration in Rare Earth Element, high ratio of Zr/Hf but low Rb/Sr ratio while Ba/Rb is increasing. That indicates that Nyanza-Burenge pegmatites are not evolved, and their formation took place at high temperature with high Nb/Ta ratio greater than five, but Rb/Sr and Ba/Rb show that they have been subjected to hydrothermal alteration which is not significant because of low concentration of 3Ts. The pegmatites are of NYF-type with Nb>Ta, they display a magmatic-hydrothermal deposit in an upper-crust environment where Nb, Ta, Sn, and W are both present.

For both sites, the mineralization in pegmatite is located at muscovite rich portion, and decrease as the core of pegmatite is reached.

CHAPTER FIVE: CONCLUSION AND RECOMMENDATIONS

During this work, different methods were applied in order to respond to the different objectives which are on the base of this research project in the locality of the Runyankezi perimeter in northern Burundi. These included fieldwork including observation of the various lithologies hosting 3Ts mineralizations, sampling campaign to obtain samples that were used in the petrographic analysis by thin sections and in the geochemical analysis. By combining the results from field observations, the results from the analysis of the geochemical data by different methods as well as the results of the microscopic analysis of the thin section from the rock samples, following conclusions can be released:

1. All mineralizations of Tin, Tungsten, and Columbo-Tantalite are hosted by pegmatites. These pegmatites are subdivided into two groups: those which are independent, not associated with granite are rich in mineralization and are highly altered and those which are directly associated with granites that are less enriched in mineralization relating to the previous. In both cases the mineralization is located at the greisen-rich (muscovite-Rich) portion and decreases as the core of the pegmatite approaches, those pegmatites belong to subalkaline rocks, range from low-K to medium-K and are peraluminous;
2. The pegmatites with high mineralization are of LCT-Type associated with S-type granite show that their formation took place at low temperature. They are more evolved with Ta>Nb and are not directly associated with the parent granite. These pegmatites are located at Buvyukana site. In contrast, pegmatites with low concentration are of NYF-Type associated with I-type granite and are not far from their parent granites, their formation took place at high temperature and are not more evolved with Nb>Ta. They are found in Nyanza-Burenge site;
3. Those pegmatites have undergone post-magmatic alteration evidenced by Rb/Sr and Ba/Rb ratios (fig. 4.21; fig. 4.24);
4. The genetic setting of Tin, Tungsten, and Columbo-Tantalite is associated with hydrothermal alteration such as sericitization, tourmalinization, albitization, muscovitization, kaolinization, and greisenization which affected the rocks hosting those mineralizations;
5. The principal minerals compositions of rocks hosting 3Ts mineralization in Runyankezi are Li-rich tourmaline (elbaite), muscovite, biotite with zircon inclusion,

hornblende, feldspars, sericite, and quartz. It is noted that muscovite, biotite, sericite, and tourmaline come from replacement during hydrothermal alteration.

6. Runyankezi accounts only single association such $(Nb,Ta)_2O_5$, and SnO2 as mined ore but $(Fe, Mn)WO_4$ is not present. And those mineralizations define Ta deposits related rare-metal granite as the type of deposits.

From this study, one recommendation can be formulated:

1. It is necessary to investigate the source of the liquid which involved in crystallization and fractionation of pegmatites not directly associated with granite at Buvyukana site, which displays a high concentration of Ta and Nb.

REFERENCES

Antony, B.T., Wenner, W., David, S. and Earle, B. A., 2014. International Strategic Mineral Issues Summary Report-Tungsten. *U.S. Geological Survey Circular* 930-0, V.**1**, n°1, 86 P.

Arrachart, G., Duhamet, J., Pellet-Rostaing, S., Toure, M. and Turgis, R., 2018. Tantalum and Niobium Selective Extraction by Alkyl-Acetophenone. *Metals 2018*, Vol. **8**, N°. 654; 11p doi:10.3390/met8090654

Ballouard, C., Poujol, M., Boulvais, P. and Branquet, Y., 2016. 'Hydrothermal transition Nb-Ta fractionation in peraluminous granites : A marker of the magmatic-hydrothermal transition'. *Research gate*, pp1–5. doi: 10.1130/g37475.1.

Baudet, D., Hanon, M., Lenonne, E., Teunissen, K., 1988. Lithostratigraphie du domaine sédimentaire de la chaîne kibarienne au Rwanda. Annales de la Société Géologique de Belgique, T112 (fascicules 1): pp.225-246.

Barker, D.S., 1989. Field relations of carbonatites, in Bell, Keith, ed., *Carbonatites Genesis and evolution*: London, United Kingdom, Unwin Hyman, p. 38–69.

Barker, D.S., 1996. Carbonate volcanism. In: Mitchell Rh (ed.) *Undersaturated Alkaline Rocks: Mineralogy, Petrogenesis, and Economic Potenti*al. *Mineralogical Association of Canada* Short Course Series, vol**.24**, pp.23-61

Best, M. G., 1988. *Igneous and metamorphic petrology*. Blackwell Science Ltd, 729p.

Bhatia, M.R.,1983."Plate tectonic sand geochemical composition of sandstones,"*Journal of Geology*,**vol.91**,no.6, pp 611–627.

Bidou, J.E., 1991. Production vivrière et autossufisance alimentaire au Burundi, *Histoire sociale de l'Afrique de l'est*. Paris, Karthala, pp 260-277.

Bourgeois, F., Andreiadis, E. and Lambert, J., 2017. Tantalum and Niobium production. *State of the art*, (Match), pp 9-10.

Brinckmann, J., Lehmann, B., Hein, U., Höhndorf, A. Mussallam, K., Weiser, Th and Timm Fr. (2001) - La Géologie et la Minéralisation Primaire de l'Or de la Chaîne Kibarienne, Nord-Ouest du Burundi, Afrique orientale. *Geol. Jahrbuch Reihe*, pp 3-195.

Brinckmann, J., 1988. The post Kibaran tin and tungsten mineralization in North Burundi (Mulehe and Nyabisaka). *International Geological correlation program 255 Newsleter/bulletin,* V.**1**: pp 41-56.

Brinckmann,J., Lehmann,B and Gast, L., (1986 et 1987). Exploration de la Cassitérite et de la Wolframite dans le nord du Burundi. *Ministry of Public Work, Energy and Mines, Bujumbura, Burundi*. Rapport **1, 2 and 3**.

Brinckmann, J. and Haut, F., 1981 Rapport de la fact-finding-Mission au Burundi 1980. 135P.,

British Geological Survey, 2011. Niobium-tantalum: Keyworth, Nottingham, United Kingdom, British Geological Survey Mineral Profile, April, 27 p., accessed April 19, 2012, at *http://www.bgs.ac.uk/mineralsuk/ statistics/mineralProfiles.html*.

Cahen, L., Snelling, N.J., 1966. The geochronology of Equatorial Africa. *North-Holland Publishing company*, Amsterdam; 195pp.

Cahen, L., Lebdent,D. & Snelling, N. 1975. Données Géochronologiques dans Katangien inférieur du Kasai Oriental et du Shaba nord-oriental (République du Zaïre). *Mus. roy. Afr. Centr., Tervuren*, Dépt. Géol. Min., Rapp. ann. 1974, Pp 59-70.

Cahen, L., Snelling, N.J., Delhal, J., Vail, J.R., Bonhomme, M. & Ledent, D., 1984. The geochronology and evolution of Africa, *Clarendon Press Oxford*, 512 p.

Černý, P., and Ercit, T.S., 2005. The classification of granitic pegmatites revisited: *Canadian Mineralogist*, v. **43**, no. 6, p. 2005–2026.

Černý,P., London, D. and Novák,M., 2012. Granitic pegmatites as reflections of their sources.Elements no **8**, pp 289-294.

Chen,Y. and Zheng, Y., 2015. Science Direct Extreme Nb / Ta fractionation in metamorphic titanite from ultrahigh-pressure metagranite. *GEOCHEMICA ET COSMOCHIMICA*

ACTA, v. **150**, pp 53-73. http://dx.doi.org/10.1016/j.gca.2014.12.002

Claessens, W., and Dreesen, R., 1983. Carte Géologique du burundi, Feuille Ngozi –S 3/29-S.F 1 :100,000.

Claiborne, L.L., Miller, C.F., Walker, B.A., Wooden, J.L., Mazdab, F.K., and Bea, F., 2006. Tracking magmatic processes through Zr/Hf ratios in rocks and Hf and Ti zoning in zircons: An example from the Spirit Mountain batholith, *Nevada: Mineralogical Magazine*, v. **70**, pp 517–543, doi: 10.1180 /0026461067050348.

Deblond, A.,1993. Géologie et Pétrologie des massifs basiques et ultrabasiques de la ceinture Kabanga-Musongati au Burundi. PhD Thesis (unpublished). Université de Liège (Belgium), 235 pp.

De Clercq, F., 2012. Metallogenesis of the Nb-Ta, Sn and W ore deposits in the northern Kibara belt (Rwanda). Unpublished doctoral dissertation, K.U.Leuven, Belgium.

Demaiffe,D., Theunissen, K., 1979. Données géochronologiques U-Pb et Rb-Sr. B relatives au complexe archéen de Kikuka (Burundi). Rapp.ann. 1978, *Mus. roy . afr. Centr., Tervuren* ; Pp 65-69

Dewaele, S., Tack, L., Fernandez-Alonso, M., Boyce, A., Muchez, P., 2007a. Cassiterite and columbite-tantalite mineralization in pegmatites of the northern part of the Kibaran orogeny (Central Africa): the Gatumba area (Rwanda). In: 9th Biennal SGA Meeting. *Mineral Exploration and Research: Digging Deeper, Dublin, Ireland*, pp 1489-1492.

Dewaele, S., Tack, L., Fernandez, A.M., 2008. Cassiterite and columbite-tantalite (coltan) mineralization in in the Mezoproterozoic rocks of the northern part of the Kibaran orogen (Central Africa): preliminary results, pp 341-357.

Dewaele, S., De Clerq, F., Muchez, P., Schneider, J., Burgess, R., Boyce, A., Fernandez-Alonso, M., 2010. Geology of the cassiterite mineralisation in the Rutongo area, Rwanda (Central Africa): current state of knowledge. Geol. Belg. 13 (1-2), 91-112.

Dewaele, S., Henjes-Kunst, F.,Melcher, F., Sitnikova, M., Burgess, R., Gerdes, A., Fernandez-Alonso, M., De Clerq, F., Muchez, P. and Lehmann, B., 2011. Late Neoproterozoic overprinting of the cassiterite and columbite-tantalite bearing pegmatites of the Gatumba area, Rwanda (Central Africa): *Journal of African Earth Sciences*, v.**61**, pp 10-26.

Dewaele, S., Goethals, H. and Thys, T., (2013).'Mineralogical characterization of cassiterite concentrates from quartz vein and pegmatite mineralization of the Karagwe-Ankole and Kibara Belts, Central Africa', *Geologica Belgica*, v.**16,** n° 1 and 2, pp 66–75.

Dostal, J., Keppie, D. and Jutras, P., 2006. Evidence for the granulite–granite connection: Penecontemporaneous high-grade metamorphism, granitic magmatism and core complex development in the Liscomb Complex , *Nova Scotia , Canada*. V.**86**, pp 77-90,doi: 10.1016/j.lithos.2005.04.002

Eern, P., 1998. Tantalum oxide Niobium Minerals from complex Pegmatites in the Moldanubicum, CZECH Republiuc: *The Canadian Mineralogist*, v .**36**, pp 659-672.

Etrology, P., Li, L., and Xiong, 2017. Nb / Ta Fractionation by Amphibole in Hydrous Basaltic Systems : Implications for Arc Magma Evolution and Continental Crust Formation. V. **58**, pp 3-28, doi: 10.1093/petrology/egw070

Fernandez-Alonso, M., Cutten, H., De Waele, B., Baudet, D., Tahon, A. & Tack, L., 2012. 'The Mesoproterozoic Karagwe-Ankole Belt (formerly the NE Kibara Belt): The result of prolonged extensional intracratonic basin development punctuated by two short-lived far-field compressional events', *Precambrian Research*. *Elsevier B.v.*, **216**–**219**,pp.63–86.doi: 10.1016/j.precamres.2012.06.007.https://doi.org/10.1002/9781118755341.ch15.

Hulsbosch, N.,2015. Geological setting and timing of the world-class Sn, Nb-Ta and Li

mineralization of Manono-Kitotolo (Katanga , Democratic Republic of Congo). *Elsevier B.v* , vol. **72**,Pp373-390, doi: 10.1016/j.oregeorev.2015.07.004

Imeokparia, E., 1981. Ba/Rb and Rb/Sr ratios as indicators of magmatic fractionation, post-magmatic alteration, and mineralization- Afu younger granite complex, Northern Nigeria, Depoartment of Geology, University of Ibadan, Ibadan-Nigeria, *Geochemical Journel*, Vol.**15**, pp 209-219.

Imeokparia, E.,G., 1985. Mesozoic granite magmatism and tin mineralization in Nigeria. In:Taylor,R,P. and Strong,D,F. *Recentadvances in the Geology of Granite-related Mineral Deposits*, the Canadian Institute of Mining and Metallurgy Press,Québec, **v.39**, pp133-141.

ISABU, 2011. Burundi relief and flood risk map.

ISABU, 2002. Subdivision of Burundi in Eco-Climatic zones.

Jamali, H., 2016. The behavior of rare-earth- element, Zirconium and hafnium during magama evolution and their application in detrmining mineralized magmatic suites in subduction zones: constrains from the Cenozoic belts of Iran, *Ore geology reviews*, article: 34p, doi 10.1016/j.oregeorev.2016.10.006.

John, F. 2013. Niubium (Columbium) and Tantalum: *Minerals Yearbook (USGS):* Is. November, 2015, 18p. **http://prometia.eu/msp-reframe**

Joseph, B., Kenneth, L. and Bruce, w., 1987. A-type granites: Geochemical characteristics discrimination and petrogenesis: *Spring. Verlag/ Geological Survey of Canada*, v.**95**, pp 407-419.

Hayashi, K.I., Fujisawa, H., Holland, H. D., and Ohmoto, H., 1997. "Geochemistry of ~1.9Ga sedimentary rocks from Northeastern Labrador, Canada,"*Geochimica et Cosmochimica Acta*,**vol.61**,no.19,pp 4115–4137.

Kinnaird, J.A., Nex, P.A.M. and Milani L., 2016. Tin in Africa.

Klerks,J., 1983. The Kibaran in Burundi: a possible mode for a Proterozoic belt. 12th Colloquium of African geology, Brussels, 6-8 April 1983, Abstracts volume, 53p

Knorring, O., 1958. Niobium and Tantalum Minerals: *Communs Geol.Surv.S.W.AFr./Namibia,* v. **1**, pp 85-88.

Kokonyangi, J., 2004. Structural Constraints on Cassiterite and Columbite-Ntatalite mineralization in the kibaran Belt; D.R. Congo (Central Africa): implication for the timing of ore formation. *Journal of Geosciences, Osaka city University*. Vol. **17**: pp127-140.

Küster and Dirk, 2009. Granitoid-hosted Ta mineralization in the Arabian-Nubian Shield-Ore deposit types, tectonometallogenetic setting and petrogenetic framework: *Ore Geology Reviews*, v. **35**, no. 1, pp 68–86.

Lavreau, J., Liégeois, 1982. Granites à étain et granito-gneiss burundien au Rwanda (région de Kibuye) : âge et signification. Ann. Soc. Geol. Belg, 105: 289-294.

Ledent, D ., Cahen, L., 1979. Précision sur l'âge, la pétrogenèse et la position stratigraphique des « granites à étain » dans l'est de l'Afrique centrale. *Bull. Soc. Belge Géol*. Vol. **88**, Pp 33-39.

Le Maitre RW., 1989. A classification of igneous rocks and glossary of terms.*Oxford, Blackwell Scientific Ltd*.

Le Maitre, R.W., 2002. Igneous Rocks: A Classification and Glossary of Terms: Cambridge, Cambridge University Press, 236 p., https://doi.org/ 10.1017/CBO9780511535581.

Liegeois, J.and Lavreau., 1984. The Alkaline plutonic complex of the Upper Ruvubu (Burundi): Geology, Age, Isotopic Geochemistry and Implications for the Regional Geology of the western Belt. *Géologie afraicain- African-geology*., pp 91-114.

Linnen, R. and Ontario, W., 2014. Geochemistry of the Rare-Earth Element, Nb , Ta , Hf , and Zr Deposits. Treatise on Geochemistry. 2nd edn. *Elsevier Ltd*. doi: 10.1016/B978-0-08-095975-7.01124-4.

Linnen, R.L., Trueman, D.L., and Burt, R.O., 2014. Tantalum and niobium, in Gunn, G., ed., *Critical Minerals Handbook,* pp 361–384.

Linnen, R.L., and Cuney, Michel, 2005. Granite-related rare-element deposits and experimental constraints on Ta-Nb-W-Sn-Zr-Hf mineralization, in Rare-element geochemistry and mineral deposits: St. John's, New found land and Labrador, Canada, *Geological Association of Canada, Short Course Notes*, v. **17**, p 45–68.

Linnen, R.L., and Keppler, H., 2002, Melt composition control of Zr/Hf fractionation in magmatic processes: *Geochimica et Cosmochimica Acta*, v. **66**, pp 3293–3301. doi:10.1016 /S0016 -7037 (02) 00924-9.

Llorens, T., 2017. Tin-tantalum-niobium mineralization in the Penouta deposit (NW Spain): Textural features and mineral chemistry to unravel the genesis and evolution of cassiterite and columbite group minerals in a peraluminous system. *Elsevier B.V*, vol. **81**, Pp79-95, doi: 10.1016/j.oregeorev.2016.10.034.

London, D., 2008. *Pegmatites*: Canadian Mineralogist, Special Publication, v. **10**, 347 p.

London, D., 2014. A petrologic assessment of internal zonation in granitic pegmatites: Lithos, v. **184**–**187**, pp 74–104. https://doi.org/10.1016/ j.lithos.2013.10.025.

McQueen, K. G. (2005). '*Ore deposit types and their primary expressions'*, *Regolith Expression of Australian Ore Systems:* pp 1–14. Available at: http://www.munkhiinvolcan.mn/Images/1_OreDepositTypes.pdf.

Melcher, F. (2017). 'ranites of Africa Tantalum- (niobium-tin) mineralisation in pegmatites and rare-metal granites of Africa'. 120p, (October). doi: 10.25131/gssajg.120.1.77.

Mining, G., Materials, R. and Lima, N., 2018. Potential of Tin and tantalum / niobium in Rondônia , Brazil and the optimization of the processing methods Rondônia tin ores and their potential of Sn , Ta / Nb, (June). 27p.

Muller, D., Rock, N.M.S. and Groves, D.I., 1992. Geochemical discrimination between shoshonitic and potassic volcanic rocks in different tectonic setting: a pilot study. *Mineralogy and Petrology*, **v.46**: pp259– 286, DOI 10.1007/BF01173568.

Ntiharirizwa, S., 2013. Le potantiel en resource minérale du Burundi, nord-est de la ceinture orogénique Kibarienne, Afrique central-orientale. Maîtise inter universitaire en Science de la Terre.Québec, Canada : 120p.

OBM., 2019. Evaluation du secteur Minier et Carrier du Burundi.

Olushpla, S. and Folahan,A., 2011. A Review of Niobium-Tantalum Separation in Hydrometallurgy. *Journal of Minerals & Materials Characterization & Engineering*, Vol. **10**, n°.3, pp.245-256, 2011

Papp, J.F., 2013b. Niobium (columbium): *U.S. Geological Survey* Mineral Commodity Summaries 2013, p 110-111. [Also available at http://minerals.usgs.gov/minerals/pubs/ mcs/2013/mcs2013.pdf.]

Papp, J.F., 2013c. Tantalum: *U.S. Geological Survey* Mineral Commodity Summaries 2013, pp 162-163. [Also available at http://minerals.usgs.gov/minerals/pubs/mcs/2013/ mcs2013.pdf.]

Parker, R., and Fleischer, M., 1968. Geochemistry of niobium and tantalum: *U.S. Geological Survey* Professional Paper **612**, 43 p.

Perks, R., and Karen. H., 2016. Transparency in Revenues from Artisanal and Small-Scale Mining of Tin, Tantalum, Tungsten and Gold in Burundi. Washington, DC: *World Bank.*

Pirajno, F., 2013. Effects of metasomatism on mineral systems and their host rocks: Alkali metasomatism, skarns, greisens, tourmalinites, rodingites, black-wall alteration and listevenites, in Harlov, D.E., and Austrheim, H., eds, *Metasomatism and the Chemical Transformation of Rock*: Lecture Notes in Earth System Sciences: Berlin, *Springer Berlin Heidelberg*, pp203–252.

Richard, N. and David, M., 1993. International Strategic Minerals Inventory Summary

Report- Niobium (Columbium) and Tantalum: *U.S Geological Survey*, pp 3-13.

Rollinson, H. R.,1993. *Using Geochemical data*: Evaluation, Presentation, Interpretation. Pearson Education Limited, Edinburgh, 380p.

Roskill Information Services Ltd., 2012. Tantalum-Market outlook to 2016 (11th ed.): London, United Kingdom, *Roskill Information Services Ltd*., 164 p.

Schulz, K.J., Piatak, N.M., and Papp, J.F., 2017. Niobium and tantalum, chap. M of Schulz, K.J., DeYoung, J.H., Jr., Seal, R.R., II, and Bradley, D.C., eds., *Critical mineral resources of the United States-Economic and environmental geology and prospects for future supply*: *U.S.Geological Survey* Professional Paper **1802**, p. M1– M34, https://doi.org/ 10.3133/pp1802M.

Schwela, U., 2010. Tantalum (A supplement to Mining Journal), with a section on the state of tantalum mining: *Mining Journal*, special publication London, United Kingdom, Aspermont, September, 11 p., accessed December 15, 2012, at *http://www.mining-journal.com/__data/assets/supplement_file_attachment/0011/237287/Tantalum2010_scr.pdf*.

Scotia, N. and Dostal, J., 2018. Contrasting behaviour of Nb / Ta and Zr / Hf ratios in a peraluminous granitic plutons NovaScotia, Canada. *CHEMICAL GEOLOGY*: V.**2541**, pp 207-2018, doi: 10.1016/S0009-2541(99)00113-8.

Selway, J. B., (2006). 'A Review of Rare-Element (Li-Cs-Ta) Pegmatite Exploration Techniques for the Superior Province , Canada , and Large Worldwide Tantalum Deposits Overview of Parental Fertile Granites', **14**, pp1-30.

Shand, S.J., 1943. *The eruptive rocks*: 2nd edition, John Wiley, New York, 444p.

Shaw, D., 1968, A review of K-Rb fractionation trends by covariance analysis: *Geochimica et Cosmochimica Acta*, v. **32**, p 573-601, doi: 10.1016 /0016 -7037 (68) 90050-1.

Simandl, G. J. and Columbia, B. 2016. Geology, market and supply chain of niobium and tantalum-a Review, 263p, doi: 10.1007/s00126-014-0551-2.

Simandl, R., Burr, D., Trueman, D., and Paradis, S., 2018. Tantalum and Niobium: Deposits, Resources, Exploration Methodes and Market-A Primer for Geoscientists. *Geoscience Canada*: Vol. **45**, pp 85-94.

Sinclair, W.D., 1986, Molybdenum, tungsten and tin deposits and associated granitoid intrusions in the northern Canadian Cordillera and adjacent parts of Alaska, in Morin, J.A., ed., *Mineral deposits of northern Cordillera*: The Canadian Institute of Mining and Metallurgy Special Volume **37**, p 216-233.

Skinner, B. J., 2005. Introduction To Ore-Forming Processes, *American Mineralogist*, v.**90**, doi: 10.2138/am.2005.426, 276p.

Stepanov, A., Hermann, J., 2013. Fractionation of Nb and Ta by biotite and phengite: implications for the ‘‘missing Nb paradox’’. Geology , v.**41**, pp 303–306. doi:10.1130/G33781.1.

Stepanov, A., Mavrogenes, J.A., Meffre, S., and David son, P., 2014. The key role of mica during igneous concentration of tantalum: Contributions to Mineralogy and Petrology, v. **167**, p. 1009– 1016, doi:10.1007/s00410-014-1009-3.

Sto-Viruet, B.Y., 2013. An Exploration in Mineral Supply Chain Mapping Using Tantalum as an Example: *USGS.*

Tack, L., Duchesne, J.C., Liégeois, J.P. and Deblond, A. (1994). Two successive mantle-derived A-type granitoids in Burundi: Kibaran late-orogenic extensional collapse and lateral shear along the edge of the Tanzania craton. - *Precambr. Res.,* v.**68**, pp323-356.

Tack, L. Baudet, D., Chartry, G., Deblond, A., Fernandez-Alonso, M., Lavreau, J., Liégeois, J.P., Tahon, A., Theunissen, K., Trefois, Ph. and Wingate, M., 2002. ‘The “northeastern Kibaran belt” (NKB) and its mineralisations reconsidered: new constraints from a revised lithostratigraphy, a GIS-compilation of existing geological maps and a review of recently published as well as unpublished igneous emplacement ages ’, *11th IAGOD Quadrennial Symposium and Geocongress*, 42p.

Tack, L., Baudet, D., Tahon, A., De waele, B., Fernandez-Alonso, M., Dewaele, S., Cutten.H., 2006 The northeastern Kibaran Belt (NKB): a long-lived Proterozoic interplete history. In:*21st Colloquium African Geology (CAG21*), 03-05.07.2006, Maputo, Mozambique, Abstract volume, pp 149-151.

Tack, L., Wingate,M.T.D., DeWaele, B., Meet, J., Belousova, E., Griffin, B., Tahona, A., Fernandez-Alonso, M., (2010). 'The 1375 Ma "Kibaran event" in Central Africa: Prominent mplacement of bimodal magmatism under extensional regime', *Precambrian Research. Elsevier B.V.*, **180,** pp. 63–84. doi: 10.1016/j.precamres.2010.02.022.

Tarek, A.,2016. Niobium and Tantalum: Geology, mineralogy, geochemistry and industrial applications, 61p.

Theunissen, K., 1979 Caractère et evolution tectonométamorphiques du Précambrien de la Feuille S3/29Sw Cibitoke (NW Burundi). *Ms. Roy. Afr. Centr., Tervuren (Belg.),* Dépt. Géol. Min., Rapp. ann. 1978, pp 135-168

Theunissen . K., and Klerks,J., 1980. The structural evolution of the Kibaran orogeny in Rwanda and Burundi in the light of the presently available radiometric data in the Kibaran belt from Shaba to Uganda. – Rapp; annu. *Mus. R; Afr. Centr Tervuren (Belg.),* dépt. Géol. Min. (1979) Pp 215-217.

Theunissen, K., 1983 Pan-African and late Kibaran tectonics in Western Burundi. *12th Colloquium of African Geol*., Brussel, 97p

Theunissen, K., 1983. Tectonics of the Kibaran belt. Unesco sponsored workship on the Kibaran, *ministry of Public Work, Energy and Mines, Bujumbura, Burundi*, pp 16-23, Is: october 1983, 8p.

USGS. U.S. Geological Survey, 2017, Appendix C -Reserves and resources: Mineral Commodity Summaries 2017: *U.S. Geological Survey,* p 195-198, https://doi.org/10.3133/70180197.

USGS. U.S. Geological Survey, 2018, Final List of Critical Minerals 2018: Executive Order 13817, Department of the Interior, https://www.federalregister.gov/documents/2018/05/18/2018-10667/final-list-of-critical-minerals-2018, accessed June 14, 2018.

Thompson, R.N., 1982. British Tertiary volcanic province. *Scott. F. Geol*., v.**18**, pp 49-107.

Wood, S., 2005. The aqueous geochemistry of zirconium, hafnium, niobium, and tantalum, in Linnen, R.L., Samson, I.M., and Martin, R.F., eds., *Rare-element geochemistry and mineral deposits*: St. Johns, Newfoundland and Labrador, Canada, *Geological Association of Canada*, Short Course Notes, v. **17**, pp 217–26.

Zaraisky, G.P., Aksyuk, A.M., Devyatova, V.N., Udoratina, O.V., and Chevychelov, V.Y., 2009. The Zr/Hf ratio as a fractionation indicator of rare-metal granites: Petrology, v. **17**, pp 25-45, doi: 10 .1134 /S0869591109010020.

LIST OF APPENDICES

Appendix A: Chemical analyses of Whole Rock from Buvyukana (in ppm)

Sample Number	Co	Co Error	Ni	Ni Error	Rb	Rb Error	Sr	Sr Error	Y	Y Error	Zr	Zr Error	Target	Type of sample	Datum: WGS_84 X	Y	LITHO
M0001	< LOD	82,81	< LOD	42,96	760,83	11,39	25,19	1,66	< LOD	5,55	40,5	2,32	Buvyukana	Pit sample	29,96318	-2,63913	PEG
M0002	< LOD	90,49	< LOD	44,43	863,89	13,31	31,5	1,85	< LOD	6,12	65,28	2,82	Buvyukana	Pit sample	29,96318	-2,63913	PEG
M0003	< LOD	92,6	< LOD	45,96	1456,66	22,32	26,43	1,86	< LOD	8,31	55,66	2,84	Buvyukana	Pit sample	29,96318	-2,63913	PEG
M0004	< LOD	82,67	< LOD	45,09	931,46	14,22	20,81	1,62	< LOD	6,38	67,38	2,86	Buvyukana	Pit sample	29,96318	-2,63913	PEG
M0005	< LOD	87,06	< LOD	47,13	1429,8	21,78	21,98	1,75	< LOD	8,21	30,36	2,39	Buvyukana	Pit sample	29,96318	-2,63913	PEG
M0006	< LOD	166,61	< LOD	48,68	424,2	8,38	30,62	1,86	< LOD	4,4	143,95	4,3	Buvyukana	Pit sample	29,96319	-2,63993	PEG
M0007	< LOD	113,86	< LOD	42,01	358,15	6	18,57	1,41	< LOD	3,59	84,34	2,87	Buvyukana	Pit sample	29,96319	-2,63993	PEG
M0008	< LOD	75,6	< LOD	40,11	423,11	6,49	16,32	1,3	< LOD	3,67	33,4	1,97	Buvyukana	Pit sample	29,96319	-2,63993	PEG
M0009	< LOD	94,29	< LOD	43,08	461,36	7,69	19,61	1,47	< LOD	4,14	30,44	2,07	Buvyukana	Pit sample	29,96319	-2,63993	PEG
M0011	< LOD	110,62	< LOD	42,94	268,32	5,05	15,57	1,35	< LOD	3,19	61,56	2,58	Buvyukana	Pit sample	29,96319	-2,63993	PEG
M0012	< LOD	66,18	< LOD	37,63	212,78	3,7	10,48	1,07	< LOD	2,39	25,67	1,72	Buvyukana	Pit sample	29,96319	-2,63993	PEG
M0013	< LOD	107,48	< LOD	43	336,4	5,9	31,54	1,72	< LOD	3,53	82,61	2,91	Buvyukana	Pit sample	29,96329	-2,63992	PEG
M0014	< LOD	111,2	< LOD	42,23	229,06	4,31	31,31	1,67	< LOD	2,88	113,03	3,27	Buvyukana	Pit sample	29,96329	-2,63992	PEG
M0015	< LOD	95,34	< LOD	41,18	326,39	5,57	37,33	1,78	< LOD	3,33	72,16	2,67	Buvyukana	Pit sample	29,96329	-2,63992	PEG
M0016	< LOD	249,86	< LOD	49,2	448,22	8,3	28,42	1,82	< LOD	4,64	138,79	4,14	Buvyukana	Pit sample	29,96319	-2,63993	PEG
M0017	< LOD	98,4	< LOD	43,43	388,64	6,47	57,63	2,25	< LOD	3,86	40,78	2,32	Buvyukana	Pit sample	29,96329	-2,63992	PEG
M0018	< LOD	93,46	< LOD	48,47	1435,9	22,95	20,75	1,76	< LOD	8,31	34,28	2,48	Buvyukana	Pit sample	29,96318	-2,63913	PEG
M0019	< LOD	76,95	< LOD	41,73	512,32	7,85	14,06	1,31	< LOD	4,27	19,12	1,81	Buvyukana	Pit sample	29,96321	-2,6399	PEG
M0021	< LOD	61,09	< LOD	38,45	306,89	4,97	11,23	1,13	< LOD	2,99	12,91	1,56	Buvyukana	Pit sample	29,96321	-2,6399	PEG
M0022	< LOD	57,85	< LOD	38,93	161,9	3,25	9,98	1,1	< LOD	2,15	15,61	1,61	Buvyukana	Pit sample	29,96321	-2,6399	PEG
M0023	< LOD	57,77	< LOD	40,78	206,26	3,87	6,53	1,04	< LOD	2,6	9,67	1,54	Buvyukana	Pit sample	29,96321	-2,6399	PEG

Sample Number	Co	Co Error	Ni	Ni Error	Rb	Rb Error	Sr	Y	Y Error	Zr	Zr Error	Target	Type of sample	Datum: WGS_84 X	Y	LITHO
M0025	< LOD	70,39	< LOD	41,14	591,18	9,03	14,84	< LOD	4,56	18,96	1,83	Buvyukana	Pit sample	29,96321	-2,6399	PEG
M0026	< LOD	70,66	< LOD	41,2	493,53	7,62	14	< LOD	4,18	26,83	1,95	Buvyukana	Pit sample	29,96321	-2,6399	PEG
M0027	< LOD	98,8	< LOD	42,96	753,65	11,51	21,31	< LOD	5,43	62,43	2,65	Buvyukana	Pit sample	29,96318	-2,63913	PEG
M0028	< LOD	82,24	< LOD	39,57	536,55	8,16	14,79	< LOD	4,15	42,41	2,12	Buvyukana	Pit sample	29,96318	-2,63913	PEG
M0029	< LOD	80,23	< LOD	40,63	501,24	7,67	12,82	< LOD	4,12	24,24	1,89	Buvyukana	Pit sample	29,96318	-2,63913	PEG
M0031	< LOD	62,94	< LOD	40,12	326,61	5,39	10,36	< LOD	3,22	13,72	1,64	Buvyukana	Pit sample	29,96321	-2,6399	PEG
M0032	< LOD	71,89	< LOD	41,02	651,66	9,58	13,16	< LOD	4,82	27,72	1,98	Buvyukana	Pit sample	29,96321	-2,6399	PEG
M0033	< LOD	72,55	< LOD	41,99	602,54	9,2	10,92	< LOD	4,73	35,87	2,14	Buvyukana	Pit sample	29,96321	-2,6399	PEG
M0034	< LOD	93,01	< LOD	41,3	216,11	4,06	34,61	< LOD	2,74	83,84	2,81	Buvyukana	Pit sample	29,96322	-2,63932	PEG
M0035	< LOD	73,11	< LOD	38,51	188,48	3,53	19,96	< LOD	2,41	77,27	2,58	Buvyukana	Pit sample	29,96322	-2,63932	PEG
M0036	< LOD	130,44	< LOD	47,08	642,72	10,78	25,66	< LOD	5,4	99,48	3,42	Buvyukana	Pit sample	29,96321	-2,63923	PEG
M0037	< LOD	116,11	< LOD	44,25	767,16	13,96	23,05	< LOD	5,63	102,93	3,5	Buvyukana	Pit sample	29,96321	-2,63923	PEG
M0039	< LOD	312	119,3	49,25	40,59	2,47	56,86	18,82	2,75	247,9	9,16			29,96221	-2,64052	LAT
M0041	< LOD	101,45	< LOD	40,24	187,02	3,67	48,9	< LOD	2,45	88,33	2,85	Buvyukana	Pit sample	29,96329	-2,63992	PEG
M0042	< LOD	101,09	< LOD	42,29	333,96	5,72	27,49	< LOD	3,48	76,53	2,78	Buvyukana	Pit sample	29,96329	-2,63992	PEG
M0043	< LOD	99,55	< LOD	42,4	401,82	7	30,96	< LOD	3,88	66,47	2,68	Buvyukana	Pit sample	29,96329	-2,63992	PEG
M0044	< LOD	88,95	< LOD	41,92	410,58	6,56	34,93	< LOD	3,83	37,62	2,18	Buvyukana	Pit sample	29,96329	-2,63992	PEG
M0045	< LOD	105,58	< LOD	42,57	496,38	7,88	17,21	< LOD	4,28	22,8	1,91	Buvyukana	Pit sample	29,96321	-2,6399	PEG
M0046	< LOD	123,53	< LOD	43,38	666,81	10,3	24,14	< LOD	5,06	108,18	3,32	Buvyukana	Pit sample	29,96321	-2,63923	PEG
M0047	< LOD	86,4	< LOD	41,91	425,92	6,85	17,72	< LOD	3,93	31,56	2,05	Buvyukana	Pit sample	29,96321	-2,6399	PEG

Sample Number	Ag	Ag Error	Cd	Cd Error	Sb	Ba	Ba Error	La	La Error	Ce	Ce Error	Target	Type of sample	Datum: WGS_84 X	Y	LITHO
M0001	< LOD	5,84	< LOD	7,04	< LOD	217,23	30,09	< LOD	65,67	77,86	43,98	Buvyukana	Pit sample	29,96318	-2,63913	PEG
M0002	< LOD	3,95	9,09	4,91	< LOD	262,81	31,38	65,67	40,49	134,48	45,84	Buvyukana	Pit sample	29,96318	-2,63913	PEG
M0003	< LOD	4,6	< LOD	8,33	< LOD	284,32	35,96	< LOD	92,47	95,13	52,18	Buvyukana	Pit sample	29,96318	-2,63913	PEG
M0004	< LOD	4,04	8,79	4,98	< LOD	198,29	31,28	< LOD	73,33	125,86	46,41	Buvyukana	Pit sample	29,96318	-2,63913	PEG
M0005	< LOD	6,53	9,82	5,34	< LOD	271,78	34,08	< LOD	85,5	95,24	49,44	Buvyukana	Pit sample	29,96318	-2,63913	PEG
M0006	< LOD	4,63	< LOD	8,8	< LOD	639,77	40,04	125,17	47,31	178,59	53,44	Buvyukana	Pit sample	29,96319	-2,63993	PEG
M0007	< LOD	4,07	10,24	5,01	< LOD	218,26	31,48	71,39	41,17	121,88	46,44	Buvyukana	Pit sample	29,96319	-2,63993	PEG
M0008	< LOD	4,85	< LOD	6,83	< LOD	107,85	28,28	< LOD	62,79	93,16	42,53	Buvyukana	Pit sample	29,96319	-2,63993	PEG
M0009	< LOD	4,75	8,69	4,83	< LOD	207,03	30,33	< LOD	84,97	< LOD	66,32	Buvyukana	Pit sample	29,96319	-2,63993	PEG
M0011	< LOD	6,4	< LOD	10,29	< LOD	210,1	31,18	< LOD	94,72	83,42	45,75	Buvyukana	Pit sample	29,96319	-2,63993	PEG
M0012	< LOD	5,14	10,81	4,61	< LOD	96,2	27,7	< LOD	71,73	< LOD	62,13	Buvyukana	Pit sample	29,96319	-2,63993	PEG
M0013	< LOD	5,08	< LOD	8,35	< LOD	333,35	32,42	< LOD	92,88	82,45	46,19	Buvyukana	Pit sample	29,96329	-2,63992	PEG
M0014	< LOD	3,93	< LOD	9,8	< LOD	344,62	31,53	61,82	39,91	79,63	44,75	Buvyukana	Pit sample	29,96329	-2,63992	PEG
M0015	< LOD	3,78	< LOD	7,82	< LOD	345,13	30,87	62,44	38,98	85,45	43,75	Buvyukana	Pit sample	29,96329	-2,63992	PEG
M0016	< LOD	4,69	< LOD	8,17	< LOD	630,38	39,48	107,01	46,82	136,1	52,67	Buvyukana	Pit sample	29,96319	-2,63993	PEG
M0017	< LOD	4,92	< LOD	7,17	< LOD	229,38	30,76	< LOD	94	< LOD	67,1	Buvyukana	Pit sample	29,96329	-2,63992	PEG
M0018	< LOD	4,38	< LOD	7,76	< LOD	246,35	33,48	< LOD	63,19	90,3	48,75	Buvyukana	Pit sample	29,96318	-2,63913	PEG
M0019	< LOD	5,01	12,21	4,89	< LOD	158,5	29,66	< LOD	57,28	< LOD	106,7	Buvyukana	Pit sample	29,96321	-2,6399	PEG
M0021	< LOD	5,29	7,28	4,39	< LOD	164,17	27,28	< LOD	73,65	< LOD	60,07	Buvyukana	Pit sample	29,96321	-2,6399	PEG
M0022	< LOD	6,17	13,02	4,65	< LOD	100,42	27,51	< LOD	53,67	< LOD	88,88	Buvyukana	Pit sample	29,96321	-2,6399	PEG
M0023	< LOD	4,9	18,42	4,97	< LOD	58,62	28,49	< LOD	56,2	< LOD	62,99	Buvyukana	Pit sample	29,96321	-2,6399	PEG
M0024	< LOD	3,56	< LOD	9,77	< LOD	67,89	26,79	< LOD	52,49	< LOD	87,52	Buvyukana	Pit sample	29,96321	-2,6399	PEG

Sample Number	Ag	Ag Error	Cd	Cd Error	Sb	Ba	Ba Error	La	La Error	Ce	Ce Error	Target	Type of sample	Datum: WGS_84 X	Y	LITHO
M0025	< LOD	6,52	6,87	4,53	< LOD	188,51	28,51	< LOD	54,38	< LOD	70,81	Buvyukana	Pit sample	29,96321	-2,6399	PEG
M0026	< LOD	5,46	< LOD	6,61	< LOD	211,14	28,16	< LOD	86,73	64,79	40,98	Buvyukana	Pit sample	29,96321	-2,6399	PEG
M0027	< LOD	6,68	8,63	4,96	< LOD	313,37	32,09	< LOD	59,38	< LOD	66,62	Buvyukana	Pit sample	29,96318	-2,63913	PEG
M0028	< LOD	5,36	< LOD	6,98	< LOD	216,86	29,52	< LOD	74,18	< LOD	64,29	Buvyukana	Pit sample	29,96318	-2,63913	PEG
M0029	< LOD	3,72	< LOD	6,77	< LOD	235,81	29,11	< LOD	62,22	< LOD	97,09	Buvyukana	Pit sample	29,96318	-2,63913	PEG
M0031	< LOD	3,55	9,85	4,48	< LOD	201,39	27,83	< LOD	54,4	< LOD	60,86	Buvyukana	Pit sample	29,96321	-2,6399	PEG
M0032	< LOD	3,96	< LOD	6,87	< LOD	195,38	29,05	< LOD	71,84	< LOD	63,6	Buvyukana	Pit sample	29,96321	-2,6399	PEG
M0033	< LOD	3,7	< LOD	6,78	< LOD	172,27	28,59	< LOD	54,57	< LOD	61,35	Buvyukana	Pit sample	29,96321	-2,6399	PEG
M0034	< LOD	3,72	< LOD	6,87	< LOD	195,63	29,23	< LOD	57,22	< LOD	104,32	Buvyukana	Pit sample	29,96322	-2,63932	PEG
M0035	< LOD	4,7	< LOD	9,26	< LOD	57,76	25,49	< LOD	49,98	< LOD	56,04	Buvyukana	Pit sample	29,96322	-2,63932	PEG
M0036	< LOD	6,93	< LOD	11,43	< LOD	282,98	33,76	< LOD	103,49	96,84	48,85	Buvyukana	Pit sample	29,96321	-2,63923	PEG
M0037	< LOD	6,06	< LOD	7,61	< LOD	254,43	32,78	< LOD	61,6	< LOD	70,63	Buvyukana	Pit sample	29,96321	-2,63923	PEG
M0039	< LOD	11,34	< LOD	10,21	< LOD	828,54	60,78	337,28	70,29	504,07	81,08			29,96221	-2,64052	LAT
M0041	< LOD	5,22	< LOD	6,81	< LOD	245,67	29,38	< LOD	91,5	82,15	42,62	Buvyukana	Pit sample	29,96329	-2,63992	PEG
M0042	< LOD	4,46	< LOD	10,28	< LOD	291,97	30,13	< LOD	57,76	112,89	43,5	Buvyukana	Pit sample	29,96329	-2,63992	PEG
M0043	< LOD	3,91	< LOD	7,74	< LOD	379,16	31,55	< LOD	93,69	< LOD	66,04	Buvyukana	Pit sample	29,96329	-2,63992	PEG
M0044	< LOD	3,86	< LOD	9,05	< LOD	175,77	29,66	< LOD	84,87	86,16	43,88	Buvyukana	Pit sample	29,96329	-2,63992	PEG
M0045	< LOD	3,93	< LOD	8,27	< LOD	265,45	31,14	< LOD	85,34	72,03	44,93	Buvyukana	Pit sample	29,96321	-2,6399	PEG
M0046	< LOD	4,31	9,54	5,2	< LOD	334,02	33,85	< LOD	64,57	112,79	48,56	Buvyukana	Pit sample	29,96321	-2,63923	PEG
M0047	< LOD	5,49	9,36	4,69	< LOD	188,53	29,19	79,49	38,45	107,04	43,18	Buvyukana	Pit sample	29,96321	-2,6399	PEG

Sample Number	Pr	Pr Error	Nd	Hf	Re	Au	Th	Th Error	Mo	Mo Error	Pd	Target	Type of sample	Datum: WGS_84 X	Y	LITHO
M0001	75,35	47,85	< LOD	< LOD	113,95	< LOD	< LOD	9,12	< LOD	2,03	< LOD	Buvyukana	Pit sample	29,96318	-2,63913	PEG
M0002	145,93	50,06	104,22	< LOD	107,44	< LOD	8,98	4,68	< LOD	2,18	< LOD	Buvyukana	Pit sample	29,96318	-2,63913	PEG
M0003	125,83	57,19	< LOD	< LOD	240,98	56,57	17,09	6,02	< LOD	2,52	< LOD	Buvyukana	Pit sample	29,96318	-2,63913	PEG
M0004	< LOD	75,08	114,5	< LOD	146,23	< LOD	10,44	4,87	< LOD	2,25	< LOD	Buvyukana	Pit sample	29,96318	-2,63913	PEG
M0005	< LOD	80,4	< LOD	< LOD	205,95	27,92	12,52	5,87	< LOD	3,16	< LOD	Buvyukana	Pit sample	29,96318	-2,63913	PEG
M0006	201,1	58,7	298,49	< LOD	108,02	< LOD	7,34	4,04	< LOD	3,22	< LOD	Buvyukana	Pit sample	29,96319	-2,63993	PEG
M0007	< LOD	75,19	< LOD	< LOD	41,76	< LOD	< LOD	4,99	< LOD	3,47	< LOD	Buvyukana	Pit sample	29,96319	-2,63993	PEG
M0008	< LOD	82,18	< LOD	< LOD	45,99	< LOD	< LOD	4,86	< LOD	1,8	< LOD	Buvyukana	Pit sample	29,96319	-2,63993	PEG
M0009	< LOD	116,65	< LOD	< LOD	63,73	< LOD	< LOD	5,34	< LOD	2,82	< LOD	Buvyukana	Pit sample	29,96319	-2,63993	PEG
M0011	79,2	49,77	< LOD	< LOD	59,19	< LOD	< LOD	6,34	< LOD	3,25	< LOD	Buvyukana	Pit sample	29,96319	-2,63993	PEG
M0012	< LOD	67,62	< LOD	< LOD	28,75	< LOD	< LOD	3,69	< LOD	2,45	< LOD	Buvyukana	Pit sample	29,96319	-2,63993	PEG
M0013	86,87	50,39	143,47	47,99	47,58	< LOD	< LOD	4,92	< LOD	2,88	< LOD	Buvyukana	Pit sample	29,96329	-2,63992	PEG
M0014	108,62	49,04	143,74	36,25	47,64	< LOD	< LOD	4,46	< LOD	1,94	< LOD	Buvyukana	Pit sample	29,96329	-2,63992	PEG
M0015	132,56	48,09	110,58	36,09	44,09	< LOD	5,18	3,18	< LOD	2,76	< LOD	Buvyukana	Pit sample	29,96329	-2,63992	PEG
M0016	193,9	58,19	252,45	55,36	73,96	< LOD	11,32	4,27	6,52	2,22	< LOD	Buvyukana	Pit sample	29,96319	-2,63993	PEG
M0017	< LOD	73,12	147,94	< LOD	49,33	< LOD	< LOD	3,99	< LOD	2,29	< LOD	Buvyukana	Pit sample	29,96329	-2,63992	PEG
M0018	< LOD	79,52	< LOD	< LOD	206,85	< LOD	< LOD	13,35	< LOD	2,52	< LOD	Buvyukana	Pit sample	29,96318	-2,63913	PEG
M0019	< LOD	99,19	< LOD	< LOD	57,82	< LOD	< LOD	4,65	< LOD	3,04	< LOD	Buvyukana	Pit sample	29,96321	-2,6399	PEG
M0021	< LOD	83,31	< LOD	< LOD	45,04	< LOD	< LOD	4,01	< LOD	2,52	< LOD	Buvyukana	Pit sample	29,96321	-2,6399	PEG
M0022	< LOD	104,46	< LOD	< LOD	37,58	< LOD	< LOD	3	< LOD	1,6	< LOD	Buvyukana	Pit sample	29,96321	-2,6399	PEG
M0023	< LOD	88,42	< LOD	< LOD	< LOD	< LOD	< LOD	3,01	< LOD	2,72	< LOD	Buvyukana	Pit sample	29,96321	-2,6399	PEG
M0024	< LOD	64,05	< LOD	< LOD	31,99	< LOD	< LOD	3,78	< LOD	2	< LOD	Buvyukana	Pit sample	29,96321	-2,6399	PEG

Sample Number	Pr	Pr Error	Nd	Hf	Hf Error	Re	Au	Th	Th Error	Mo	Pd	Target	Type of sample	Datum: WGS_84 X	Y	LITHO
M0025	< LOD	87,47	< LOD	< LOD	36,7	51,25	< LOD	< LOD	5,89	< LOD	< LOD	Buvyukana	Pit sample	29,96321	-2,6399	PEG
M0026	< LOD	66,81	< LOD	42,73	24,96	51,7	< LOD	< LOD	6,31	< LOD	4,26	Buvyukana	Pit sample	29,96321	-2,6399	PEG
M0027	< LOD	75,39	< LOD	< LOD	41,21	94,71	< LOD	< LOD	6,31	< LOD	< LOD	Buvyukana	Pit sample	29,96318	-2,63913	PEG
M0028	< LOD	74,98	< LOD	38,41	24,54	73,72	< LOD	< LOD	6,38	< LOD	< LOD	Buvyukana	Pit sample	29,96318	-2,63913	PEG
M0029	< LOD	98,5	< LOD	< LOD	36,97	72,33	< LOD	6,16	3,6	< LOD	< LOD	Buvyukana	Pit sample	29,96318	-2,63913	PEG
M0031	< LOD	95,82	< LOD	< LOD	32,29	39,78	< LOD	< LOD	5,24	< LOD	< LOD	Buvyukana	Pit sample	29,96321	-2,6399	PEG
M0032	< LOD	69,16	< LOD	< LOD	48,6	76,29	< LOD	6,38	3,93	< LOD	< LOD	Buvyukana	Pit sample	29,96321	-2,6399	PEG
M0033	< LOD	83,69	< LOD	< LOD	62,44	73,8	< LOD	< LOD	5,74	< LOD	< LOD	Buvyukana	Pit sample	29,96321	-2,6399	PEG
M0034	< LOD	69,61	< LOD	< LOD	33,31	23,81	< LOD	5,05	2,91	< LOD	< LOD	Buvyukana	Pit sample	29,96322	-2,63932	PEG
M0035	< LOD	71	< LOD	< LOD	45,75	25,3	< LOD	< LOD	3,99	3,51	< LOD	Buvyukana	Pit sample	29,96322	-2,63932	PEG
M0036	103,72	53,3	< LOD	< LOD	64,9	90,09	< LOD	9,34	4,43	< LOD	< LOD	Buvyukana	Pit sample	29,96321	-2,63923	PEG
M0037	< LOD	120,01	< LOD	< LOD	59,24	94,94	< LOD	8,19	4,45	< LOD	< LOD	Buvyukana	Pit sample	29,96321	-2,63923	PEG
M0039	570,01	89,69	798,46	111,9	42,33	100,08	< LOD	< LOD	8,63	8,21	< LOD			29,96221	-2,64052	LAT
M0041	< LOD	69,46	< LOD	< LOD	33,74	40,49	< LOD	5,49	2,79	< LOD	< LOD	Buvyukana	Pit sample	29,96329	-2,63992	PEG
M0042	110,03	47,39	152,43	< LOD	36,51	43,6	< LOD	< LOD	6,06	< LOD	< LOD	Buvyukana	Pit sample	29,96329	-2,63992	PEG
M0043	89,62	48,25	116,91	38,12	25,34	60,03	< LOD	7,25	3,53	< LOD	< LOD	Buvyukana	Pit sample	29,96329	-2,63992	PEG
M0044	< LOD	71,35	< LOD	44,45	25,47	58,91	< LOD	< LOD	3,85	< LOD	< LOD	Buvyukana	Pit sample	29,96329	-2,63992	PEG
M0045	< LOD	115,62	< LOD	< LOD	37,54	59,44	< LOD	< LOD	7,22	< LOD	< LOD	Buvyukana	Pit sample	29,96321	-2,6399	PEG
M0046	135,41	53,17	170,56	< LOD	41,9	97,48	< LOD	8,02	4,15	3,74	< LOD	Buvyukana	Pit sample	29,96321	-2,63923	PEG
M0047	< LOD	70,02	< LOD	< LOD	55,47	39,74	< LOD	< LOD	7,31	< LOD	< LOD	Buvyukana	Pit sample	29,96321	-2,6399	PEG

Sample Number	Cl	Cl Error	K	K Error	Ca	Ca Error	Ti	Ti Error	V	Cr	Mn	Target	Type of sample	Datum: WGS_84 X	Y	LITHO
M0001	< LOD	143,9	34667,83	543,11	< LOD	170,72	< LOD	1786,28	< LOD	< LOD	< LOD	Buvyukana	Pit sample	29,96318	-2,63913	PEG
M0002	< LOD	158,26	32981,63	554,2	< LOD	223,04	< LOD	2306,33	< LOD	< LOD	< LOD	Buvyukana	Pit sample	29,96318	-2,63913	PEG
M0003	< LOD	154,55	49213,39	729,81	< LOD	265,15	< LOD	2043,01	< LOD	< LOD	660,84	Buvyukana	Pit sample	29,96318	-2,63913	PEG
M0004	< LOD	126,83	29512,37	491,54	< LOD	136,87	< LOD	1632,4	< LOD	< LOD	< LOD	Buvyukana	Pit sample	29,96318	-2,63913	PEG
M0005	< LOD	167,54	48280,56	702,02	< LOD	187,3	< LOD	1407,74	< LOD	< LOD	580,48	Buvyukana	Pit sample	29,96318	-2,63913	PEG
M0006	< LOD	175,61	36178,68	730,34	< LOD	350,21	< LOD	2939,95	< LOD	< LOD	536,4	Buvyukana	Pit sample	29,96319	-2,63993	PEG
M0007	< LOD	171,98	22707,83	460,99	224,91	97,08	< LOD	1778,44	< LOD	< LOD	< LOD	Buvyukana	Pit sample	29,96319	-2,63993	PEG
M0008	< LOD	137,75	24724,37	419,12	< LOD	190,07	< LOD	1331,11	< LOD	< LOD	< LOD	Buvyukana	Pit sample	29,96319	-2,63993	PEG
M0009	< LOD	165,12	31748,88	528,12	173,89	98,69	< LOD	1940,17	< LOD	< LOD	< LOD	Buvyukana	Pit sample	29,96319	-2,63993	PEG
M0011	< LOD	159,26	20149,78	424,99	359,72	86,46	< LOD	2530,9	< LOD	< LOD	< LOD	Buvyukana	Pit sample	29,96319	-2,63993	PEG
M0012	< LOD	138,13	13512,62	266,58	153,85	54,92	< LOD	1382,36	< LOD	< LOD	< LOD	Buvyukana	Pit sample	29,96319	-2,63993	PEG
M0013	< LOD	167,82	21271,53	421,94	< LOD	190,9	< LOD	1573,48	< LOD	< LOD	472,45	Buvyukana	Pit sample	29,96329	-2,63992	PEG
M0014	< LOD	155,28	14830,06	368,97	139,54	78,25	< LOD	1735,81	< LOD	< LOD	501,56	Buvyukana	Pit sample	29,96329	-2,63992	PEG
M0015	< LOD	158,85	20812	409,78	< LOD	180,9	< LOD	1945,63	< LOD	< LOD	484,64	Buvyukana	Pit sample	29,96329	-2,63992	PEG
M0016	< LOD	146,13	33469,37	692,76	243,18	145,17	< LOD	2827,05	< LOD	< LOD	< LOD	Buvyukana	Pit sample	29,96319	-2,63993	PEG
M0017	< LOD	143,78	21421,1	419,09	< LOD	209,05	< LOD	1847,45	< LOD	< LOD	< LOD	Buvyukana	Pit sample	29,96329	-2,63992	PEG
M0018	< LOD	189,9	57421,73	835,28	< LOD	217,08	< LOD	2302,04	< LOD	< LOD	784,63	Buvyukana	Pit sample	29,96318	-2,63913	PEG
M0019	< LOD	163,08	36178,48	534,63	< LOD	216,3	< LOD	1305,42	< LOD	< LOD	< LOD	Buvyukana	Pit sample	29,96321	-2,6399	PEG
M0021	< LOD	132,98	20040,93	335,56	147,05	64,91	< LOD	1108,67	< LOD	< LOD	< LOD	Buvyukana	Pit sample	29,96321	-2,6399	PEG
M0022	< LOD	143,13	12637,98	256,1	154,15	53,57	< LOD	1022,48	< LOD	< LOD	< LOD	Buvyukana	Pit sample	29,96321	-2,6399	PEG
M0023	< LOD	137,8	16142,16	300,45	128,07	61,52	< LOD	1123,68	< LOD	< LOD	< LOD	Buvyukana	Pit sample	29,96321	-2,6399	PEG
M0024	< LOD	159,27	16368,78	299,94	124,49	60,34	< LOD	1001,66	< LOD	< LOD	< LOD	Buvyukana	Pit sample	29,96321	-2,6399	PEG

Sample Number	Cl	Cl Error	K	K Error	Ca	Ca Error	Ti	Ti Error	V	Cr	Mn	Sample Number	Type of sample	Datum: WGS_84 X	Y	LITHO
M0025	< LOD	145,47	34803,79	515,73	< LOD	158,14	< LOD	1097,34	< LOD	< LOD	< LOD	Buvyukana	Pit sample	29,96321	-2,6399	PEG
M0026	< LOD	137,09	28473,25	459,02	< LOD	176,82	< LOD	1082,81	< LOD	< LOD	< LOD	Buvyukana	Pit sample	29,96321	-2,6399	PEG
M0027	< LOD	146,02	42261,53	662,02	< LOD	264,71	< LOD	2174,15	< LOD	< LOD	< LOD	Buvyukana	Pit sample	29,96318	-2,63913	PEG
M0028	< LOD	160,63	28671,76	482,56	< LOD	230,82	< LOD	1793,3	< LOD	< LOD	< LOD	Buvyukana	Pit sample	29,96318	-2,63913	PEG
M0029	< LOD	123,37	26384,05	443,71	< LOD	173,06	< LOD	1532,5	< LOD	< LOD	< LOD	Buvyukana	Pit sample	29,96318	-2,63913	PEG
M0031	< LOD	139,39	22596,04	372,75	121,39	70,58	< LOD	999,61	< LOD	< LOD	< LOD	Buvyukana	Pit sample	29,96321	-2,6399	PEG
M0032	< LOD	131,22	37091,05	544,91	< LOD	155,57	< LOD	1342,12	< LOD	< LOD	< LOD	Buvyukana	Pit sample	29,96321	-2,6399	PEG
M0033	< LOD	137,62	31973,81	493,83	< LOD	205,22	< LOD	1151,05	< LOD	< LOD	< LOD	Buvyukana	Pit sample	29,96321	-2,6399	PEG
M0034	< LOD	149,42	17452,04	370,64	< LOD	114,5	< LOD	1964,95	< LOD	< LOD	< LOD	Buvyukana	Pit sample	29,96322	-2,63932	PEG
M0035	< LOD	159,36	9421,39	227,79	237,68	50,31	< LOD	1320,32	< LOD	< LOD	< LOD	Buvyukana	Pit sample	29,96322	-2,63932	PEG
M0036	< LOD	180,93	33309,99	602,67	< LOD	281,95	2076,6	1352,4	< LOD	< LOD	< LOD	Buvyukana	Pit sample	29,96321	-2,63923	PEG
M0037	< LOD	174,55	39266,7	634,52	212,3	125,31	< LOD	1821,24	< LOD	< LOD	< LOD	Buvyukana	Pit sample	29,96321	-2,63923	PEG
M0039	249,87	130,06	12307,39	747,89	444,22	155,66	7281,21	3825,86	< LOD	< LOD	< LOD			29,96221	-2,64052	LAT
M0041	< LOD	132,86	10676,91	300,49	213,14	65,67	< LOD	1552,56	< LOD	< LOD	< LOD	Buvyukana	Pit sample	29,96329	-2,63992	PEG
M0042	< LOD	207,22	20981,18	417,84	< LOD	126,74	< LOD	2146,64	< LOD	< LOD	538,97	Buvyukana	Pit sample	29,96329	-2,63992	PEG
M0043	< LOD	157,17	27778,53	495,75	247,34	96,37	< LOD	2254,51	< LOD	< LOD	531,18	Buvyukana	Pit sample	29,96329	-2,63992	PEG
M0044	< LOD	156,43	22449,53	402,65	< LOD	121,54	< LOD	1385,97	< LOD	< LOD	515,1	Buvyukana	Pit sample	29,96329	-2,63992	PEG
M0045	< LOD	165,05	41655,84	618,28	176,21	111,14	< LOD	1645,62	< LOD	< LOD	< LOD	Buvyukana	Pit sample	29,96321	-2,6399	PEG
M0046	< LOD	143,26	32025,89	580,66	323,75	119,33	< LOD	2028,61	< LOD	< LOD	< LOD	Buvyukana	Pit sample	29,96321	-2,63923	PEG
M0047	< LOD	133,14	26244,78	450,1	199,08	85,47	< LOD	1384,17	< LOD	< LOD	< LOD	Buvyukana	Pit sample	29,96321	-2,6399	PEG

SAMPLE Num,	Ta	Nb	Sn	W	U	Si	Fe	Al	Mg	Bal	P	S	Target	Datum: WGS_84 X	Y	LITHO
M0001	574,12	181,17	360,29	< LOD	13,97	297975,09	11730,61	194688,72	< LOD	372070,63	1191,14	547,59	Buvyukana	29,96318	-2,63913	PEG
M0002	1507,02	331,83	532,91	< LOD	11,44	289104,19	14528,58	160821,52	< LOD	496172,56	< LOD	718,53	Buvyukana	29,96318	-2,63913	PEG
M0003	4554,77	681,61	1069,23	< LOD	24,59	300723,22	13994,56	213356,59	< LOD	334803,16	< LOD	862,44	Buvyukana	29,96318	-2,63913	PEG
M0004	2045,89	350,4	552,13	< LOD	14,11	296497,44	10728,65	156313,92	< LOD	500172	1124,34	622,68	Buvyukana	29,96318	-2,63913	PEG
M0005	3426,58	662,14	716,62	< LOD	16,49	298434,03	11763,61	145490,52	< LOD	485471,72	< LOD	574,74	Buvyukana	29,96318	-2,63913	PEG
M0006	225,18	134,88	175,11	< LOD	7,02	274589,47	64259,28	152352,47	< LOD	464054,06	2075,05	817,04	Buvyukana	29,96319	-2,63993	PEG
M0007	166,77	103,37	293,16	< LOD	5,13	340722,66	28917,04	157178,22	< LOD	346625,75	1648,51	742,37	Buvyukana	29,96319	-2,63993	PEG
M0007 DUP	159,85	113,53	295,02	< LOD	7,12	347239,53	29398,22	113506,25	< LOD	481688,47	1482,91	770,36				
M0008	220,64	118,02	452,19	< LOD	8,4	356053,28	11188,98	129760,55	< LOD	474382,22	1346,44	699,19	Buvyukana	29,96319	-2,63993	PEG
M0009	184,71	81,59	364,09	< LOD	< LOD	322303,5	16904,09	131688,67	< LOD	494828,06	< LOD	757,09	Buvyukana	29,96319	-2,63993	PEG
M0011	207,41	77,66	246,1	< LOD	< LOD	297508,47	24348,01	127779,57	< LOD	526749,44	< LOD	673,56	Buvyukana	29,96319	-2,63993	PEG
M0012	196,62	147,87	570,77	< LOD	< LOD	337484,56	8506,15	119271,73	< LOD	518918,63	< LOD	728,4	Buvyukana	29,96319	-2,63993	PEG
M0013	165,1	70,18	137,63	< LOD	6,37	305432,75	24769,76	120376,8	< LOD	523284,5	< LOD	672,33	Buvyukana	29,96329	-2,63992	PEG
M0014	191,27	72,41	140,3	< LOD	6,33	307748,53	27485,75	166677,3	98164,33	379410,75	< LOD	687,19	Buvyukana	29,96329	-2,63992	PEG
M0015	166,89	79,63	180,4	< LOD	6,5	302060,34	19488,49	133047,28	< LOD	520750,34	< LOD	787,41	Buvyukana	29,96329	-2,63992	PEG
M0016	213,71	135,34	201,2	< LOD	< LOD	288724,72	62504,14	137761,98	< LOD	469322,81	1449,44	1071,19	Buvyukana	29,96319	-2,63993	PEG
M0017	181,62	75,66	157,49	< LOD	7,21	326760,56	18430,57	122432,15	< LOD	508165,31	< LOD	844,29	Buvyukana	29,96329	-2,63992	PEG
M0018	2598,44	572,25	668,21	< LOD	30,45	310850,09	13709,08	246574,44	131001,42	231803,73	< LOD	749,43	Buvyukana	29,96318	-2,63913	PEG
M0019	247,48	97,61	1050,78	< LOD	< LOD	310980,34	10867,43	171399,28	< LOD	371681,88	< LOD	503,83	Buvyukana	29,96321	-2,6399	PEG
M0021	202,38	80,3	335,46	< LOD	< LOD	303747,34	6292,24	140158,47	< LOD	526780,25	< LOD	685,39	Buvyukana	29,96321	-2,6399	PEG
M0022	194,57	24,15	459,33	< LOD	< LOD	291556,25	5110,77	140878,66	< LOD	547094,13	< LOD	707,29	Buvyukana	29,96321	-2,6399	PEG
M0023	151,76	46,59	1714,17	< LOD	< LOD	353837	4693,08	139437,2	< LOD	420010,66	< LOD	626,66	Buvyukana	29,96321	-2,6399	PEG
M0024	152,74	65,44	178,5	< LOD	4,62	299506,03	5055,79	130502,98	< LOD	546173,13	< LOD	656,91	Buvyukana	29,96321	-2,6399	PEG

SAMPLE Num	Ta	Nb	Sn	W	U	Si	Fe	Al	Mg	Bal	P	S	Target	Datum: WGS_84 X	Y	LITHO
M0025	342,9	219,03	302,65	< LOD	7,55	302306,09	8036,52	153343,02	< LOD	497709	< LOD	667,3	Buvyukana	29,96321	-2,6399	PEG
M0026	306,69	158,11	246,03	< LOD	5,99	289537,34	8729,62	192559,58	< LOD	399090,13	< LOD	711,06	Buvyukana	29,96321	-2,6399	PEG
M0027	381,75	154,06	380,15	< LOD	17,27	287319,72	18919,76	157347,33	< LOD	489555,28	< LOD	861,28	Buvyukana	29,96318	-2,63913	PEG
M0028	256,51	132,96	270,84	< LOD	9,56	270464,16	14958,26	156975,88	< LOD	525456,75	< LOD	856,91	Buvyukana	29,96318	-2,63913	PEG
M0029	761,21	199,47	244,4	< LOD	18,93	289554,53	12165,57	152935,27	< LOD	514905,5	< LOD	937,08	Buvyukana	29,96318	-2,63913	PEG
M0031	206,24	77,53	374,27	< LOD	< LOD	297092,72	6096,91	125489,12	< LOD	546621	< LOD	601,09	Buvyukana	29,96321	-2,6399	PEG
M0032	348	198,79	303,73	< LOD	6,96	276941,53	8307,2	209297,06	124138,37	341016,47	< LOD	505,22	Buvyukana	29,96321	-2,6399	PEG
M0033	309,55	173,04	293,86	< LOD	6,62	275413,75	8603,26	153283,55	< LOD	527831,19	< LOD	840,04	Buvyukana	29,96321	-2,6399	PEG
M0034	149,78	51,22	84,68	< LOD	5,15	337582,97	17912,88	126553,38	< LOD	497627,78	< LOD	772,62	Buvyukana	29,96322	-2,63932	PEG
M0035	133,76	48,07	78,63	< LOD	4,1	305513,22	9989,9	155167,73	70361,67	447107,16	< LOD	717,36	Buvyukana	29,96322	-2,63932	PEG
M0036	371,81	124,23	405,62	< LOD	8,82	310156,34	34264,41	132271,52	< LOD	483033,34	< LOD	827,57	Buvyukana	29,96321	-2,63923	PEG
M0037	325,75	155,36	717,37	< LOD	17,94	286946,16	28574,58	152658,81	< LOD	485683,66	< LOD	718,29	Buvyukana	29,96321	-2,63923	PEG
M0039	112,65	67,64	< LOD	< LOD	< LOD	217125,52	220404,17	135250,81	< LOD	397670,66	3439,88	1389,36		29,96221	-2,64052	LAT
M0041	168,93	72,78	67,21	< LOD	5,93	294433,22	24740,82	124637,21	< LOD	541178,38	< LOD	702,37	Buvyukana	29,96329	-2,63992	PEG
M0042	193,42	82,45	150,9	< LOD	5,68	321852,88	20237,8	151342,33	< LOD	407045,81	< LOD	671,82	Buvyukana	29,96329	-2,63992	PEG
M0043	205,13	92,76	168,34	< LOD	< LOD	306612,84	20240,22	135942,44	< LOD	504497,44	1567,84	844,13	Buvyukana	29,96329	-2,63992	PEG
M0044	203,04	106,82	264,33	< LOD	< LOD	341954	14704,32	171933,09	131548,08	313616,19	< LOD	603,16	Buvyukana	29,96329	-2,63992	PEG
M0045	167,28	73,39	190,13	< LOD	< LOD	309227,16	15026,73	129319,48	< LOD	502155,06	< LOD	609,32	Buvyukana	29,96321	-2,6399	PEG
M0046	342,63	135,27	355,03	< LOD	< LOD	298020,13	34347,3	133226,23	< LOD	495472,5	1163,91	698,15	Buvyukana	29,96321	-2,63923	PEG
M0047	188,32	87,1	268,52	< LOD	< LOD	317675,97	13756,65	130075,72	< LOD	508577,09	1084,71	786,24	Buvyukana	29,96321	-2,6399	PEG

Appendices B: Chemical analyses of Whole Rock from NYANZA-BURENGE (in ppm)

SAMPLE	Pr	Rb	Sm	Sn	Sr	Ta	Tb	Th	Tm	U	V	W	Y	Yb	Zr	Target	Type of sample	Datum: WGS_84		LITHO
DESCRIPTION	ppm	ppm	ppm	ppm	ppm	ppm	ppm	ppm	ppm	ppm	ppm	ppm	ppm	ppm	ppm			X	Y	
C0189	2,61	271	1,37	43	8,9	23,2	0,19	9,41	0,1	2,84	69	15	5,7	0,75	112	NYANZA	Pit sample	29,99715	-2,74231	PEG
C0191	3,56	437	2,12	55	8,4	6,9	0,3	8,27	0,14	2,93	47	13	8,6	1,01	100	NYANZA	Pit sample	29,99715	-2,74231	PEG
C0192	2,94	408	1,76	52	7,9	3,6	0,29	5,83	0,13	2,72	35	14	8,5	0,86	80	NYANZA	Pit sample	29,99715	-2,74231	PEG
C0193	4,19	251	2,78	397	13,2	272	0,38	13,85	0,24	7,24	73	324	12,3	1,53	222	NYANZA	Pit sample	29,99715	-2,74231	PEG
C0194	4,59	58,2	2,62	47	15,6	5,6	0,32	18,5	0,19	4,36	113	17	10,2	1,37	225	NYANZA	Pit sample	29,99715	-2,74231	GRT
C0195	5,1	95,9	2,73	31	17,9	5,3	0,42	18,95	0,22	5,6	107	20	13,9	1,5	209	NYANZA	Pit sample	29,99715	-2,74231	GRT
C0196	4,08	64,2	2,35	24	17	3,4	0,29	21,5	0,21	5,97	100	25	9,1	1,35	205	NYANZA	Pit sample	29,99715	-2,74231	GRT
C0197	14,05	93,7	6,83	93	53,7	4,6	0,6	17,15	0,26	3,92	201	12	13,8	1,67	174	NYANZA	Pit sample	29,99837	-2,74527	QZT
C0198	48,3	221	21,3	81	96,6	12	1,35	10,55	0,33	3,08	112	9	18	2,26	116	NYANZA	Pit sample	29,99837	-2,74527	QZT
C0199	27,9	119,5	14,4	85	159,5	14,5	1,49	16,2	0,79	3,31	191	8	42	5,04	233	NYANZA	Pit sample	29,99837	-2,74527	QZT
C0201	5,45	55,8	2,85	19	25,4	11,6	0,32	13,9	0,18	3,13	167	11	9,6	1,22	136	NYANZA	Pit sample	29,99837	-2,74527	QZT
C0202	53,7	287	21,2	72	71,9	9,5	1,06	6,93	0,22	3,75	71	6	10,1	1,34	63	NYANZA	Pit sample	29,99837	-2,74527	QZT
C0203	34,2	156	14,75	81	132	3,8	1,19	18,4	0,53	5,56	197	10	26,9	3,86	218	NYANZA	Pit sample	29,99837	-2,74527	QZT
C0204	0,8	690	0,38	73	6	7,3	0,08	5,05	0,04	0,81	65	4	2,6	0,4	75	NYANZA	Pit sample	30,00601	-2,74712	PEG
C0205	1,34	874	0,58	94	5,8	20,7	0,08	4,27	0,04	0,81	38	3	2,3	0,28	73	NYANZA	Pit sample	30,00601	-2,74712	PEG
C0206	1,06	678	0,61	82	5,6	14	0,08	4,15	0,04	0,72	43	3	2,3	0,3	69	NYANZA	Pit sample	30,00601	-2,74712	PEG
C0207	1,77	520	0,81	70	8,4	12,4	0,11	6,51	0,07	1,19	60	4	3,5	0,5	115	NYANZA	Pit sample	30,00601	-2,74712	PEG
C0208	1,48	687	0,7	80	6	37	0,08	4,57	0,05	1,32	37	3	2,6	0,34	97	NYANZA	Pit sample	30,00601	-2,74712	PEG
C0209	0,73	442	0,36	66	3,7	24,8	0,06	2,47	0,04	0,77	55	8	1,7	0,25	44	NYANZA	Pit sample	30,008	-2,74619	PEG
C0211	1,02	318	0,55	45	3,2	7,4	0,06	3,63	0,04	1,29	40	3	1,7	0,21	76	NYANZA	Pit sample	30,008	-2,74619	PEG
C0212	0,84	392	0,49	55	2,7	7,4	0,06	3,68	0,04	1,2	24	3	1,4	0,25	72	NYANZA	Pit sample	30,008	-2,74619	PEG
C0213	0,66	586	0,33	80	2,1	15,1	0,05	2,47	0,02	0,91	23	3	0,9	0,13	47	NYANZA	Pit sample	30,008	-2,74619	PEG
C0214	0,86	480	0,47	62	2	9,3	0,05	2,61	0,02	1,17	28	2	0,9	0,13	62	NYANZA	Pit sample	30,008	-2,74619	PEG

SAMPLE	Pr	Rb	Sm	Sn	Sr	Ta	Tb	Th	Tm	U	V	W	Y	Yb	Zr	Target	Type of sample	Datum: WGS_84		LITHO
DESCRIPTION	ppm	ppm	ppm	ppm	ppm	ppm	ppm	ppm	ppm	ppm	ppm	ppm	ppm	ppm	ppm			X	Y	
C0217	2,55	432	1,94	64	10,5	9,9	0,33	9,6	0,23	3,34	183	7	11	1,49	138	NYANZA	Pit sample	30,00978	-2,74413	PEG
C0218	2,66	33,4	2,75	18	4,2	0,9	0,6	7,88	0,43	6,72	344	5	23,6	2,81	128	NYANZA	Pit sample	30,00978	-2,74413	MSC
C0219	1,67	28,4	1,73	19	3,6	0,9	0,41	8,13	0,22	10	518	7	11,6	1,62	135	NYANZA	Pit sample	30,00978	-2,74413	MSC
C0221	2,15	41,2	1,26	16	13,5	1,2	0,2	10,6	0,12	1,52	251	158	5,4	0,75	107	NYANZA	Pit sample	30,00636	-2,74385	LAT
C0222	2,58	193,5	1,64	27	36,1	20,7	0,29	17,8	0,24	3,17	352	7	10,3	1,54	224	NYANZA	Pit sample	30,00664	-2,74512	LAT
C0223	22,1	1865	5,04	237	24,8	41	0,33	5,45	0,12	2,68	72	6	6,4	0,92	79	NYANZA	Trench sample	30,00864	-2,745736408	PEG
C0224	12,65	1785	3,22	239	19,4	44,9	0,34	6,54	0,2	4,83	77	6	9,8	1,47	164	NYANZA	Trench sample	30,00864	-2,74573551	PEG
C0225	4,18	101,5	2,72	38	28,5	2,6	0,56	10,1	0,31	6,32	275	10	14,2	2,38	154	NYANZA	Trench sample	30,00864	-2,745734612	PEG
C0226	5,33	113,5	2,72	40	29,2	3	0,56	11,3	0,4	4	233	15	19,6	3,03	266	NYANZA	Trench sample	30,00864	-2,745733714	MSC
C0227	6,92	110,5	3,89	42	32,8	3	0,65	11,6	0,39	4,61	278	14	20,1	2,97	272	NYANZA	Trench sample	30,00864	-2,745732816	MSC
C0228	4,11	44,6	2,41	27	17,6	4,8	0,38	7,59	0,22	6,67	414	242	10,5	1,64	143	NYANZA	Trench sample	30,00864	-2,745731918	PEG
C0229	6,51	43,6	3,39	48	44,8	16,7	0,49	7,85	0,27	8,7	369	16	13,1	2,06	144	NYANZA	Trench sample	30,00864	-2,74573102	PEG
C0231	10,3	457	4,84	79	34,2	17,9	0,61	6,31	0,25	3,69	143	9	17,9	1,71	101	NYANZA	Trench sample	30,00864	-2,745730122	PEG
C0232	7,6	564	2,93	72	13,2	11,2	0,39	3,63	0,18	1,32	76	4	16,3	1,17	55	NYANZA	Trench sample	30,00864	-2,745729224	PEG
C0233	7,7	1135	2,52	154	9,1	22,7	0,21	3,63	0,08	0,95	64	6	6	0,55	45	NYANZA	Trench sample	30,00864	-2,745728326	PEG
C0234	2,82	1280	0,85	141	4	17,7	0,09	2,56	0,04	0,55	39	5	2,7	0,28	31	NYANZA	Trench sample	30,00864	-2,745727428	PEG
C0235	6,69	673	1,71	109	7	34,5	0,13	3,55	0,07	1,28	52	19	3,9	0,44	51	NYANZA	Trench sample	30,00864	-2,74572653	PEG
C0236	17,45	918	3,65	103	14,1	9	0,25	3,55	0,11	1,67	64	5	6,9	0,91	72	NYANZA	Trench sample	30,00864	-2,745725632	PEG
C0237	5,85	397	1,98	49	9,6	23,1	0,2	4,64	0,1	1,74	62	5	6,7	0,73	71	NYANZA	Trench sample	30,00864	-2,745724734	PEG
C0238	14,7	471	4,24	77	26,4	8,7	0,43	5,52	0,21	2,39	104	6	18,4	1,42	88	NYANZA	Trench sample	30,00864	-2,745723836	PEG
C0239	2,8	55,4	2,22	30	11,9	1,1	0,5	9,23	0,29	7,59	359	6	12,4	2,23	162	NYANZA	Trench sample	30,00864	-2,745739551	QZT
C0241	3,56	47,6	3,12	23	12,6	1,9	0,88	10,45	0,35	7,42	358	6	13,9	2,72	158	NYANZA	Trench sample	30,00864	-2,745738204	QZT
C0242	3,08	61,3	2,32	24	14,4	1,2	0,51	9,94	0,28	6	321	6	12	2,11	147	NYANZA	Trench sample	30,00864	-2,745737306	QZT
C0243	2,95	57,9	1,94	24	16,4	1,9	0,42	9,83	0,29	5,49	279	6	13,9	2,24	158	NYANZA	Trench sample	30,00864	-2,745736408	QZT
C0244	3,08	75,8	1,76	93	16,7	1,8	0,45	9,71	0,3	5,01	242	10	15,7	2,38	163	NYANZA	Trench sample	30,00864	-2,74573551	QZT

SAMPLE	Ba	Ce	Cr	Cs	Dy	Er	Eu	Ga	Gd	Hf	Ho	La	Lu	Nb	Nd	Target	Type of sample	Datum: WGS_84		LITHO
DESCRIPTION	ppm	ppm	ppm	ppm	ppm	ppm	ppm	ppm	ppm	ppm	ppm	ppm	ppm	ppm	ppm			X	Y	
C0189	43,6	47,9	230	23,8	1,16	0,69	0,29	23,4	1	3,4	0,23	15,1	0,09	64,6	8,2	NYANZA	Pit sample	29,99715	-2,74231	PEG
C0191	45	43,3	210	34,5	1,79	1,01	0,38	33,8	1,58	4,5	0,33	19,7	0,14	51	11,1	NYANZA	Pit sample	29,99715	-2,74231	PEG
C0192	47,4	31,9	250	35	1,65	0,93	0,33	30,7	1,44	4	0,33	15,8	0,12	37,5	9,3	NYANZA	Pit sample	29,99715	-2,74231	PEG
C0193	76,7	58,6	180	26,8	2,21	1,34	0,53	30,7	1,92	11,3	0,47	21,8	0,25	344	14	NYANZA	Pit sample	29,99715	-2,74231	PEG
C0194	75,8	88	210	12,35	2,06	1,22	0,51	22,9	1,8	5,9	0,4	25	0,2	32,8	14,6	NYANZA	Pit sample	29,99715	-2,74231	GRT
C0195	94,1	94,9	170	14,55	2,41	1,53	0,55	27,3	2,25	6,2	0,51	29,2	0,22	32,5	16,6	NYANZA	Pit sample	29,99715	-2,74231	GRT
C0196	96,7	83	160	11,35	1,67	1,11	0,45	25,3	1,63	5,7	0,36	24,7	0,21	27,2	12,9	NYANZA	Pit sample	29,99715	-2,74231	GRT
C0197	237	155	410	12,55	3,17	1,7	1,18	23,1	3,8	4,4	0,58	73,3	0,28	24	42,5	NYANZA	Pit sample	29,99837	-2,74527	QZT
C0198	395	548	270	24,7	5,58	2,26	3,1	27,5	9,08	3,2	0,9	262	0,32	41,3	145	NYANZA	Pit sample	29,99837	-2,74527	QZT
C0199	461	314	330	20,4	8,04	5,01	2,28	32,7	8,69	6,5	1,58	140,5	0,79	34,8	87,4	NYANZA	Pit sample	29,99837	-2,74527	QZT
C0201	115,5	64,2	410	7,6	1,9	1,24	0,5	16,6	1,88	3,4	0,41	28,8	0,19	19,7	17,3	NYANZA	Pit sample	29,99837	-2,74527	QZT
C0202	313	571	230	28,8	4,26	1,43	2,89	27,1	7,78	2,1	0,6	293	0,19	34,1	155	NYANZA	Pit sample	29,99837	-2,74527	QZT
C0203	461	372	290	27,1	6,58	3,6	2,39	31,3	7,51	6	1,2	186	0,56	25	100,5	NYANZA	Pit sample	29,99837	-2,74527	QZT
C0204	70	11,6	240	42,3	0,51	0,31	0,11	26,9	0,37	2,1	0,11	5,2	0,06	42,8	2,4	NYANZA	Pit sample	30,00601	-2,74712	PEG
C0205	63,1	11	190	58,2	0,49	0,28	0,12	31,8	0,43	2,7	0,09	7,5	0,04	60,3	3,9	NYANZA	Pit sample	30,00601	-2,74712	PEG
C0206	60,8	9,7	190	48,7	0,49	0,24	0,09	27,4	0,38	2,5	0,08	6,3	0,04	48,2	3	NYANZA	Pit sample	30,00601	-2,74712	PEG
C0207	90,8	17,2	180	46,1	0,66	0,36	0,16	29,2	0,57	4,1	0,13	11,4	0,09	37,6	4,6	NYANZA	Pit sample	30,00601	-2,74712	PEG
C0208	60,1	16,4	150	47,9	0,51	0,35	0,1	32,5	0,47	5,1	0,1	10,1	0,06	72,5	4	NYANZA	Pit sample	30,00601	-2,74712	PEG
C0209	30,4	13,6	340	39,1	0,35	0,22	0,08	16,6	0,35	2,1	0,08	4,2	0,04	72,5	2,3	NYANZA	Pit sample	30,008	-2,74619	PEG
C0211	27,3	17,8	240	28,1	0,37	0,24	0,09	20,5	0,43	6,1	0,07	6,8	0,03	27,1	2,8	NYANZA	Pit sample	30,008	-2,74619	PEG
C0212	22,5	16,4	220	35,4	0,32	0,19	0,07	23,9	0,35	6	0,06	5,9	0,03	27,5	2,6	NYANZA	Pit sample	30,008	-2,74619	PEG
C0213	17,2	17,5	250	53,7	0,22	0,13	0,06	25,2	0,25	3,8	0,05	4,4	0,02	61,1	1,9	NYANZA	Pit sample	30,008	-2,74619	PEG
C0214	13,5	18,5	220	45,7	0,26	0,13	0,05	21,7	0,27	6,3	0,05	5,9	0,02	35,4	2,4	NYANZA	Pit sample	30,008	-2,74619	PEG
C0215	90	42,8	520	6,24	1,63	0,97	0,36	11,3	1,33	2,5	0,35	16,2	0,16	15,7	11,2	NYANZA	Pit sample	30,00901	-2,74553	QZT
C0216	102,5	47,1	400	63,8	0,89	0,56	0,16	30,3	0,72	2,4	0,19	5,5	0,09	49,4	3	NYANZA	Pit sample	30,00978	-2,74413	PEG

SAMPLE	Ba	Ce	Cr	Cs	Dy	Er	Eu	Ga	Gd	Hf	Ho	La	Lu	Nb	Nd	Target	Type of sample	Datum: WGS_84		LITHO
DESCRIPTION	ppm	ppm	ppm	ppm	ppm	ppm	ppm	ppm	ppm	ppm	ppm	ppm	ppm	ppm	ppm			X	Y	
C0217	164.5	54,5	500	34,7	2,23	1,48	0,42	26,9	1,66	3,7	0,45	15	0,22	31,9	8,4	NYANZA	Pit sample	30,00978	-2,74413	PEG
C0218	95,3	164	1130	6,39	3,73	2,79	0,7	18,6	2,98	3,3	0,86	10,3	0,42	10,6	9,9	NYANZA	Pit sample	30,00978	-2,74413	MSC
C0219	99,2	625	1480	5,45	2,26	1,34	0,37	22,3	1,62	3,6	0,45	6,9	0,25	10,9	6,1	NYANZA	Pit sample	30,00978	-2,74413	MSC
C0221	71	21,1	580	5,31	1,14	0,74	0,23	15,2	1,02	2,7	0,23	12	0,14	10,7	6,9	NYANZA	Pit sample	30,00636	-2,74385	LAT
C0222	458	23,4	720	33,6	1,95	1,36	0,48	32,1	1,38	6	0,4	17,2	0,24	48,5	8,1	NYANZA	Pit sample	30,00664	-2,74512	LAT
C0223	92,3	177	190	126,5	1,63	0,83	0,7	51,4	2,3	5,9	0,29	162	0,12	132,5	51,8	NYANZA	Trench sample	30,00864	-2,745736408	PEG
C0224	112,5	116	180	143	1,84	1,17	0,5	50	1,93	17	0,39	90,3	0,22	134	29,8	NYANZA	Trench sample	30,00864	-2,74573551	PEG
C0225	331	396	740	8,96	3,2	2,15	0,65	22,2	2,85	4,9	0,66	26,8	0,34	18,3	13,3	NYANZA	Trench sample	30,00864	-2,745734612	PEG
C0226	508	157,5	370	11,35	3,59	2,36	0,66	26,5	2,74	7,9	0,79	35,4	0,42	24,1	15,9	NYANZA	Trench sample	30,00864	-2,745733714	MSC
C0227	504	120	610	11,55	3,83	2,53	0,84	27,6	3,38	8,2	0,85	42,2	0,41	24,5	21,8	NYANZA	Trench sample	30,00864	-2,745732816	MSC
C0228	135,5	77,8	1280	5,48	2,31	1,39	0,48	19,5	2	4,5	0,48	23,7	0,23	23,4	12,7	NYANZA	Trench sample	30,00864	-2,745731918	PEG
C0229	115,5	115	1240	5,53	2,86	1,73	0,76	24,2	2,59	4,3	0,59	35,9	0,3	27,3	20,4	NYANZA	Trench sample	30,00864	-2,74573102	PEG
C0231	153	110,5	380	31	3,22	1,71	0,93	27,1	4,32	3,8	0,62	61,6	0,24	61,1	32,8	NYANZA	Trench sample	30,00864	-2,745730122	PEG
C0232	96,3	52,6	210	40,8	2,22	1,36	0,55	29,4	2,98	2,6	0,44	53,4	0,16	35,2	22,3	NYANZA	Trench sample	30,00864	-2,745729224	PEG
C0233	59	105	190	66,4	1,05	0,58	0,36	40,2	1,65	2,3	0,2	56,6	0,08	73,2	20	NYANZA	Trench sample	30,00864	-2,745728326	PEG
C0234	40,2	59,8	230	77,8	0,46	0,27	0,15	40,8	0,55	1,6	0,08	19,5	0,03	75,7	6,9	NYANZA	Trench sample	30,00864	-2,745727428	PEG
C0235	55,3	71,5	180	42,5	0,82	0,43	0,27	29,8	0,98	3	0,14	47,2	0,05	67,9	16,3	NYANZA	Trench sample	30,00864	-2,74572653	PEG
C0236	97,6	76,5	170	64	1,37	0,73	0,46	36,5	1,81	5	0,26	129,5	0,13	41,4	38,5	NYANZA	Trench sample	30,00864	-2,745725632	PEG
C0237	75,7	51	220	28,9	1,06	0,7	0,33	24,3	1,36	3,6	0,23	41,8	0,11	36,7	15,3	NYANZA	Trench sample	30,00864	-2,745724734	PEG
C0238	124,5	168	190	31,1	2,47	1,35	0,7	29,2	3,59	3,7	0,5	110	0,2	27,6	37,4	NYANZA	Trench sample	30,00864	-2,745723836	PEG
C0239	367	998	1290	8,53	2,77	1,8	0,5	22,4	2,02	4,9	0,58	16,1	0,3	13,3	9,3	NYANZA	Trench sample	30,00864	-2,745739551	QZT
C0241	1070	3220	1080	6,38	3,52	2,09	0,65	28	2,91	4,4	0,69	17,7	0,36	15,4	12,2	NYANZA	Trench sample	30,00864	-2,745738204	QZT
C0242	242	622	990	9,54	2,69	1,74	0,53	21,1	2,18	4,2	0,55	17,4	0,31	13,2	10,3	NYANZA	Trench sample	30,00864	-2,745737306	QZT
C0243	237	93,5	720	7,3	2,65	1,8	0,48	19	2,14	4,6	0,62	18,1	0,3	14,7	9,3	NYANZA	Trench sample	30,00864	-2,745736408	QZT
C0244	267	117	460	9,55	2,66	2,1	0,42	18,7	2	4,9	0,63	19,3	0,35	14,8	9,3	NYANZA	Trench sample	30,00864	-2,74573551	QZT